

# MODERN DEVELOPMENT OF MAGNETIC RESONANCE

**abstracts**

**2015**

KAZAN \* RUSSIA









# MODERN DEVELOPMENT OF MAGNETIC RESONANCE

ABSTRACTS OF THE  
INTERNATIONAL CONFERENCE

Editor:  
KEV M. SALIKHOV

KAZAN, SEPTEMBER 22–26, 2015

Prof. Kev M. Salikhov  
Zavoisky Physical-Technical Institute,  
Russian Academy of Sciences, Kazan, Russian Federation  
Phone: 7 (843) 2720503  
E-mail: salikhov@kfti.knc.ru

This work is subject to copyright.

All rights are reserved, whether the whole or part of the material is concerned, specifically those of translation, reprinting, re-use of illustrations, broadcasting, reproduction by photocopying machines or similar means, and storage in data banks.

© 2015 Zavoisky Physical-Technical Institute, Kazan

© 2015 Igor A. Aksenov, graphic design

Printed in the Russian Federation

Published by Zavoisky Physical-Technical Institute, Kazan  
[www.kfti.knc.ru](http://www.kfti.knc.ru)

---

## CO-CHAIRS

Aleksei Kalachev,  
Kev Salikhov

## PROGRAM COMMITTEE

Albert Aganov (Russia)  
Vadim Atsarkin (Russia)  
Pavel Baranov (Russia)  
Marina Bennati (Germany)  
Bernhard Blümich (Germany)  
Michael Bowman (USA)  
Marina Brustolon (Italy)  
Sabine Van Doorslaer (Belgium)  
Jack Freed (USA)  
Ilgiz Garifullin (Russia)  
Graeme Hanson (Australia)  
Martina Huber (The Netherlands)  
Walter Kockenberger (UK)  
Wolfgang Lubitz (Germany)  
Klaus Möbius (Germany)  
Hitoshi Ohta (Japan)  
Igor Ovchinnikov (Russia)  
Kev Salikhov (Russia)  
Vladimir Skirda (Russia)  
Murat Tagirov (Russia)  
Takeji Takui (Japan)  
Valery Tarasov (Russia)  
Dmitrii Tayurskii (Russia)  
Yurii Tsvetkov (Russia)  
Violeta Voronkova (Russia)

## **LOCAL ORGANIZING COMMITTEE**

Tarasov V.F., chairman  
Adzhaliev Yu.A.  
Akhmin S.M.  
Chuclanov A.P.  
Falın M.L.  
Galeev R.T.  
Goleneva V.M.  
Gubaidulina A.Z.  
Guseva R.R.  
Kupriyanova O.O.  
Kurkina N.G.

Latypov V.A.  
Lvov S.G.  
Mosina L.V.  
Ovchinnikov I.V.  
Siafetdinova A.Z.  
Voronkova V.K.  
Voronova L.V.  
Yanduganova O.B.  
Yurtaeva S.V.  
Ziganshina S.A.

## **SCIENTIFIC SECRETARIAT**

Violeta K. Voronkova  
Laila V. Mosina  
Vlad A. Latypov

The conference is organized under the auspices of the AMPERE Society

## **ORGANIZERS**

Kazan E. K. Zavoisky Physical-Technical Institute  
of the Kazan Scientific Center of the Russian Academy of Sciences  
The Academy of Sciences of the Republic of Tatarstan  
Kazan Federal University

## **SUPPORTED BY**

The Government of the Republic of Tatarstan  
The Russian Foundation for Basic Research  
Bruker BioSpin Moscow

## **CONFERENCE LOCATION**

The Academy of Sciences of the Republic of Tatarstan  
Kazan, ul. Baumana 20



---

## CONTENTS

### ZAVOISKY AWARD LECTURES

- Half a Century in Magnetic Resonance: Spin Temperature and More  
*V. A. Atsarkin* 2
- Low Symmetry through EPR: 40 Years of Attraction in Florence  
*D. Gatteschi* 3

### PLENARY LECTURES

- Resonance Spin-Charge Phenomena in Manganite Thin Films and Bilayers  
*V. A. Atsarkin, B. V. Sorokin, I. V. Borisenko, V. V. Demidov, G. A. Ovsyannikov* 6
- Exploring Low Symmetry Effects in Molecular Magnets with EPR  
*D. Gatteschi, M. Fittipaldi* 7
- Magnetic Resonance in Strongly Correlated and Quantum Critical Systems  
*S. V. Demishev, A. V. Semeno, M. I. Gilmanov, V. V. Glushkov, A. N. Samarin, N. E. Sluchanko* 9

### SECTION 1

#### CHEMICAL AND BIOLOGICAL SYSTEMS

- New Approaches to Study Structure of Biopolymers  
Using Pulse EPR  
*E. Bagryanskaya, A. A. Kuzhelev, O. A. Krumkacheva, M. Fedin, O. Yu. Rogozhnikova, D. V. Trukhin, V. M. Tormyshev, G. Shevelev, A. A. Lomzov, D. Pyshnyi* 12
- Spin-Label EPR Study of Peptide-Lipid and Cholesterol-Lipid  
Interactions in Model Biological Membranes  
*S. A. Dzuba* 14
- Magnetic Interactions in Narrow-Line Trityl Biradicals  
*M. K. Bowman, H. Chen, N. P. Isaev, R. I. Samoilova, A. G. Maryasov, O. Y. Rogozhnikova, V. M. Tormyshev* 16
- Effect of Disaccharide Trehalose Glassy Matrix on Charge  
Recombination in Photosystem I  
*A. Semenov, M. Malferrari, A. Savitsky, M. Mamedov, K. Möbius, G. Venturoli* 17

|  |    |
|--|----|
| Electron Transfer between Aromatic Amino Acids and Histidine Radicals<br><i>A. Yurkovskaya, O. Morozova</i>  | 18 |
| Application of ELDOR Detected NMR to Study Hyperfine Interaction in Cu(II)-bis(oxamidato) Complexes<br><i>R. B. Zaripov, E. L. Vavilova, V. K. Voronkova, K. M. Salikhov, A. Aliabadi, A. Petr, V. Kataev, B. Büchner, M. A. Abdulmalic, T. Rüffer</i> | 19 |
| Low Field Photo CIDNP in Linked Systems<br><i>P. A. Purtoy, N. E. Polyakov, I. M. Magin, A. I. Kruppa, T. V. Leshina</i>   | 20 |
| Lesion Impact on Flipping-Unflipping Equilibrium of DNA Duplexes: an NMR Study<br><i>N. A. Kuznetsov, A. S. Kiryutin, M. S. Panov, A. V. Yurkovskaya, O. S. Fedorova</i>   | 22 |
| A Connection Between Electron Transfer and Spin Exchange<br><i>G. I. Likhtenshtein</i>   | 23 |
| Spin Effects in Chiral Linked Systems<br><i>T. V. Leshina, E. A. Khramtsova, D. V. Sosnovsky, P. A. Purtoy</i>   | 25 |
| Paramagnetic Centers Created under Mechano-Chemical Treatment of Mixed Molybdenum-Vanadium Oxides<br><i>I. V. Kolbanov, E. N. Degtyarev, M. V. Sivak, A. N. Streletsky, A. I. Kokorin</i>  | 27 |
| Electron Spin Relaxation of Nitroxide Spin Labels in the Trehalose Glassy Matrix at Room Temperature<br><i>R. K. Strizhakov, A. A. Kuzhelev, O. A. Krumkacheva, G. Y. Shevelev, I. A. Kirilyuk, M. V. Fedin, E. G. Bagryanskaya</i>                    | 28 |
| The Study of Interaction of Disaccharides with Lipid Bilayer Using Pulsed Electron Paramagnetic Resonance<br><i>K. B. Konov</i>  | 29 |
| Kinetics and Mechanism of the Reversible Photoinduced Oxidation of Purine Nucleotides in Aqueous Solutions: Time-Resolved CIDNP and Laser Flash Photolysis Study<br><i>N. N. Fishman, O. B. Morozova, M. S. Panov, G. Grampp, A. V. Yurkovskaya</i>    | 31 |

## SECTION 2

STRONGLY CORRELATED ELECTRON SYSTEMS.  
MAGNETIC RESONANCE INSTRUMENTATION

|   |    |
|---|----|
| Exotic Spin Phases in the Low-Dimensional Quantum Magnet $\text{LiCuSbO}_4$ as Seen by High-Field NMR and ESR Spectroscopies<br><i>V. Kataev, H.-J. Grafe, M. Iakovleva, E. Vavilova, A. Alfonsov, H. Nojiri, M.-I. Sturza, S. Wurmehl, S.-L. Drechsler, B. Büchner</i> | 34 |
|---|----|

|   |    |
|---|----|
| Magnetic Properties of 4f- and 5d-Metal Complexes<br>with Redox-Active Ligands: the High-Level <i>ab initio</i> Calculations<br>with Non-Perturbative Account of Spin-Orbit Coupling<br><i>N. Gritsan, E. Suturina, A. Dmitriev</i> | 35 |
| Excitonic Magnetism in Van Vleck-Type Mott Insulators<br><i>G. Khaliullin</i>   | 36 |
| Spin Fluctuations and Inhomogeneities in Iron Pnictide Superconductors<br>as Probed by NMR and NQR<br><i>H.-J. Grafe, U. Gräfe, F. Hammerath, G. Lang, A. P. Dioguardi,<br/>N. J. Curro, B. Büchner</i>                             | 37 |
| Magnetic Properties of YbMnO <sub>3</sub> Ceramic Samples<br><i>R. M. Eremina, I. V. Yatzyk, T. P. Gavrilova, V. V. Parfenov,<br/>V. I. Chichkov, N. V. Andreev</i>   | 39 |
| Unusual Quadrupole Moment Reduction and Cobalt Charge<br>Differentiation in Na <sub>x</sub> CoO <sub>2</sub><br><i>I. R. Mukhamedshin, I. F. Gilmutdinov, A. V. Dooglav, S. A. Krivenko,<br/>H. Alloul</i>                          | 41 |
| EPR of Gadolinium Cluster Centers in the Semimagnetic Narrow Gap<br>Semiconductors Pb <sub>1-x</sub> Gd <sub>x</sub> Te ( $x = 0.02$ )<br><i>E. R. Zhiteitsev, R. R. Zainullin, V. A. Ulanov, V. A. Shustov</i>                     | 43 |
| Research-Class Bench-Top EPR-Spectrometer Bruker EMXnano<br><i>S. Lyubenova, P. Hofer, D. Kuznetsov</i>   | 45 |
| <br>SECTION 3<br>LOW-DIMENSIONAL SYSTEMS AND NANO-SYSTEMS   |    |
| Spin Probes for EPR and Overhauser-Enhanced Magnetic<br>Resonance Imaging<br><i>G. Audran, P. Brémond, S. Marque</i>  | 48 |
| Magnetic Resonance of Spinons in $S = 1/2$ Antiferromagnetic<br>Spin Chains<br><i>A. I. Smirnov, T. A. Soldatov, K. Yu. Povarov</i>   | 49 |
| NMR of <sup>3</sup> He in Porous Media<br><i>A. V. Klochkov, E. M. Alakshin, R. R. Gazizulin, V. V. Kuzmin,<br/>K. R. Safiullin, M. S. Tagirov</i>  | 50 |
| Silicon-Based Hybrid Nanostructures: Magnetic State<br>and Magneto-Dependent Charge Transport<br><i>N. V. Volkov, A. S. Tarasov, M. V. Rautskii, S. N. Varnakov,<br/>S. G. Ovchinnikov</i>  | 51 |
| Electronic and Magnetic Structures of Nanographites and Their<br>Changes Influenced by Adsorbed Molecules: EMR and MS Studies<br><i>A. M. Ziatdinov</i>   | 52 |

|   |    |
|---|----|
| Investigation of Magnetoelastic Effect in Permalloy Microparticles by Ferromagnetic Resonance and Magnetic Force Microscopy Techniques<br><i>D. A. Biziyayev, A. A. Bukharaev, Yu. E. Kandrashkin, R. V. Gorev, L. V. Mingalieva, V. L. Mironov, N. I. Nurgazizov, T. F. Khanipov</i> | 54 |
| Features of Ferromagnetic Resonance and Exchange Interaction in Structures CoPt with not Collinear Magnetizations<br><i>A. A. Fraerman, N. S. Gusev, V. L. Mironov, E. S. Demidov, L. I. Budarin</i>  | 56 |
| Ferromagnetic Resonance in Permalloy Microstrips<br><i>E. Skorohodov, R. Gorev, R. Yakubov, Yu. Khivintzev, Yu. Filimonov, E. Demidov, V. Mironov</i>   | 58 |
| Magnetic Resonance Studies of Ion-Beam Implanted Single Crystal Oxides<br><i>B. Rameev, R. Khaibullin</i>   | 60 |
| One-Third Magnetization Plateau and Spin Dynamics in Low-Dimensional Magnet $\text{NaFe}_3(\text{HPO}_3)_2(\text{H}_2\text{PO}_3)_6$<br><i>E. A. Zvereva, I. Munao, P. Lightfoot, A. A. Tsirlin, Y. A. Ovchenkov, O. S. Volkova, C. Koo, R. Klingeler, A. N. Vasiliev</i>             | 61 |
| SECTION 4   |    |
| THEORY OF MAGNETIC RESONANCE  |    |
| Distance Measurements by Peldor Spectroscopy in Systems Containing Photoexcited Triplet States and Nitroxides<br><i>D. Carbonera, M. Di Valentin, M. Albertini, E. Zurlo, M. Gobbo</i>  | 66 |
| Applications of Information Geometry to Saturated Spectra<br><i>K. A. Earle, T. Broderick</i>   | 68 |
| Investigation of Quantum Correlations and Quantum Computations with NMR Methods<br><i>E. B. Fel'dman</i>  | 69 |
| Resonance Line Shape and Orthogonal Two-Spin Correlation Functions in Magnetically Disordered Systems<br><i>F. S. Dzheparov</i>   | 70 |
| Exploiting the Concept of Avoided Level Crossings for Analysing Magnetic Field Dependence of Solid-State CIDNP<br><i>D. Sosnovsky, J. Matysik, G. Jeschke, K. Ivanov</i>  | 71 |
| Intrinsic Gilbert Damping in Polycrystalline Multilayer Structures with Exchange Bias NiFe/Cu/NiFe/IrMn<br><i>A. N. Orlova, A. Y. Zubin, G. S. Kupriyanova</i>  | 72 |

## SECTION 5

MODERN METHODS OF MAGNETIC RESONANCE.  
OTHER APPLICATIONS OF MAGNETIC RESONANCE

|  |    |
|--|----|
| RF-SABRE and PH-INEPT Sequences Make High Field<br>SABRE Feasible<br><i>A. N. Pravdivtsev, A. V. Yurkovskaya, H.-M. Vieth, K. L. Ivanov</i>  | 74 |
| Electron Paramagnetic Resonance Study of Color Centers<br>in Silicon Carbide. From Identification to Quantum Applications<br><i>V. Soltamov, B. Yavkin, G. Astakhov, V. Dyakonov, H. Kraus,<br/>F. Fuchs, S. B. Orlinskii, P. G. Baranov</i>   | 75 |
| POSTERS  |    |
| NMR Studies of the Solution of Mechanically Activated<br>Calcium Gluconate<br><i>M. M. Akhmetov, G. G. Gumarov, V. Yu. Petukhov, G. N. Konygin,<br/>D. S. Rybin, A. B. Konov</i>   | 78 |
| Influence of Uniaxial Compression on EPR Spectra of Nickel Chloride<br>with 3-Amino-4-Ethoxycarbonylpyrazol Compound<br><i>A. S. Berezin, V. A. Nadolinniy, L. G. Lavrenova</i>  | 80 |
| Development of the Method of Indirect Registration of D <sub>2</sub> O Involved<br>in a Chemical Exchange<br><i>A. Bogaychuk, G. Kupriyanova, N. Sinyavsky, A. Gorkin</i>  | 82 |
| Photo- and Thermo-Active Magnetic Properties of Iron-Containing<br>Dendrimers<br><i>N. Domracheva, V. Vorobeva, M. Gruzdev, U. Chervonova,<br/>A. Kolker, A. Pyataev</i>   | 84 |
| Ferromagnetic Resonance of Deposited from Laser Plasma Nanosized<br>Layers of the Diamond-Like Diluted Magnetic Semiconductor<br>on the Basis of Si, Doped by Mn<br><i>E. S. Demidov, V. V. Podol'skii, V. P. Lesnikov, V. V. Karzanov,<br/>A. A. Tronov, L. I. Budarin</i>  | 86 |
| Synthesis and ESR Investigations of Gd <sub>1-x</sub> Sr <sub>x</sub> MnO <sub>3</sub><br><i>R. M. Eremina, T. Maiti, A. K. Shukla</i>   | 89 |
| AFM-PM Phase Transitions in Nano-Composite Materials<br>(SrFe <sub>12</sub> O <sub>19</sub> ) <sub>x</sub> (CaCu <sub>3</sub> Ti <sub>4</sub> O <sub>12</sub> ) <sub>1-x</sub><br><i>R. M. Eremina, K. R. Sharipov, I. V. Yatsyk, N. M. Lyadov,<br/>T. P. Gavrilova, I. F. Gilmudinov, A. G. Kiyamov, Yu. V. Kabirov,<br/>V. G. Gavrilyachenko, T. I. Chupakhina</i> | 90 |
| Electron Paramagnetic Resonance Study of Yb <sup>3+</sup> in Hexagonal<br>Perovskite RbMgF <sub>3</sub> Crystal<br><i>M. L. Falin, V. A. Latypov, S. V. Petrov</i>   | 92 |

---

|   |     |
|---|-----|
| CIDNP Study of Biradicals from Nucleotide-Photosensitizer and Amino Acid-Photosensitizer Conjugates<br><i>N. Fishman, A. Kiryutin, O. Morozova, M. Panov, T. Abramova, A. Yurkovskaya</i>   | 93  |
| The Modes of the Superconducting Triplet Spin-Valve and Distribution of Condensate Functions<br><i>R. R. Gaifullin, R. G. Deminov, L. R. Tagirov, T. Yu. Karminskaya, M. Yu. Kupriyanov, Ya. V. Fominov, A. A. Golubov</i>                                    | 95  |
| EPR Study of Nitric Oxide Production in Brain, Heart and Liver of Rats after Hemorrhagic Insult Modeling<br><i>Kh. L. Gainutdinov, V. V. Andrianov, V. S. Iyudin, G. G. Yafarova, A. A. Denisov, M. O. Khotyanovich, S. G. Pashkevich, V. A. Kulchitchkii</i> | 96  |
| Effect of Levels Anticrossing on the EPR Spectra and the Dynamic Susceptibility<br><i>R. T. Galeev</i>  | 98  |
| ESR Study of Electron Beam Irradiated Calcium Gluconate<br><i>I. A. Goenko, V. Yu. Petukhov, I. V. Yatsyk, G. G. Gumarov, M. M. Akhmetov, G. N. Konygin</i>   | 99  |
| Electron Spin Resonance in 1-2-2 Pnictides $\text{EuCd}_2\text{As}_2$ and Influence Substitutions on its Parameters<br><i>Yu. Goryunov, A. Nateprov</i>   | 101 |
| Spin Dynamics in the Frustrated System $\text{CoAl}_2\text{O}_4$<br><i>M. Iakovleva, E. Vavilova, H.-J. Grafe, S. Zimmermann, A. Alfonsov, H. Luetkens, H.-H. Klauss, A. Maljuk, S. Wurmehl, B. Büchner, V. Kataev</i>  | 103 |
| Abnormal Absorption Lines in ESR Spectra of Sportsmen Serum Samples<br><i>M. I. Ibragimova, A. I. Chushnikov, G. V. Cherepnev, V. Yu. Petukhov, I. V. Yatsyk</i>  | 104 |
| In-Plane Magnetic Anisotropy Constants of Thin Films from Angular FMR Dependence<br><i>A. V. Izotov, B. A. Belyaev</i>  | 106 |
| Orientalional Self-Ordering of Spin-Labeled Cholesterol Analog in Lipid Bilayers<br><i>M. E. Kardash, S. A. Dzuba</i>   | 107 |
| Development of Four-Pulse ELDOR Theory for the Case of Overlapping EPR Spectra and Overlapping Excitation Bands Taking into Account Nonsecular Part of the Dipole-Dipole Interaction<br><i>I. T. Khairuzhdinoy, K. M. Salikhov</i>                            | 109 |

|   |     |
|---|-----|
| Spin-Dependent Transport in Bismuth Doped Silicon<br><i>A. V. Koroleva, A. V. Soukhorukov, D. V. Guseinov, A. V. Kudrin,<br/>S. A. Popkov, A. A. Detochenko, A. A. Ezhevskii, A. A. Konakov,<br/>N. V. Abrosimov, H. Riemann</i>    | 110 |
| NMR Bottle Scanner<br><i>A. B. Konov, M. F. Sadykov, A. Turkiya</i>   | 111 |
| Investigation of the $T_1$ and $T_2$ Relaxation of Polyamides NMR<br>in the Low Magnetic Field<br><i>G. S. Kupriyanova, V. V. Molchanov, E. A. Severin, G. V. Mozzhukhin</i>  | 112 |
| Pulse and CW EPR Study of Triarylmethyl Radicals<br>at Room Temperature<br><i>A. A. Kuzhelev, O. A. Krumkacheva, D. V. Trukhin,<br/>O. Yu. Rogozhnikova, T. I. Troitskaya, V. M. Tormyshev, M. V. Fedin,<br/>E. G. Bagryanskaya</i> | 114 |
| Electron Paramagnetic Resonance of $Ce^{3+}$ Ions<br>in $KZnF_3$ Single Crystal<br><i>V. A. Latypov, M. L. Falin, S. L. Korableva</i>   | 115 |
| Membrane-Sucrose Interactions Probed by Spin-Label Pulsed EPR<br><i>D. V. Leonov, K. B. Konov, K. Yu. Fedotov, N. P. Isaev,<br/>V. K. Voronkova, S. A. Dzuba</i>  | 116 |
| Magnetic Properties of Crystals of Partially Stabilized Zirconia<br><i>E. E. Lomonova, F. O. Milovich, N. Yu. Tabachkova, R. M. Eremina,<br/>I. I. Fazlizhanov</i>  | 117 |
| Calculations of Time-Resolved EPR Spectra in Photovoltaic Pair:<br>Polymer Poly(3-Hexylthiophene) and [6-6]-Phenyl C61 –<br>Butyric Acid Methyl Ester<br><i>N. Lukzen, J. Behrends</i>  | 119 |
| Non Resonance Double Frequency NQR in $NaNO_2$<br><i>S. Mamadazizov, G. Mozzhukhin, B. Rameev, G. Kupriyanova</i>   | 120 |
| Compensation of the NQR Frequency Offset with Composite Pulses<br><i>I. Mershiev, G. Kupriyanova</i>  | 122 |
| Population Transfer in NQR of Compounds with Long $T_1$ Relaxation<br>Parameter<br><i>G. V. Mozzhukhin, J. Barras, B. Rameev, G. Kupriyanova</i>  | 124 |
| Spin-Polarized Time-Resolved EPR Spectra of Pentadentate<br>Fe(III) Complexes with Imidazole or Picoline as Co-Ligandes<br><i>I. Ovchinnikov, T. Ivanova, A. Sukhanov, O. Turanova</i>  | 125 |
| Low-Temperature Dynamical Transition in Glassy o-Terphenyl<br><i>E. A. Pushkina, D. V. Leonov, S. A. Dzuba</i>  | 126 |
| To the ESR Studies of the Topological Insulators<br><i>V. O. Sakhin, E. F. Kukovitsky, Yu. I. Talanov, G. B. Teitel'baum</i>  | 128 |

---

|   |     |
|---|-----|
| Development of a Method for Separating Exchange and Dipole-Dipole Interactions to the Shape of EPR Spectra of Nitroxyl Radicals with Unresolved Proton Hyperfine Structure<br><i>K. M. Salikhov, R. T. Galeev, B. Bales, M. M. Bakirov</i>                        | 129 |
| Nuclear Magnetic Resonance in Low-Dimensional Compound $A_3Ni_2SbO_6$ ( $A = Na, Li$ )<br><i>T. Salikhov, M. Iakovleva, K. Safullin, A. Klochkov, M. Tagirov, M. Stratan, E. Zvereva, V. Nalbandyan, E. Vavilova</i>  | 130 |
| High-Frequency EPR Spectroscopy of ZnSe:Fe<br><i>G. S. Shakurov, D. S. Pytalev, V. I. Kozlovsky, Yu. V. Korostelin</i>  | 131 |
| EPR Study of the Inclusion Complex of Nitronyl Nitroxide Covalently Linked with Permethyl-B-Cyclodextrin<br><i>R. K. Strizhakov, O. A. Krumkacheva, E. V. Tretyakov, A. S. Medvedeva, V. V. Novokshonov, V. G. Vasiliev, V. I. Ovcharenko, E. G. Bagryanskaya</i> | 132 |
| Influence of Fe-Fe and Fe-Ln Spin-Spin Interactions on the Magnetisation Dynamics of Mixed Clusters<br><i>A. Sukhanov, R. Galeev, L. Mingalieva, V. Voronkova, A. Baniodeh, A. Powell</i>   | 134 |
| ESR Study of the $Bi_2Te_3$ Doped with Manganese<br><i>Yu. Talanov, E. Kukovitsky, V. Sakhin, G. Teitel'baum</i>  | 136 |
| Dimer Self-Organization of $Er^{3+}$ Impurity Ions in Synthetic Forsterite<br><i>V. F. Tarasov, L. V. Mingalieva, K. A. Subbotin, R. B. Zaripov, E. V. Zharikov</i>   | 138 |
| Formation of $(Ni^{3+}-F_{int}^-)$ Associates in the $BaF_2$ Crystals Activated by Nickel: Results of EPR Study<br><i>V. A. Ulanov, R. R. Zainullin, I. V. Yatsyk, E. R. Zhiteitsev</i>   | 139 |
| EPR Investigation of Trinuclear Copper Cluster in Hyperbranched Polyesterpolyacrylic Acid<br><i>S. V. Yurtaeva, I. V. Ovchinnikov, M. P. Kutyreva, A. R. Gataulina, N. A. Ulakhovich, A. A. Rodionov</i>  | 142 |
| The Influence of the Frequency of the Microwave Field on the Dispersion Curves of the Spin-Wave Resonance Spectra<br><i>A. M. Zuyzin, M. A. Bakulin, S. V. Bezborodov, V. V. Radaikin, S. N. Sabaev</i>   | 144 |
| Spin-Wave Resonance in Films with a Uniform Gradient of Field Uniaxial Anisotropy<br><i>A. M. Zyuzin, N. V. Yantsen</i>   | 146 |
| AUTHOR INDEX  | 149 |



---

## ZAVOISKY AWARD LECTURES

## **Half a Century in Magnetic Resonance: Spin Temperature and More**

**V. A. Atsarkin**

Kotel'nikov Institute of Radio Engineering and Electronics of RAS, Moscow 125009,  
Russian Federation, atsarkin@cplire.ru

# **Low Symmetry through EPR: 40 Years of Attraction in Florence**

**D. Gatteschi**

Department of Chemistry, University of Florence, Sesto Fiorentino 50019, Italy,  
dante.gatteschi@unifi.it

---

---

## PLENARY LECTURES

## Resonance Spin-Charge Phenomena in Manganite Thin Films and Bilayers

**V. A. Atsarkin, B. V. Sorokin, I. V. Borisenko, V. V. Demidov,  
and G. A. Ovsyannikov**

Kotel'nikov Institute of Radio Engineering and Electronics of RAS, Moscow 125009,  
Russian Federation, atsarkin@cplire.ru

The dc voltage generated by microwave pumping under conditions of ferromagnetic resonance has been studied in thin epitaxial films of the manganite  $\text{La}_{0.67}\text{Sr}_{0.33}\text{MnO}_3$  and bilayer structures manganite/non-magnetic metals (Au, Pt, and  $\text{SrRuO}_3$ ) grown on the  $\text{NdGaO}_3$  substrate. The studies were performed in the temperature range up to the Curie point ( $T_C \sim 340$  K). The effect is shown to be caused by two different phenomena: (1) the resonance dc electromotive force related to anisotropic magnetoresistance in the manganite film and (2) pure spin current (spin pumping) generated in the FMR-excited ferromagnet and flowing across the interface with the non-magnetic metal, where it is registered by means of the inverse spin Hall effect. The two phenomena were separated using the angular dependence of the effect, the external magnetic field  $H_0$  being rotated in the film plane. The physical mechanism of the electromotive force caused by anisotropic magnetoresistance in the manganite films, as well as the anisotropic magnetoresistance itself, were found to differ considerably from similar effects in traditional ferromagnetic metals. It was proved experimentally that in the manganite films with in-plane magnetic anisotropy the main role is played by colossal magnetoresistance which provides resistivity variations depending on the angle between the sample magnetization and easy axis. This model is related with the theory accounting for spin fluctuations when approaching  $T_C$ .

The dc voltage corresponding to the spin pumping was found to be considerably lower than that reported previously for other ferromagnet/metal structures. This may be attributed to some peculiarities of the manganite films.

The work was supported by the Russian Foundation for Basic Research (grants 14-02-00165, 14-07-93105, and 14-07-00258).

## Exploring Low Symmetry Effects in Molecular Magnets with EPR

**D. Gatteschi<sup>1</sup>** and **M. Fittipaldi<sup>2</sup>**

<sup>1</sup> Department of Chemistry, University of Florence, Sesto Fiorentino 50019, Italy, dante.gatteschi@unifi.it

<sup>2</sup> Department of Physics, University of Florence, Sesto Fiorentino 50019, Italy, maria.fittipaldi@unifi.it

EPR is a very useful tool to identify and characterize low symmetry effects in magnetic materials, particularly as such features are difficult to monitor otherwise. This is particularly true for Molecular Magnets (MM), which are a class of materials which have been rapidly developing in the last few years [1, 2]. The key feature of MM is that of using molecules rather than metals or oxides to make new types of magnets. The approach has been successful and new classes

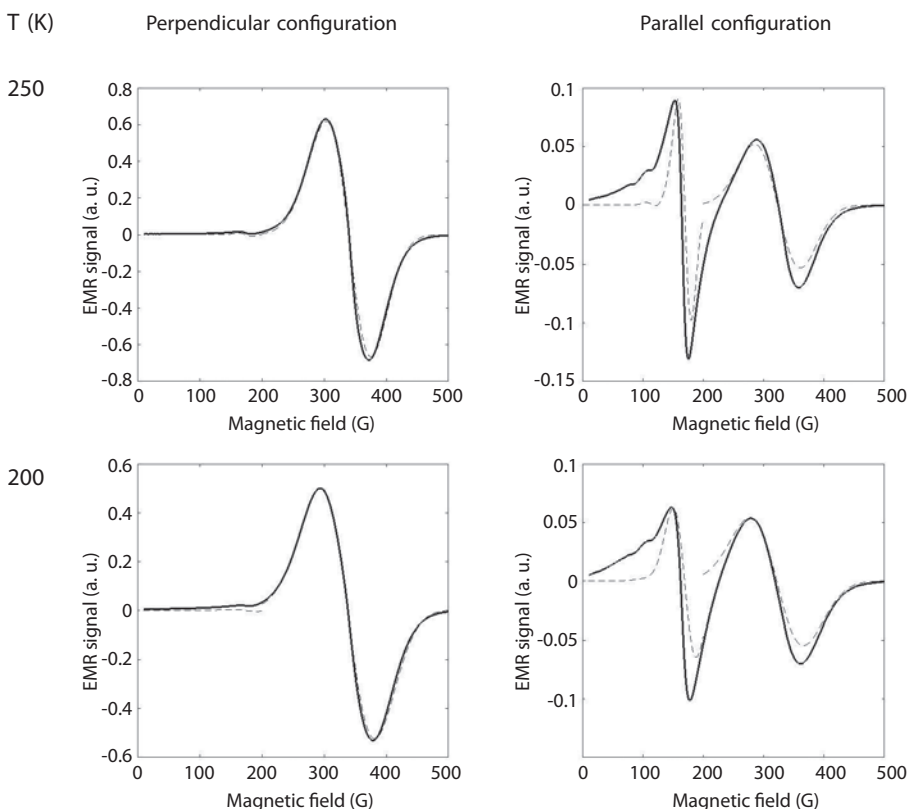


**Fig. 1.** Experimental EPR spectra (solid) of magnetic nanoparticles in ferritins acquired in the parallel and perpendicular configurations at 250 K and 200 K, and simulations (dotted) using an equivalent spin system  $S_{\text{eq}} = 10$ ,  $D_{\text{eq}} = -100$  MHz.

of 0, 1, 2, 3 dimensional magnets were obtained. Here we will consider some examples in detail to demonstrate the potentialities of EPR in this field. These will include, for instance, the effect of vibronic coupling in single molecules, and the properties of finite size clusters including Single Molecule Magnets.

In fact, an expanding field is that of nano objects containing  $10\text{--}10^3$  magnetic bricks. The finite size of the particles can be used to monitor the upsurge of quantum size effects, a field which is being intensively explored [3] also for characterizing biological magnets. In this respect, EPR is a privileged technique to reveal these effects, as shown for systems obtained by inorganic and molecular and biological techniques employing ferritins (Fig. 1). The characterization of large but finite size particles requires different approaches as compared to systems of infinite size and approaches which use mixed quantum-classical techniques are under development.

1. Benelli C., Gatteschi D.: "Introduction to Molecular Magnetism. From Transition Metals to Lanthanides", Wiley VCH, Weinheim, 2015
2. Gatteschi D., Sessoli R., Villain J.: "Molecular Nanomagnets" Oxford University Press, Oxford, 2006
3. Gatteschi D., Fittipaldi M., Sangregorio C., Sorace L.: *Angew. Chem. Int. Ed. Engl.* **51**, 4792–4800 (2012)



## Magnetic Resonance in Strongly Correlated and Quantum Critical Systems

**S. V. Demishev, A. V. Semeno, M. I. Gilmanov, V. V. Glushkov,  
A. N. Samarin, and N. E. Sluchanko**

Prokhorov General Physics Institute of RAS, Moscow 119991, Russian Federation, demis@lt.gpi.ru

In the present talk various aspects of probing of the quantum critical (QC) systems and strongly correlated electron systems (SCES) by electron spin resonance (ESR) technique are reviewed. As an experimental objects dielectrics ( $\text{CuGeO}_3$  doped with magnetic impurities), bad conductors ( $\text{VO}_x$  nanomaterials) and magnetic metals ( $\text{Mn}_{1-x}\text{Fe}_x\text{Si}$ ,  $\text{Eu}_{1-x}\text{M}_x\text{B}_6$  ( $M = \text{Gd}, \text{Ca}$ ) solid solutions) are considered. We aim to show that magnetic resonance studies may provide unique information about quantum criticality, which is inaccessible by other experimental methods. A straightforward use of the ESR technique consists in monitoring of the part of the magnetic system responsible for quantum criticality, which leads to unambiguous experimental determination of magnetization structure. This direction of research was implemented for doped  $\text{CuGeO}_3$  [1] and  $\text{VO}_x$  nanomaterials [2] and resulted in the simple analytical description of the magnetic susceptibility at arbitrary temperature in quantum critical regime [3].

However, most interesting physics consists in analysis of the spin relaxation in SCES and QC systems. In the case of  $\text{CuGeO}_3$  ESR has revealed that in the QC state the anomalous low temperature broadening (ALTB) of the ESR line width  $W(T)$  is characterized by the validity of a universal relation between the line width and  $g$ -factor shift,  $W/\Delta g = 1.99 T k_B / \mu_B$ , which is a consequence of the staggered field in  $S = 1/2$  spin chain systems [4]. Therefore it is possible to consider a scenario, where suppression of long-range magnetic order and QC regime is caused by the change of the local field configuration and appearance of the staggered magnetization. Recent experiments show that this mechanism may be responsible for suppression of the spin-Peierls state in  $\text{CuGeO}_3$  nanorods and onset of a disorder driven QC regime.

The ALT B effects in line width are not confined to the case of antiferromagnetic (AF)  $S = 1/2$  quasi-1D chain systems, but were also observed in 3D SCES like  $\text{VO}_x$  nanomaterials [2],  $\text{MnSi}$  [5, 6] and  $\text{EuB}_6$  [7]. In some cases, ALT B may be attributed to AF correlations in proximity to Neel transition in accordance with the standard theory. Nevertheless, similar peculiarities of the  $W(T)$  occur below magnetic transitions in SCES driven by ferromagnetic (FM) interactions. Recent experiments in  $\text{Eu}_{1-x}\text{M}_x\text{B}_6$  system revealed that suppression of FM magnetic order results in vanishing of the line width ALT B. At the same time, in contrast to AF case, there is no theory accounting observed behavior for FM SCES.

Another fascinating example is the application of the ESR technique to the QC metallic system  $\text{Mn}_{1-x}\text{Fe}_x\text{Si}$ . These solid solutions are characterized by the presence of two QC points  $x^* \sim 0.11$  and  $x_c \sim 0.24$  corresponding to suppression

of long-range chiral magnetic order and chiral spin liquid state respectively [8]. In  $\text{Mn}_{1-x}\text{Fe}_x\text{Si}$  we find anomalous spin relaxation, which is marked by violation of the classical Korringa-type relaxation and scaling behavior [9]. At QC points  $x^*$  and  $x_c$  the non-Fermi-liquid effects in the temperature dependence of the ESR line width, which may be quantitatively described in the theory of Wölfle and Abrahams, are observed. Analysis of experimental data shows that ESR may be considered as a unique tool for visualization of the hidden QC points at the magnetic phase diagram.

In summary, it is possible to mark that, from the general point of view, all studied systems are characterized by the interplay between QC phenomena, nanoscale magnetism and disorder effects, which indicates the directions for the future development of the theory describing ESR in strongly correlated electron systems. This work was supported by Programmes of Russian Academy of Sciences “Electron spin resonance, spin-dependent electronic effects and spin technologies”, “Electron correlations in strongly interacting systems” and by RFBR grant 13-02-00160.

1. Demishev S.V. *et al.*: *J. Magn. Magn. Mat.* **300**, e346 (2006)
2. Demishev S.V. *et al.*: *Phys. Rev. B* **84**, 094426 (2011)
3. Demishev S.V.: *phys. status solidi (b)* **247**, No. 3, 676 (2010)
4. Demishev S.V. *et al.*: *Europhys. Lett.* **63**, 446 (2003)
5. Demishev S.V. *et al.*: *JETP Letters* **93**, 213 (2011)
6. Demishev S.V. *et al.*: *Phys. Rev.* **85**, 045131 (2012)
7. Semeno A.V. *et al.*: *Phys. Rev. B* **79**, 014423 (2009)
8. Demishev S.V. *et al.*: *JETP Letters* **98**, 829 (2013)
9. Demishev S.V. *et al.*: *JETP Letters* **100**, 28 (2014)

---

## SECTION 1

# CHEMICAL AND BIOLOGICAL SYSTEMS

## New Approaches to Study Structure of Biopolymers Using Pulse EPR

**E. Bagryanskaya<sup>1</sup>, A. A. Kuzhelev<sup>1</sup>, O. A. Krumkacheva<sup>2</sup>, M. Fedin<sup>2</sup>,  
O. Yu. Rogozhnikova<sup>1</sup>, D. V. Trukhin<sup>1</sup>, V. M. Tormyshev<sup>1</sup>,  
G. Shevelev<sup>3</sup>, A. A. Lomzov<sup>3</sup>, and D. Pyshnyi<sup>3</sup>**

<sup>1</sup> N. N. Vorozhtsov Novosibirsk Institute of Organic Chemistry, Novosibirsk, Russian Federation, [egbagryanskaya@nioch.nsc.ru](mailto:egbagryanskaya@nioch.nsc.ru)

<sup>2</sup> International Tomography Center SB RAS, Novosibirsk, Russian Federation

<sup>3</sup> Institute of Chemical Biology and Fundamental Medicine SB RAS, Novosibirsk 630090, Russian Federation

Site-directed spin labeling (SDSL) is widely applied for structural studies of biopolymers by pulsed dipolar EPR spectroscopy (PELDOR/DEER and DQC methods). Although significant progress has been achieved in this field, a number of challenges still remain. One of the requirements for the spin labels application is their stability in reducing media. The advantages of new sterically-substituted nitroxide application in biophysics will be demonstrated using our recent results [1–3]. The new spin labels demonstrated clear advantages over 2,2,5,5-tetramethylpyrroline nitroxides with respect to stability and electron spin relaxation rates, which should allow PELDOR distance measurements at liquid nitrogen temperature range [2,3].

Another challenge in pulsed dipolar EPR spectroscopy is a design of spin labels and SDSL strategies for distance measurements in nucleic acids at room/physiological temperature. For this purpose, relaxation properties of trityl radicals represent a significant advantage. Electron spin relaxation of a series of trityl radicals with different substituents was measured using pulse EPR spectroscopy in X- and Q-band at different temperatures. The analysis of these data allows separating the contribution of different mechanisms of electron spin relaxation [4]. We report synthesis and comparative study of series of model DNA duplexes, 5'-spin-labeled with TAMs and nitroxides and have found that the accuracy of distance distributions obtained by DEER strongly depends on the type of radical. Replacement of both nitroxides by TAMs in the same spin-labeled duplex allows narrowing of the distance distributions by a factor of three. Replacement of one nitroxide by TAM leads to a less pronounced narrowing, but at the same time gains sensitivity in DEER experiment due to efficient pumping on narrow EPR line of TAM. Distance distributions in nitroxide/nitroxide pairs are influenced by the structure of linker: the use of a short amine-based linker improves the accuracy by a factor of two. At the same time, negligible dependence on the linker length is found for distribution width in TAM/TAM pairs. Molecular dynamics calculations indicate greater conformational disorder of nitroxide labels compared to TAM ones, thus rationalizing the experimentally observed trends [4].

Room-temperature distance measurement in trityl-labeled immobilized DNA duplexes was performed. The synthesis of optimal trityl-based spin labels, efficient SDSL and immobilization approaches that, working together, allowed to

measure as long distances as ~4.5 nm with high accuracy at room and 37 °C [6]. The peculiarities of different approaches for the immobilization procedure (nucleosil@DMA, trehaloza, sucrose, agaroza, glucose, etc.) and measurements of distances at room temperatures were studied. A novel SDSL approach suitable for long natural RNAs, was proposed [3] and it's applicability to long RNAs structural studies using pulse EPR was shown.

This work is supported by Russian Scientific Fund ((№14-14-00922).

1. Bagryanskaya E.G., Marke S.R.A.: *Chem. Rev.* **114**, 5011– 5056 (2014)
2. Kirilyuk I.I. *et al.*: *J. Org. Chem.* **77**, 8016–8027 (2012)
3. Babaylova E. *et al.*: *Org. Biomol. Chem.* **12**, 3129–3136 (2014)
4. Shevelev G. *et al.*: *J. Phys. Chem.* DOI: 10.1021/acs.jpcc.5b03026 (2015)
5. Kuzhelev A. *et al.*: *J. Phys. Chem.* DOI: 10.1021/acs.jpcc.5b03027 (2015)
6. Shevelev G.Yu. *et al.*: *J. Amer. Chem. Soc.*: **136**, 9874–9877 (2014)
7. Krunkacheva O. *et al.*: *J. Phys. Chem. B.* submitted (2015)

## Spin-Label EPR Study of Peptide-Lipid and Cholesterol-Lipid Interactions in Model Biological Membranes

**S. A. Dzuba**

Voevodsky Institute of Chemical Kinetics and Combustion, Russian Academy of Sciences;  
Novosibirsk State University, Novosibirsk 630090, Russian Federation, dzuba@kinetics.nsc.ru

The number of pathogenic bacterial strains which in its evolution became resistant to the known antibiotics is growing. Therefore, there exists a need to develop new antibiotics to which the resistance of bacteria is weakened or even absent. The promising class of such substances is antimicrobial membrane-active peptides. Trichogin GA IV belongs to the family of naturally occurring peptaibols that display antibiotic properties. Different electron spin echo (ESE) spectroscopic techniques were employed to study a set of spin labelled analogues of trichogin GA IV in model and natural membranes [1]. Pulsed Electron-electron Double Resonance (PELDOR) enabled the elucidation of the peptide conformation; while the ESE envelope modulation (ESEEM) technique was applied to study the insertion of the site specifically spin labeled peptide into the core of the membrane. The latter technique was also used to examine the water accessibility for peptide-attached spin labels at different levels of membrane depth. Measurement of the ESE decays at different temperatures reveals molecular information on the mobility of the transmembrane lipopeptide aggregate. The experimental results are discussed in terms of the antibiotic and toxic activities of trichogin GA IV.

PELDOR is based on pulsed modulation of magnetic dipole-dipolar interaction between spin labels by microwave pulses, most often it is used to study distances in a pair of spin labels. Suggested recently [2] another approach in pulsed EPR employs effects of so-called “instantaneous diffusion” in electron spin echo (ESE) formation. It is also based on pulsed modulation of the magnetic dipole-dipolar interactions between spin labels and can be used to study nanoclusters of spin labels. Nanoclusters were found for spin-labeled analog of cholesterol, 3 $\beta$ -doxyl-5 $\alpha$ -cholestane (cholestane) dissolved at concentrations between 0.1 mol% and 2 mol% in phospholipid bilayers. The observed effects of instantaneous diffusion were explained by assuming that neighboring cholestane molecules are oriented similarly. As conventional CW EPR spectra do not show aggregation of spin labels, cholestane molecules remain spatially diluted. These results evidence that cholestane molecules at low concentrations in biological membranes can interact via large distances of several nanometers, forming spatially diluted microdomains of nearly the same molecular orientation (i.g. stacking self-ordering with intercalated lipid layers). However this long-range orientational self-ordering of cholestane molecules in the bilayer was found to be destroyed in presence of cholesterol [3]. This is because cholesterol molecules contain a hydroxyl group that strongly interacts with lipid heads via formation of hydrogen bonds.

There is accumulating evidence for the compositional heterogeneous structure in the lipid content of the plasma membranes, which are assumed to contain lipid rafts – fluctuating nanoscale assemblies of lipids, cholesterol, peptides and proteins. Lipid rafts are thought to form platforms that function in membrane signaling and trafficking. To explore properties of lipid rafts, ESE spectroscopy of spin labels can be employed as well [3]. The ESE decays recorded at 77 K were found to become faster with increase of cholestane concentration. The cholestane-dependent contribution to ESE decay is remarkably non-exponential; however, the logarithm of this contribution can be rescaled for different cholestane concentrations to a universal function with the rescaling factor approximately proportional to concentration. This result shows that the cholestane-dependent contribution to the ESE decay can be employed to estimate the local (at the nanometer scale of distances) cholestane concentration. Analogous rescaling behavior is also observed for the bilayers with different cholesterol concentrations, with the rescaling factor increasing with increase of the cholesterol concentration. This result evidences that cholestane molecules are distributed heterogeneously in the cholesterol-containing bilayer and form clusters with enhanced cholestane (and probably cholesterol) local concentration. From the obtained data the enhancement factor can be easily derived.

1. Dzuba S.A., Raap J.: *Chem. Biodivers.* **10**, 864–875 (2013)
2. Kardash, M.E., Dzuba, S.A.: *J. Chem. Phys.* **141**, 211101 (2014)
3. Kardash M.E, Isaev N.P, Dzuba S.A.: *J. Phys. Chem. B*, in press (2015). DOI: 10.1021/acs.jpcc.5b03080.

## Magnetic Interactions in Narrow-Line Trityl Biradicals

**M. K. Bowman<sup>1</sup>, H. Chen<sup>1</sup>, N. P. Isaev<sup>2</sup>, R. I. Samoilova<sup>2</sup>,  
A. G. Maryasov<sup>2</sup>, O. Yu. Rogozhnikova<sup>3</sup>, and V. M. Tormyshev<sup>3</sup>**

<sup>1</sup> Department of Chemistry, University of Alabama, Tuscaloosa, Alabama 35487-0336, USA, [mkbowman@ua.edu](mailto:mkbowman@ua.edu)

<sup>2</sup> V. V. Voevodsky Institute of Chemical Kinetics and Combustion, Novosibirsk 630090, Russian Federation, [maryasov@kinetics.nsc.ru](mailto:maryasov@kinetics.nsc.ru)

<sup>3</sup> N. N. Vorozhtsov Novosibirsk Institute of Organic Chemistry, Novosibirsk 630090, Russian Federation, [Torm@nioch.nsc.ru](mailto:Torm@nioch.nsc.ru)

A series of trityl biradicals have been synthesized with short linkers, Fig. 1. These biradicals have substantial exchange interaction with a ( $S = 0$ ) singlet state lying 40 K or about 1 THz above the ( $S = 1$ ) triplet ground state as determined by spin susceptibility measurements and from the Orbach-Aminov spin-lattice relaxation process. ENDOR measurements show a decrease in hyperfine couplings by a factor of 1/2, and have sharp  $^{13}\text{C}$  and  $^1\text{H}$  lines from the  $m_s = 0$  sublevel. The biradicals have a relatively small Zero-Field Splitting,  $D \sim 19$  MHz. This results in a very narrow EPR spectrum that allows coherent excitation of the entire EPR spectrum of the triplet by microwave pulses in frozen solutions for spin dynamics study in triplet ground-state molecules. These synthetic biradicals have EPR properties and dynamics very similar to self-assembled dimers that form in concentrated solutions of trityl radicals but dilute biradical solutions lack the strong spectral diffusion and spin diffusion seen in those concentrated solutions of self-assembled dimers.

Supported by RFBR N0. 14-03-93180 ICCh-a (VMT) and NSF 1416238 (MKB).

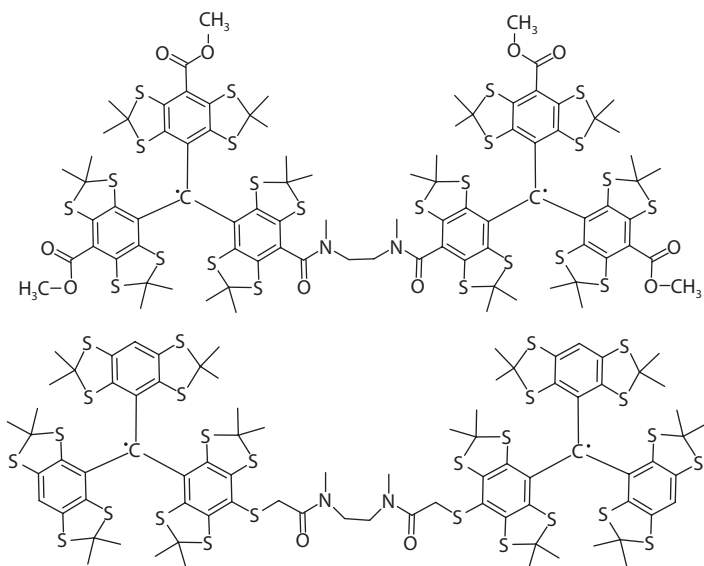


**Fig. 1.** Trityl biradicals composed of asymmetric and symmetric tritylsubunits.



## Effect of Disaccharide Trehalose Glassy Matrix on Charge Recombination in Photosystem I

**A. Semenov<sup>1</sup>, M. Malferrari<sup>2</sup>, A. Savitsky<sup>3</sup>, M. Mamedov<sup>1</sup>,  
K. Möbius<sup>3</sup>, and G. Venturoli<sup>1</sup>**

<sup>1</sup> A. N. Belozersky Institute of Physical-Chemical Biology, Moscow State University

<sup>2</sup> Department of Pharmacy and Biotechnology, University of Bologna, Bologna, Italy

<sup>3</sup> Max Planck Institute for Chemical Energy Conversion, Mülheim (Ruhr), Germany

Flash-induced charge recombination kinetics has been studied in Photosystem I (PS I) complexes from cyanobacterium *Synechocystis* sp. PCC 6803, embedded into trehalose matrices at different hydration levels, obtained by equilibration at relative humidity,  $r$ , between 11% and 63%. High-field EPR studies in the presence of nitroxide spin label demonstrated the structural homogeneity of the dry PS I-trehalose matrix. The W-band EPR spectra of spin-correlated  $P700^+A_1^-$  radical-pair exhibit no difference for PS I in solution and in the dried matrix both at room and cryogenic temperature, implying no alteration of the distance and relative orientation of the cofactors. PS I was stable at room temperature in dried trehalose matrices for several months. The kinetics of the flash-induced charge recombination in PS I-trehalose matrices, measured at comparable hydration, by W-band transient EPR and by absorption flash spectrometry at 810 nm, were similar. The recombination kinetics in hydrated PS I-trehalose glasses and in solution are comparable and mostly reflect the reduction of the photooxidized primary donor, a special chlorophyll pair, P700, from the reduced terminal iron-sulphur clusters. The optically detected  $P700^+$  decay gradually accelerated and became more distributed upon dehydration from  $r = 63\%$  to  $r = 11\%$ . The Maximum Entropy Method analysis of the recombination kinetics showed that upon dehydration the contribution of the slowest kinetic component with an average lifetime  $\tau \sim 130\text{--}250$  ms gradually decreased in parallel with the increase of the fastest component with  $\tau \sim 100\text{--}200$   $\mu\text{s}$ . At  $r < 53\%$ , two additional distributed components appear in the range of 1–30 ms. The effects of dehydration at room temperature mimic those observed upon freezing water-glycerol PS I systems at cryogenic temperatures, suggesting an impairment of PS I protein dynamics in the trehalose glass. Acceleration of the kinetics most likely reflects inhibition of the forward electron transfer to the iron-sulphur centers. At  $r = 11\%$ , as well as at low temperature, the main kinetic component is attributed to the back reaction from the photoreduced phylloquinone acceptor  $A_1^-$ .

This work was supported by Grants from the RFBR (13-04-40299, 15-04-04252 and 15-43-02538).

## Electron Transfer between Aromatic Amino Acids and Histidine Radicals

**A. Yurkovskaya and O. Morozova**

International Tomography Center, Novosibirsk 630090, Russian Federation,  
yurk@tomo.nsc.ru

An alternative source of experimental information on transient radicals that are too ephemeral for EPR detection is nuclear hyperpolarization termed CIDNP (Chemically Induced Dynamic Nuclear Polarization), which manifests itself as anomalous spectral intensity pattern in the NMR spectra of chemically reacting systems. This type of hyperpolarization is particularly useful in the study of the reactions of short-lived and optically silent radicals of amino acids, such as histidyl<sup>1</sup>. In the oxidation process of peptides or proteins histidine may either act as a mediator in the transfer of an unpaired electron to the final acceptor or may participate directly. Utilizing the kinetics of hyperpolarization obtained with microsecond time resolution we were able to perform measurements of the rate constant of intramolecular electron transfer in the oxidized peptides Tyr-His, His-Tyr, His-Trp, Trp-His and of intermolecular electron transfer from tyrosine and tryptophan to the histidyl radical for free amino acids and their N-acetyl derivatives. Histidine is a particularly important protein residue because its imidazole side chain is frequently involved in catalysis and in ligation of essential metal ions.

While the acid-base properties of histidine residues in peptides and in proteins have been extensively studied in solution, little is known about radicals produced by one-electron oxidation of His. Usually, the reactivity of histidine toward the endogenous oxidation is much lower than that of tryptophan and tyrosine. We found that 3,3',4,4'-benzophenone tetracarboxylic acid can be used to form radicals with high efficiency because its photo-excited triplet state is quenched with comparable efficiencies by tryptophan, tyrosine, and histidine in neutral to basic aqueous solution<sup>2</sup>. This opens the possibility to study the reaction of electron transfer from tyrosine and tryptophan to a transient histidyl radical by time-resolved CIDNP. The strong pH dependence of the reaction rate was explained in terms of the acidity constants of the peptides or free amino acids. The presence of a positive charge at the amino group of a tyrosine residue decreases the reaction rate constant by an order of magnitude. Also, the protonation state of the diamagnetic product is important for the reaction of the histidyl radical and tyrosine: when the product includes imidazole with a positive charge, the observed reaction rate constant is negligibly low in the pH range studied. The high NMR signal enhancement, the good time resolution and the possibility to work at biocompatible conditions make CIDNP the method of choice for studying radical-related processes in biosystems.

This work was supported by RSF (project 15-13-20035)

1. Morozova O.B., Yurkovskaya A.V.: *Angew. Chem. Int. Edit.* **49**, 7996–7999 (2010)
2. Saprygina N.N., Morozova O.B., Grampp G., Yurkovskaya A.V.: *J. Phys. Chem. A* **118**, 339–349 (2014)

## Application of ELDOR Detected NMR to Study Hyperfine Interaction in Cu(II)-bis(oxamidato) Complexes

**R. B. Zaripov<sup>1</sup>, E. L. Vavilova<sup>1</sup>, V. K. Voronkova<sup>1</sup>,  
K. M. Salikhov<sup>1</sup>, A. Aliabadi<sup>2</sup>, A. Petr<sup>2</sup>, V. Kataev<sup>1,2</sup>, B. Büchner<sup>2</sup>,  
M. A. Abdulmalic<sup>3</sup>, and T. Ruffer<sup>3</sup>**

<sup>1</sup> Zavoisky Physical-Technical Institute, Russian Academy of Sciences, Kazan 420029, Russian Federation, zaripovruslan@gmail.com

<sup>2</sup> Institute of Solid State Research IFW Dresden, Dresden D-01171, Germany

<sup>3</sup> Technical University of Chemnitz, Chemnitz D-09107, Germany

In this work we present a study of two complexes by the pulse ELDOR detected NMR (ED NMR) technique, named as complex P1 and complex P2. The difference between two complexes is in the ligands R. The P1 and P2 complexes contained ethanol and propyl ligands respectively (see Fig. 1) [1].

It is well known that ED NMR technique is useful at high microwave frequencies [2, 3]. We show that pulse ELDOR detected NMR at the Q-band is a very promising method to study such kind of systems. It has enabled us to accurately determine the hyperfine interaction parameters of individual nitrogen ligands.

Moreover, we provide more detailed theoretical consideration for the model system  $S = 1/2$  and  $I = 1$ .

This work was supported by the Deutsche Forschungsgemeinschaft through project FOR 1154 "Towards Molecular Spintronics", by the Russian leading scientific school grant NSh-4653.2014.2, by the Russian Foundation for Basic Research through project RFBR 14-02-01194, and by the President Grant for Government Support of Young Russian Scientists MK-4957.2014.2.

1. Abdulmalic M.A. *et al.*: Dalton Trans. **44**, 8062 (2015)
2. Kaminker I. *et al.*: J. Magn. Reson. **240**, 77 (2014)
3. Nalepa A. *et al.*: J. Magn. Reson. **242**, 203 (2014)

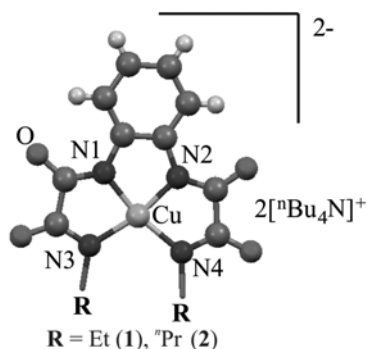


Fig. 1. Structure of the samples.

## Low Field Photo CIDNP in Linked Systems

**P. A. Purtoy, N. E. Polyakov, I. M. Magin, A. I. Kruppa,  
and T. V. Leshina**

Institute of Chemical Kinetics and Combustion, Novosibirsk 630090, Russian Federation

Electron transfer (ET) is the most widespread and universal chemical process, this is why ET attracts the permanent interest of researchers. This interest extends in particular on the photoinduced electron transfer (PET). PET processes in linked systems, dyads and triads, are often used as a model of enzyme-substrate interaction, as well as individual stages of photosynthesis. The main attention in such studies is paid to the detection and the role of the short-lived particles with partial and full charge transfer, i.e., namely exciplexes and radical ion pairs (RIP). One of the ways to study the connection between exciplex and RIP is to analyze the effect of an external magnetic field (MFE) on time-resolved pulse photolysis or fluorescence. Another promising approach has been applied in the study of photoinduced processes involving partial (exciplex) and full (bi-radical ion) charge transfer in the dyad NPX-PYR, containing a widely studied anti-inflammatory drug naproxen and N-methyl pyrrolidine using CIDNP and time-resolved fluorescence techniques [1]. The reaction mechanism, in which the formation of the exciplex precedes the stage of complete charge transfer and biradical ion is in a rapid dynamic equilibrium with the exciplex has been established. In this regard, it seems interesting to us to study the CIDNP effects in NPX-PYR dyads in low magnetic fields. Since the chemical polarization is a differential effect, unlike the integral MFE, one would expect a significant diversity in the CIDNP field dependences in the media of different polarity due to the change in the ratio exciplex/biradical ion, as well as in the Coulomb

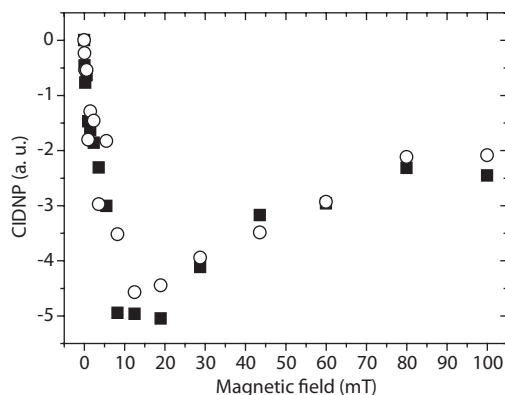


**Fig. 1.** CIDNP field dependence (low field region) for N-CH<sub>3</sub> protons measured after laser irradiation (308 nm) of 2 mM solutions of R,S- (■) and S,S-NPX-PYR (○) dyads in CD<sub>3</sub>CN ( $\epsilon = 36.8$ ).

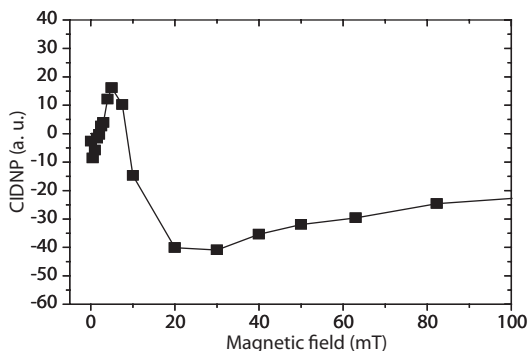


**Fig. 2.** CIDNP field dependence for N-CH<sub>3</sub> protons measured after laser irradiation (308 nm) of 2 mM solution *R,S*-NPX-PYR dyad in CD<sub>3</sub>CN/benzene mixture at  $\epsilon = 10$ .

interaction. Besides that, the lifetimes of states with partial and full charge transfer in the dyad naproxen – pyrrolidine are in the nanosecond range, this let us expect the impact of the rapid exchange between the exciplex and biradical ion on the spin evolution.

Low field photo CIDNP (chemical induced dynamics nuclear polarization) for these processes in dyads including drug – (S) and (R) naproxen and (S) N-methyl pyrrolidine in solutions with strong and weak polarity has been measured. A dramatic influence of solvent polarity on the field dependences of the N-methyl pyrrolidine H<sup>1</sup> CIDNP effects has been found. The field dependences of both *R,S*- and *S,S*-dyads in polar medium are the curves with a single extremum in the area of the S-T<sub>+</sub> terms intersection (Fig. 1). Meanwhile, the CIDNP field dependences of the same protons measured in low polar medium present curves with several extrema (Fig. 2). The shapes of experimental CIDNP field dependences with two extrema are described using Green function approach for the calculations of CIDNP effects in the system without electron exchange interaction. The report discusses possible causes of the difference between CIDNP field dependences detected in the solution of low polarity with the strong Coulomb interaction and in a polar solvent.

The work was supported by the Russian Foundation for Fundamental Research grant 14-03-00192.

1. Magin I.M., Polyakov N.E., Khramtsova E.A., Kruppa A.I., Tsentlovich Yu.P., Leshina T.V., Miranda M.A., Nuin E., Marin M.L.: Dyad. Chem. Phys. Lett. **516**, 51–55 (2011)

## Lesion Impact on Flipping-Unflipping Equilibrium of DNA Duplexes: an NMR Study

N. A. Kuznetsov<sup>1,3</sup>, A. S. Kiryutin<sup>2,3</sup>, M. S. Panov<sup>2,3</sup>, A. V. Yurkovskaya<sup>2,3</sup>,  
and O. S. Fedorova<sup>1</sup>

<sup>1</sup> Institute of Chemical Biology and Fundamental Medicine, Novosibirsk 630090, Russian Federation

<sup>2</sup> International Tomography Center SB RAS, Novosibirsk 630090, Russian Federation,  
mike.p@tomo.nsc.ru

<sup>3</sup> Department of Natural Sciences, Novosibirsk State University, Novosibirsk 630090,  
Russian Federation

DNA molecules in living cells are known to be continuously exposed to exogenous and endogenous factors, which may lead to chemical changes in the DNA structure. Until now, it is an open question, how the lesion sites are recognized by enzymatic repair systems. One hypothesis is that the chemically modified nitrogenous bases form less stable hydrogen bonds than their native analogues, shifts the equilibrium between the flipped and unflipped state of the DNA double helix for such sites to the open form. In turn, elongation of the time spent in the open state may be a signal for enzymatic repair system to start on this particular segment of DNA.

The aim of this study was to investigate the balance between flipped and unflipped forms in the DNA duplex by modern NMR methods. In present study four tridecamer DNA duplexes were investigated, for which the only difference was a nitrogenous base in the centre (seventh position) while maintaining the entire nucleotide sequence chains unchanged. For comparison, it was studied by a DNA duplex with a canonical pair of nitrogenous bases (A), two duplexes containing hypoxanthine (Hx) and 1-N6-ethenoadenine ( $\epsilon$ A) instead of an adenine, and the fourth does not contain any nitrogenous base complementary to T in seventh position (THF). The polarization transfer from water protons to the imino protons in duplex unflipped form was studied, the speed of which depends on the rate of proton exchange between water and imino protons in the open form DNA and increases with the addition of ammonia. As a result, site-specific data about flipping-unflipping equilibrium constants were obtained, which reflects the dynamics of hydrogen bonds breaking between the nitrogen bases. Proton exchange rates were found to be the slowest for the native duplex and increases in the row  $A < Hx < \epsilon A < THF$ . In addition, there is a rate increase of flipping GC-pairs neighbouring to the lesion site, which indicates a weakening of the stacking interaction of bases along the DNA helix. These results allow us to say that DNA double helix stability indeed depends on chemical modifications of nitrogenous bases.

## A Connection Between Electron Transfer and Spin Exchange

**G. I. Likhtenshtein**

Department of Chemistry, Ben-Gurion University, Beer-Sheva 84105, Israel,  
gertz@bgu.ac.il

Electron transfer (ET) is one of the most ubiquitous and fundamental phenomena in chemistry, physics and biology. The spin exchange (SE) interaction integral ( $J$ ) is the key quantity for a microscopic description and understanding of molecular magnetism and an instrument for study structure of compounds and mechanisms of physical and chemical processes. The SciFinder (Chemical Abstracts Service) provides access to more than 240000 and 36000 references for ET and SE respectively. In spite of importance of problem connection between ET and SE only limited studies have been made up in this area to the present.

A semi-empirical approach for the quantitative estimation of the effect of intermediated and bridging the group on ET was developed in [1–3]. The basic idea underlying this approach is an analogy between superexchange in electron transfer and such electron exchange processes as spin-exchange (SE) and triplet-triplet energy transfer (TTET). Electronic coupling term (resonance integral) in ET ( $V_{ET}^2$ ) and exchange integrals,  $J_{SE}$  and  $J_{TT}$ , are related to the overlap integral ( $S_i$ ), which quantitatively characterizes the degree of overlap of orbitals involved in these processes. Thus

$$V_{ET}^2, J_{SE}, J_{TT} \propto S_n^i \propto \exp(-\beta_i R_i) \quad (1)$$

where  $R_i$  is the distance between the interacting centers and  $\beta_i$  is a coefficient which characterizes the degree of the integral decay. In the first approximation  $n = 2$  for the ET and SE processes with the overlap of two orbitals and  $n = 4$  for the TT process in which four orbitals overlap (of ground and triplet states of the donor and ground and triplet states of the acceptor). Therefore we can use Eq. 1 with  $\beta_{ET} = \beta_{SE} = 0.5\beta_{TT}$  for estimation of contribution of the coupling term in electron transfer rate. According to experiments, for systems in which the centers are separated by a “non-conductive” medium (molecules or groups with saturated chemical bond) [2]  $\beta_{TT}$  equal  $2.6 \text{ \AA}^{-1}$  and consequently  $\beta_{ET} = \beta_{SE} = 1.3 \text{ \AA}^{-1}$ . Closs *et al.* analyzing experimental data on ET and TT in a donor acceptor system also came to conclusion that  $\beta_{SE} = \beta_{ET} = 0.5\beta_{TT}$ .

An examination of the empirical data on the exchange integral values ( $J_{ET}$ ) for the spin-spin interactions in systems with known structure, that is, biradicals, transition metal complexes with paramagnetic ligands and monocrystals of nitroxide radicals, allows the value of the attenuation parameter  $\gamma_X$  for the exchange interaction through a given group  $X$  to be estimated. By our definition, the attenuation factor  $\gamma_X$  is

$$\gamma_X = J_{RYPZP} / J_{RXXZP} \quad (2)$$

where  $R$  is a nitroxide or organic radical,  $P$  is a paramagnetic complex or radical and  $X$ ,  $Y$ , and  $Z$  are chemical groups in the bridge between  $R$  and  $P$ . Exchange integral a bridged donor acceptor pair can be estimated by Eq. 3.

$$J_{SE} = J_0 \rho_D \rho_A \prod_i \gamma_i^{-1} \quad (3)$$

where  $J_0$  is the exchange integral at Van der Waals contact,  $\rho_{S_i}^2$  is the spin density in donor and acceptor at contact in non-bridged DA pair, and  $\gamma_i$  is the attenuation factor.

$$k_{ET} = k_0 \rho_D \rho_A \prod_i \gamma_i^{-1} \quad (4)$$

where  $k_0$  is the rate constant of ET in in non-bridged DA pair, can be used for calculation rate constants of electron transfer.

In given presentation, it is shown that the application of aforementioned semi-empirical approach to experimental data in systems, in which  $k_{ET}$  and  $J_{SE}$  were measured, demonstrated reasonable agreement between calculated and experimental quantities in a number biological and model systems.

1. Kotelnikov A.I., Fogel V.R., Likhtenshtein G.I., Postnikova G.B.: Mol. Biol. (Moscow) **15**, 281–289 (1981)
2. Likhtenshtein G.I.: J. Photochem Photobiol A Chem., 79–92 (1996)
3. Likhtenshtein G.I.: Solar Energy Conversion. Chemical Aspects WILEY-VCH, 2012.



## Spin Effects in Chiral Linked Systems

**T. V. Leshina, E. A. Khramtsova, D. V. Sosnovsky, and P. A. Purtov**

Institute of Chemical Kinetics and Combustion, Novosibirsk 630090, Russian Federation

Stereoisomerism (optical isomerism), as well as it is known, plays a significant role in the nature and human life. Indeed, the majority of biological molecules are optically active agents (amino acids are laevorotatory, on the contrary – carbohydrates are dextrorotatory). It is known that 60% of produced pharmacy contains optically active (chiral) compounds. Moreover, the only one of enantiomers is a drug in 90% of these cases. Among them the non-steroidal anti-inflammatory drugs (NSAIDs), which demonstrate a noticeable difference in the healing qualities of chiral isomers, are widely studied. In case of naproxen (NPX, S or R-6-methoxy- $\alpha$ -methyl-2-naphthaleneacetic acid), that is one of the successfully used NSAIDs, the only (S)-isomer has a therapeutic activity. In discussing the nature of the therapeutic effects of chirality on drug activity, it is usually taken into

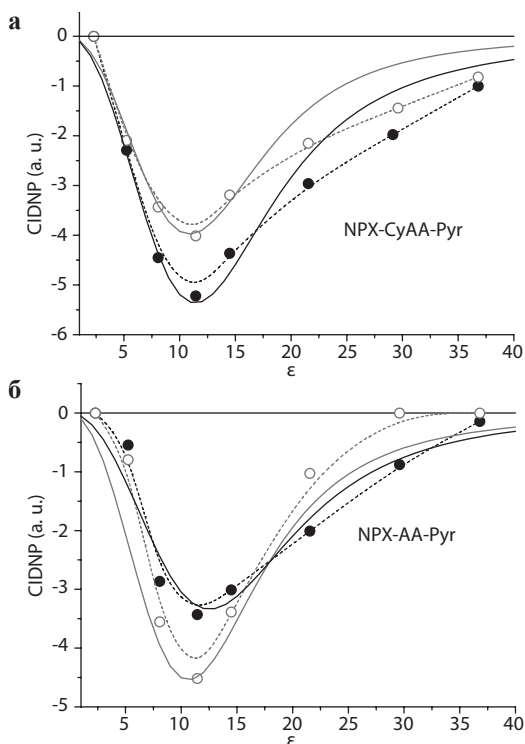


**Fig. 1.** Dependences on solvent polarity of CIDNP effects for (R,S)- (●) and (S,S)- (○) configurations of the dyad NPX-CyAA-Pyr (a) and NPX-AA-Pyr (b). Solid lines are calculated.

account that chiral drug in enzyme or receptor active sites always interacts with another chiral particle. In living systems it is the amino acid residues located in the active sites. The chemical nature of the chiral centers impact on reactivity still remains unclear for today. Because there is a process of the two chiral centers interaction which differs only in the spatial arrangement of electron clouds at the relevant bonds, it seems to us that the spin effects in donor-acceptor systems that includes charge transfer will be sensitive to the chirality manifestation (for example through electronic exchange interaction). In this work we have tried to explore the nature of chiral effects in terms of the spin chemistry methods in specially selected systems, modeling the naproxen binding with chiral electron donors. Photoinduced processes in the linked systems – dyads and triads are frequently used for the simulation of binding between the drug molecules and the active sites of receptors and various transport proteins. Using photoinduced processes to model these interactions is based on an opinion that the donor-acceptor properties of such particles would not be highly dependent on their generation pathway: photoirradiation or thermal electron transfer.

It can be expected that the analysis of the CIDNP effects in different polarity environments will set the main factors responsible for the impact of the chiral centers in diastereomers on the charge transfer. Indeed, the joint analysis of both fluorescence quenching and the  $H^1$  CIDNP effects in two dyads of (S)- and (R)-NPX-Pyr with different bridges between the donor and acceptor have demonstrated the stereoselectivity of the rates of partial and complete charge transfer processes. To describe the dependence of CIDNP on solvent permittivity theoretically we used the method of calculation based on the solution of the master-equation of spin chemistry using Liouville equation. The experimental and calculated CIDNP dependences of two dyads (R,S)- and (S,S)-configurations on the solvent polarity are presented in the figure. The curves show a satisfactory agreement between theory and experiment. The area of the greatest discrepancy relates to the strong polarity. There are several reasons for this. Firstly, the theory has been developed for the motion of the paramagnetic centers of dyads in the Coulomb field. Meanwhile, it is known that in highly polar media charged particles act as neutral. The second reason is a change in the relationship of back electron transfer constants from the singlet and triplet state of biradical-ion:  $k_S$  and  $k_T$  values, as a function of the polarity. These changes are not considered in the calculations. Thus, the analysis of CIDNP data allows to trace the states with partial (exciplex) and full electron transfer (biradical-ion) involved in the excitation quenching (R,S)- and (S,S)-configuration of both NPX-Pyr dyads. While the exciplex is in rapid dynamic equilibrium with the biradical-ion, it influence both the form of the CIDNP dependence on the solvent polarity and the field dependence of the CIDNP in weak magnetic fields. In the latter case (weak magnetic fields), the rapid exchange between states with partial and complete charge transfer effects on the spin evolution through the loss of spin correlations in the biradical-ion.

## Paramagnetic Centers Created under Mechano-Chemical Treatment of Mixed Molybdenum-Vanadium Oxides

I. V. Kolbanev, E. N. Degtyarev, M. V. Sivak, A. N. Streletsky, and A. I. Kokorin

N. Semenov Institute of Chemical Physics RAS, Moscow 119991, Russian Federation, alex-kokorin@yandex.ru

The mechanochemical activation (MCA) of oxides was carried out using the Aronov vibratory mill (frequency: 50 Hz, amplitude: 5 mm) fractional mode during 30 s with the interval of 5–10 min afterwards. Before the experiment, powders (powder mass ~15 g, ball mass ~270 g) were charged into the drum, which was purged with argon. Thus, the mechanochemical treatment of powders was realized in the inert media. The degree of MCA was characterized by the value of dose  $D$  of the mechanical treatment which was calculated by the Eq.:  $D = J_g \cdot t$ , where  $J_g$  (W/g) is the specific power intensity of activator,  $t$  is the duration of machining [1].  $J_g$  was equal to 8 W/g). Individual:  $V_2O_5$ ,  $MoO_3$ , and mixed oxides  $xV_2O_5:(1-x)MoO_3$  were investigated by several physical methods including EPR.

EPR spectra were recorded on X-band Bruker EMX-8 spectrometer at 77 & 298 K, and spin-Hamiltonian parameters were calculated as described in [2].

In the paper, our recent results obtained for mixed Mo:V oxides prepared by the mechano-chemical method will be analyzed as a function of the oxide composition, time of mechanical treatment, high temperature heating, etc. Changes in EPR spectra, morphology, conductivity and some other features of such materials will be discussed.

This work was partially supported by the RFBR project No. 14-03-90020-a.

1. Streletskii A.N.: Proc. 2nd Int. Conf. on Structural Applications of Mechanical Alloying. Ed. deBarbadillo J.J. *et al.*, p. 51, 1993.
2. Sviridova T.V. *et al.*: Russian J. Chem. Phys. B **9**, no. 1, 22 (2015)

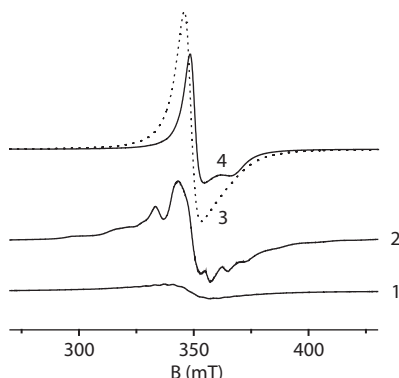


**Fig. 1.** EPR spectra at 77 K (normalized to equal weight of samples) of mixed oxides  $3V_2O_5:1MoO_3$  initial (1), after mechanical treatment (2) and after heating at  $600^\circ\text{C}$  (3). 4 is  $1V_2O_5:3MoO_3$  analogous to (3). (3) and (4) were recorded at five-fold smaller RG than (1) and (2).

## Electron Spin Relaxation of Nitroxide Spin Labels in the Trehalose Glassy Matrix at Room Temperature

R. K. Strizhakov<sup>1</sup>, A. A. Kuzhelev<sup>1,2</sup>, O. A. Krumkacheva<sup>2,3</sup>,  
G. Y. Shevelev<sup>4</sup>, I. A. Kirilyuk<sup>1,2</sup>, M. V. Fedin<sup>2,3</sup>, and E. G. Bagryanskaya<sup>1,2</sup>

<sup>1</sup> Novosibirsk Institute of Organic Chemistry, Novosibirsk 630090, Russian Federation

<sup>2</sup> Novosibirsk State University, Novosibirsk 630090, Russian Federation

<sup>3</sup> International Tomography Center, Novosibirsk 630090, Russian Federation

<sup>4</sup> Institute of Chemical Biology and Fundamental Medicine, Novosibirsk 630090, Russian Federation  
Rodion.Strizhakov@tomo.nsc.ru

Nitroxide spin labels are extensively used in studies of structure of biomolecules by pulse electron double resonance (PELDOR) spectroscopy. The range of distances available for PELDOR measurements depends on the values of phase memory time ( $T_m$ ). As a rule, PELDOR experiments with nitroxide spin labels are carried out in frozen solutions at low temperatures 50–80 K in order to obtain long enough  $T_m$  values.

Recently, in order to perform PELDOR measurements at room temperature, the immobilization of the biomolecules in the trehalose glassy matrix combined with spirocyclohexane-substituted nitroxide spin label has been proposed. It prevented motional averaging of anisotropic dipolar interaction between spin labels and suppressed the influence of motional averaging of  $g$ - and  $A$ -tensors on room-temperature  $T_m$  values.

In this study we investigated the electron spin relaxation properties of nitroxide spin labels with diverse structure immobilized by trehalose glassy matrix at 300 K. The effects of nitroxide structure on electron spin relaxation properties were analyzed. We found that the replacement of the gem-methyl groups with spirocyclohexyl groups and rigidity of nitroxide ring have the most significant effect on  $T_m$  values at room temperature in trehalose.

The financial support of the Russian Science Foundation (No. 14-14-00922).

1. Meyer V., Swanson M., Eaton G. *et al.*: Biophys. J. **108**, 1213 (2015)

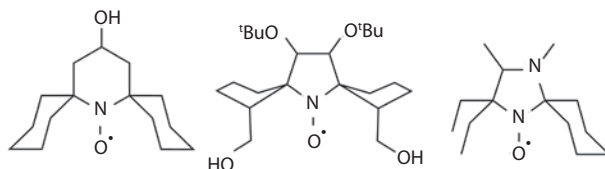


Fig. 1. Several investigated nitroxides.

## The Study of Interaction of Disaccharides with Lipid Bilayer Using Pulsed Electron Paramagnetic Resonance

**K. B. Konov**

Zavoisky Physical-Technical Institute, Russian Academy of Sciences, Kazan 420029,  
Russian Federation, kostyakonov@gmail.com

Disaccharides, mainly sucrose and trehalose, are known for their cryoprotective activity. These sugars can stabilize membrane under unfavorable conditions of low temperature and low humidity. The action of disaccharides could be explained by specific interaction with lipid bilayer or by vitrification of solvating shell of the cell membrane.

Electron spin echo envelope modulation (ESEEM) technique was applied to investigate local concentration of deuterated sucrose and trehalose molecules near spin label attached to lipid polar group. ESEEM is capable to probe weak magnetic interaction between electron spin (nitroxide spin label) and nuclear spin (deuterium atoms in disaccharide molecules). This interaction lead to modulation of the electron spin echo amplitude. The depth of modulation depends on

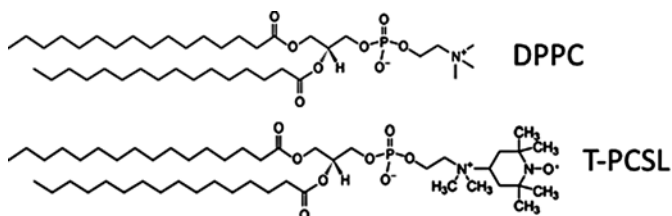


Fig. 1.

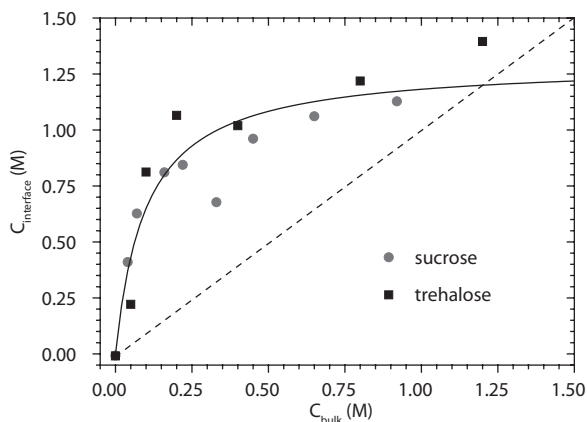


Fig. 2.

distance between electron and nuclear spin. In the case of disordered samples ESEEM can provide information about local concentration of deuterated molecules near nitroxide spin label.

The samples were prepared using 1,2-dipalmitoyl-*sn*-glycero-3-phosphocholine (DPPC) and spin labeled lipid 1,2-dipalmitoyl-*sn*-glycero-3-phospho(TEMPO) choline (T-PCSL) hydrated with aqueous disaccharide solution. The obtained data show preferable accumulation of disaccharides molecules near lipid bilayer surface according to Langmuir model of monolayer adsorption. This result supports the hypothesis of direct interaction between disaccharides molecules and lipid bilayer. In addition, evidences were obtained that membrane solvation shell in both sucrose and trehalose solutions is in glassy state.

1. Konov K.B., Isaev N.P., Dzuba S.A.: Appl. Magn. Res. **45**, 1117–1126 (2014)
2. Konov K.B., Isaev N.P., Dzuba S.A., J. Phys. Chem. B **118** (43), 12478–12485 (2014)

## **Kinetics and Mechanism of the Reversible Photoinduced Oxidation of Purine Nucleotides in Aqueous Solutions: Time-Resolved CIDNP and Laser Flash Photolysis Study**

**N. N. Fishman<sup>1</sup>, O. B. Morozova<sup>1</sup>, M. S. Panov<sup>1,2</sup>, G. Grampp<sup>3</sup>,  
and A. V. Yurkovskaya<sup>1,2</sup>**

<sup>1</sup> International Tomography Center, Novosibirsk 630090, Russian Federation

<sup>2</sup> Novosibirsk State University, Novosibirsk 630090, Russian Federation

<sup>3</sup> Institute of Physical and Theoretical Chemistry, Graz University of Technology, Graz 8010, Austria,  
n\_s@tomo.nsc.ru

Free radicals, resulting from electron transfer, are often observed in living biological systems to give rise to many important, functional processes. Nucleic acids and their building blocks are involved in the pathological damage of DNA due to electron removal from DNA bases. Ionizing radiation, photoionization, photosensitized oxidation by endogenous and exogenous chromophores such as flavins, porphyrins, benzophenones, results in the formation of short-lived radicals of easily oxidized nucleotides. This makes the characterization of the nucleotides radicals and the study of their reactions extremely important. In order to study the chemical reactivity of two purine nucleotides, adenosine-5'-monophosphate (AMP) and guanosine-5'-monophosphate (GMP), towards 3,3',4,4'-benzophenone tetracarboxylic acid (TCBP) in the triplet-excited state in aqueous solutions of different pH at room temperature and to provide further information on the acid-base properties of radical intermediates observed in the photo-oxidation reactions of purines in aqueous solution, we have used two techniques, namely the Time-Resolved laser flash photolysis (LFP) and the Time-Resolved Chemically Induced Dynamic Nuclear Polarization (CIDNP). The pH dependence of the observed quenching rate constant was measured by LFP and explained in terms of reactants pKa values. As a result, the quenching rate constants for each pair of reactants were determined by simulating the pH dependence of the quenching rate constant observed. A complimentary study on the pH dependence of the geminate CIDNP intensity by time-resolved CIDNP enabled us to get information on transient radical intermediates and to establish detailed mechanisms for the reactions between the triplet TCBP and GMP or AMP.

This work was supported by the program of RFBR (Projects No. 14-03-31563, No. 14-03-00453).

---



---

## SECTION 2

STRONGLY CORRELATED ELECTRON SYSTEMS.  
MAGNETIC RESONANCE INSTRUMENTATION

## Exotic Spin Phases in the Low-Dimensional Quantum Magnet $\text{LiCuSbO}_4$ as Seen by High-Field NMR and ESR Spectroscopies

**V. Kataev<sup>1,2</sup>, H.-J. Grafe<sup>1</sup>, M. Iakovleva<sup>2</sup>, E. Vavilova<sup>2</sup>,  
A. Alfonsov<sup>1</sup>, H. Nojiri<sup>3</sup>, M.-I. Sturza<sup>1</sup>, S. Wurmehl<sup>1</sup>,  
S.-L. Drechsler<sup>1</sup>, and B. Büchner<sup>1</sup>**

<sup>1</sup> Leibniz Institute for Solid State and Materials Research IFW, Dresden D-01069, Germany

<sup>2</sup> Zavoisky Physical-Technical Institute, Russian Academy of Sciences, Kazan 420029,  
Russian Federation

<sup>3</sup> Institute of Materials Research, Tohoku University, Sendai 980-8577, Japan

Quantum spin-1/2 networks in reduced spatial dimensions are predicted to exhibit a plethora of novel ground states beyond classical ferro- or antiferromagnetic phases. Quest for experimental realizations of such theoretical models is majorly focused on complex transition metal (TM) oxides where magnetic coupling between the spins of the TM ions can be confined to one or two spatial directions. In this talk, we will present our recent results of high-field NMR and sub-THz ESR studies of the quantum magnet  $\text{LiCuSbO}_4$  (LCSO). In this material  $\text{Cu}^{2+}$  ions ( $S = 1/2$ ) are exchange-coupled along the crystallographic  $a$ -axis and form well-isolated one-dimensional Heisenberg antiferromagnetic spin chains. Absence of a long-range magnetic order down to sub-Kelvin temperatures is suggestive of the realization of a quantum spin liquid state. Our NMR and ESR measurements in strong magnetic fields up to 16 Tesla reveal clear indications for the occurrence of an exotic field-induced nematic quadrupolar phase which has been long sought in different materials. We will discuss a relationship of our experimental findings with recent theories of low-dimensional quantum spin magnets.

# Magnetic Properties of 4f- and 5d-Metal Complexes with Redox-Active Ligands: the High-Level *ab initio* Calculations with Non-Perturbative Account of Spin-Orbit Coupling

**N. Gritsan<sup>1,2</sup>, E. Suturina<sup>2</sup>, and A. Dmitriev<sup>1,2</sup>**

<sup>1</sup> Institute of Chemical Kinetic and Combustion, Novosibirsk 630090, Russian Federation, [grisan@kinetics.nsc.ru](mailto:grisan@kinetics.nsc.ru)

<sup>2</sup> Physics Department, Novosibirsk State University, Novosibirsk 630090, Russian Federation

Molecular magnetic materials, especially single molecule and single ion magnets, are of high interest in the development of new advanced functional materials [1]. Analysis of the experimental magnetic data for molecular materials is a challenging task. In recent years, the quantum chemistry is increasingly being used to predict the electronic structure of the individual paramagnetic centers as well as the interactions between them. The most difficult task is to correctly predict the properties of 5d- and 4f-metal complexes exhibiting fundamentally important relativistic effects.

In this project, the explicitly correlated CASSCF and NEVPT2 approaches with non-perturbative account of spin-orbit coupling have been applied to calculate the electronic structure and low-energy spectra of the paramagnetic complexes. Magnetic properties were calculated using the CASSCF/SO-RASSI/SINGLE-ANISO procedure [2].

The report will present and discuss the results of calculations for several types of complexes, namely, rhenium complex with non-innocent redox-active dioxolene ligand [3] as well as samarium, europium and ytterbium complexes with redox-active thiadimidate-type ligand. All these magnetically active materials have been recently synthesized and characterized by XRD and magnetic susceptibility measurements in a wide temperature range. In some cases, the EPR or UV-vis spectra have been also recorded.

The work was supported in part by Russian Foundation for Basic Research (grant 15-03-03242).

1. Benelli C., Gatteschi D.: Introduction to Molecular Magnetism. From Transition Metals to Lanthanides. Weinheim: Wiley-VCH 2015.
2. Chibotaru L.F., Ungur L.: J. Chem. Phys. **137**, 064112 (2012)
3. Abramov P.A., Gritsan N.P., Suturina E.A. *et al.*: Inorg. Chem. DOI: 10.1021/acs.inorgchem.5b00407 (2015)

## Excitonic Magnetism in Van Vleck-Type Mott Insulators

**G. Khaliullin**

Max Planck Institute for Solid State Research, Stuttgart 70569, Germany

In Mott insulators with the  $t_{2g}^4$  electronic configuration such as of Re, Ru, Os, and Ir ions, spin-orbit coupling dictates a Van Vleck-type ground state, and the magnetic response is governed by gapped singlet-triplet excitations. The exchange interactions as well as crystal fields may close the spin gap, resulting in a Bose condensation of spin-orbit excitons. In addition to usual magnons, a “Higgs” amplitude mode, most prominent near the quantum critical point, is predicted. Upon electron doping, an unconventional triplet superconductivity may emerge. We discuss these theoretical predictions [1, 2] in the context of recent experiments in ruthenium oxides.

1. Khaliullin G.: Phys. Rev. Lett. **111**, 197201 (2013)
2. Chaloupka J., Khaliullin G. (unpublished).

## Spin Fluctuations and Inhomogeneities in Iron Pnictide Superconductors as Probed by NMR and NQR

**H.-J. Grafe<sup>1</sup>, U. Gräfe<sup>1</sup>, F. Hammerath<sup>1</sup>, G. Lang<sup>2</sup>, A. P. Dioguardi<sup>3</sup>,  
N. J. Curro<sup>3</sup>, and B. Büchner<sup>1</sup>**

<sup>1</sup> IFW Dresden, Institute for Solid State Research, Dresden 01171, Germany,  
h.grafe@ifw-dresden.de

<sup>2</sup> LPEM UMR8213, CNRS-ESPCI ParisTech-UPMC, Paris 75005, France

<sup>3</sup> Department of Physics, University of California, Davis, California 95616, USA

The interplay of superconductivity and magnetism is one of the utmost concerns of the research on iron pnictide superconductors. Both phases are adjacent to each other in the phase diagram, and can even coexist as, for example, in underdoped  $\text{BaFe}_{2-x}\text{Co}_x\text{As}_2$ . Magnetic fluctuations are therefore believed to mediate the Cooper pairing, experimentally substantiated by a critical enhancement of the nuclear spin-lattice relaxation rate at optimal doping. Since their discovery, evidence has mounted that the physics of iron pnictides can be described in a simple band picture in which the spin density wave order is enabled by nesting of the equally sized electron and hole Fermi surfaces. Doping electrons increases (decreases)

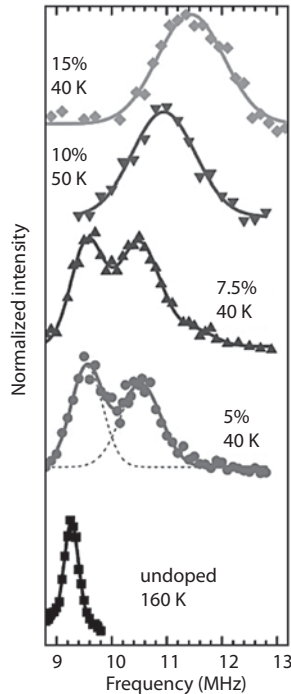


**Fig. 1.**  $^{75}\text{As}$  NQR spectra of  $\text{LaO}_{1-x}\text{F}_x\text{FeAs}$  for different F contents [4].

the size of the electron (hole) Fermi surfaces, thus hampering the formation of spin density wave (SDW) order. On the other hand, many peculiarities of the magnetic properties of the iron pnictides evidence the importance of electronic correlations and inhomogeneities in these fascinating, multifaceted materials. Here, we present NMR data in Co and Cu doped  $\text{BaFe}_2\text{As}_2$  evidencing that the spin fluctuations probed by the nuclear spin-lattice relaxation rate  $(T_1T)^{-1}$  are identical for both dopings down to  $T_c$  [1]. Since Cu is not adding electrons to the Fermi surface, our results show that increasing (decreasing) the size of the electron (hole) Fermi surfaces has a negligible effect on the magnetic fluctuations, in contrast to the simple band picture. Moreover, we show that the spin fluctuations in  $\text{BaFe}_{2-x}\text{Co}_x\text{As}_2$  are glassy and inhomogeneous [2], reflecting a broad distribution of locally frustrated domains. These results suggest that disorder induced frustration plays a significant role in suppressing long-range antiferromagnetic order and in the emergence of superconductivity. A strong field dependence of the spin lattice relaxation rate  $(T_1T)^{-1}$  and similar inhomogeneities in the spin fluctuations in underdoped  $\text{LaO}_{1-x}\text{F}_x\text{FeAs}$  reflect a progressive slowing down of the spin fluctuations down to the superconducting phase transition in this compound, suggesting a competition between superconductivity and slow magnetic correlations [3]. Finally, we present NQR data featuring low-doping-like and high-doping-like regions in the paramagnetic state of underdoped  $\text{LaO}_{1-x}\text{F}_x\text{FeAs}$  (see Fig. 1) [4]. A detailed analysis of the temperature and doping dependence of these peaks shows that the low-doping-like regions fully account for the orthorhombicity and static magnetism of the system, which are not hindered by superconductivity but limited by percolation effects. Consequently, the loss of static magnetism when doping cannot be related to a degradation of the nesting properties of the Fermi surface. In conclusion, our results in both families of iron based superconductors evidences the existence of inhomogeneities, and their important role for the suppression of magnetism and the emergence of superconductivity, going beyond the simple band picture of Fermi surface nesting and doping dependent hampering of the spin density wave order.

1. Grafe H.-J., Gräfe U., Dioguardi A.P., Curro N.J., Aswartham S., Wurmehl S., Büchner B.: *Phys. Rev. B* **90**, 094519 (2014)
2. Dioguardi A.P., Lawson M.M., Bush B.T., Crocker J., Shirer K.R., Nisson D.M., Kissikov T., Ran S., Bud'ko S.L., Canfield P.C., Yuan S., Kuhns P.L., Reyes A.P., Grafe H.-J., Curro N.J.: arXiv:1503.01844v1 (2015)
3. Hammerath F., Gräfe U., Kühne T., Kühne H., Kuhns P.L., Reyes A.P., Lang G., Wurmehl S., Carretta P., Büchner B., Grafe H.-J.: *Phys. Rev. B* **88**, 104503 (2013)
4. Lang G., Grafe H.-J., Paar D., Hammerath F., Manthey K., Behr G., Werner J., Büchner B.: *Phys. Rev. Lett.* **104**, 097001 (2010)

## Magnetic Properties of $\text{YbMnO}_3$ Ceramic Samples

**R. M. Eremina<sup>1,2</sup>, I. V. Yatzyk<sup>1,2</sup>, T. P. Gavrilova<sup>1,2</sup>, V. V. Parfenov<sup>2</sup>,  
V. I. Chichkov<sup>3</sup>, and N. V. Andreev<sup>3</sup>**

<sup>1</sup> Zavoisky Physical-Technical Institute, Russian Academy of Sciences, Kazan 420029,  
Russian Federation, R Eremina@yandex.ru

<sup>2</sup> Kazan Federal University, Kazan 420008, Russian Federation

<sup>3</sup> National University of Science and Technology MISiS, Moscow 119991, Russian Federation

Polycrystalline samples of ytterbium manganites  $\text{YbMnO}_3$  were synthesized according to two different ceramic technologies ( $\text{YbMnO}_3$ -I and  $\text{YbMnO}_3$ -II). These technologies differ in the sintering time and annealing temperature. The X-ray analysis of the synthesized manganites (I and II) showed that both samples belong to the space group  $P6_3cm$  and they are in single-phase state. The analysis of the XRD peak intensities demonstrated the difference in the atom site occupancy for Yb ions between two samples. Electron spin resonance (ESR) was much more sensitive to such differences in the crystal structure.

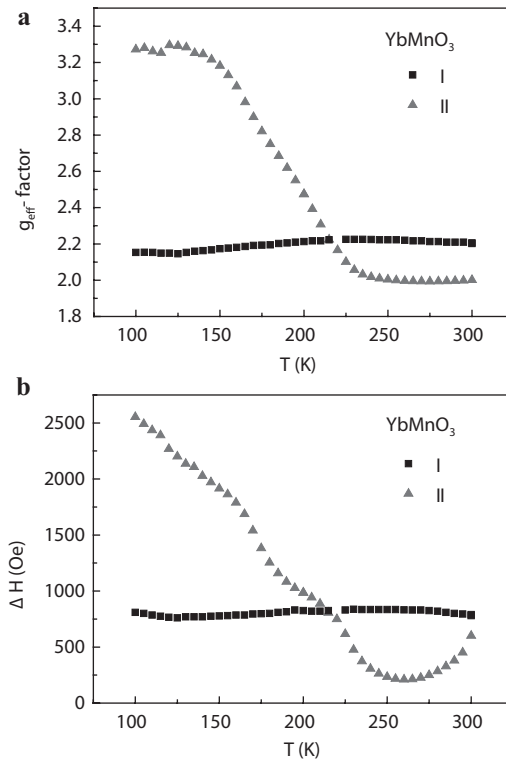


**Fig. 1.** Temperature dependence of  $g$ -factor (a) and ESR linewidth (b) in  $\text{YbMnO}_3$ .

ESR measurements were carried out in the temperature range of 100–320 K at the frequency of 9.48 GHz. The ESR spectrum of ytterbium manganite  $\text{YbMnO}_3$  (I and II) consists of one broad exchange-narrowed resonance line in all temperature range for both samples. The fitting of the ESR spectrum of  $\text{YbMnO}_3$ -I gives the  $g$ -factor above 2.1 (Fig. 1a), which is unusual for  $\text{Mn}^{3+}$  ions. The  $g$ -factor of  $\text{YbMnO}_3$ -II changes from 1.99 to 3.3 (Fig. 1b), that corresponds to middle  $g$ -factors of  $\text{Mn}^{3+}$  and  $\text{Yb}^{3+}$  ions systems, respectively. This temperature dependencies  $g$ -value and linewidth suggests the strong exchange interaction between  $\text{Mn}^{3+}$  and  $\text{Yb}^{3+}$  ions. The ESR linewidth is about 800 Oe in room temperature in both cases. The possible reasons of the phenomenon are under discussion.



## Unusual Quadrupole Moment Reduction and Cobalt Charge Differentiation in $\text{Na}_x\text{CoO}_2$

**I. R. Mukhamedshin<sup>1</sup>, I. F. Gilmutdinov<sup>1</sup>, A. V. Dooglav<sup>1</sup>, S. A. Krivenko<sup>1</sup>,  
and H. Alloul<sup>2</sup>**

<sup>1</sup>Institute of Physics, Kazan Federal University, Kazan 420008, Russian Federation

<sup>2</sup>Laboratoire de Physique des Solides, Université Paris-Sud, Orsay 91405, France

Among the various families of correlated electron systems the layered cobaltates  $\text{Na}_x\text{CoO}_2$  are quite original due to the triangular arrangement of the Co atoms in the  $\text{CoO}_2$  layers. In the trigonally distorted  $\text{CoO}_6$  octahedra, which build up the layered structure, the strong crystal field induced on the Co lowers the  $t_{2g}$  ionic levels with respect to the  $e_g$  levels. This favors for the cobalt electronic structure the low spin configurations in which the 5 to 6 electrons on the Co reside on the  $t_{2g}$  ionic levels. This electronic structure and the variation of the interlayer charge density, that is, here the Na content, are at the origin of many singular physical properties of sodium cobaltates, such as large thermoelectric effects, superconductivity, ordered magnetic states, high Curie-Weiss magnetism and metal insulator transition etc [1].

We have synthesized and characterized different stable phases of sodium cobaltates  $\text{Na}_x\text{CoO}_2$  with sodium content  $0.65 < x < 0.80$ . Our NMR/NQR study allowed us to evidence that in the sodium cobaltates  $\text{Na}_x\text{CoO}_2$  a large interplay between the Na atomic ordering and the electronic density on the Co sites occurs.  $^{23}\text{Na}$  NMR allows to determine the difference in the susceptibility of the phases and reveals the presence of Na order in each phase.  $^{59}\text{Co}$  NMR experiments give clear evidence that Co charge disproportionation is a dominant feature of Na cobaltates [2]. Only a small fraction ( $\approx 25\%$ ) of cobalts are in a non-magnetic  $\text{Co}^{3+}$  charge state, which correspond to filled  $t_{2g}$  levels, whereas electrons delocalize on the other cobalts with an average charge state close to  $\text{Co}^{3.5+}$ .

For sodium cobaltates with  $x \geq 0.5$  we found that the magnetic and charge properties of the Co sites are highly correlated with each other as magnetic shift KZZ scale linearly with quadrupolar frequency  $\nu_Q$  [3]. Such correlations can be understood as both measured values  $\nu_Q$  and KZZ contain terms proportional to the quadrupole moment of the  $t_{2g}$  hole density distribution which involves as a coefficient the hole concentration on the Co site. Therefore this correlations reflect the fact that the hole content on the Co orbitals varies from site to site and the hyperfine coupling (or the local magnetic susceptibility) scales with the on site delocalized charge.

We found that in cobaltates for  $x \geq 0.5$  a local charge contribution to the  $\nu_Q$  equal  $\approx 3.3$  MHz per hole on Co site. A theoretical estimate gives that single hole (or electron) on a given  $t_{2g}$  orbital should correspond for  $^{59}\text{Co}$  to about 20 MHz per hole which is about six times larger than our experimental value.

This discrepancy evidence that quadrupole moment of cobalt  $t_{2g}$ -shells in cobaltates are greatly reduced and the local charge is not evenly distributed on the Co  $t_{2g}$  orbitals. We can suggest that this can be explained either that the holes are distributed over the three orbital states within the  $t_{2g}$ -shells due to the thermal/quantum fluctuations or by the specific in-plane correlations. Such unusual quadrupole moment reduction and cobalt charge differentiation found in this system calls for better theoretical understanding of the incidence of the Na atomic order on the electronic structures of sodium cobaltates.

This work was partially supported by the RFBR under project 14-02-01213a and performed according to the Russian Government Program of Competitive Growth of Kazan Federal University. I.R.M. and I.F.G. thank for the support of a visit to Orsay by “Investissements d’Avenir” LabEx PALM (ANR-10-LABX-0039-PALM).

1. Mukhamedshin I.R., Alloul H.: *Physica B* **460**, 58–63 (2015)
2. Mukhamedshin I.R., Alloul H., Collin G., Blanchard N.: *Phys. Rev. Lett.* **94**, 247602 (2005)
3. Mukhamedshin I.R., Dooglav A.V., Krivenko S.A., Alloul H.: *Phys. Rev. B* **90**, 115151 (2014)

## EPR of Gadolinium Cluster Centers in the Semimagnetic Narrow Gap Semiconductors $\text{Pb}_{1-x}\text{Gd}_x\text{Te}$ ( $x = 0.02$ )

E. R. Zhiteitsev<sup>1</sup>, R. R. Zainullin<sup>2</sup>, V. A. Ulanov<sup>1,2</sup>, and V. A. Shustov<sup>1</sup>

<sup>1</sup> Zavoisky Physical-Technical Institute, Russian Academy of Sciences, Kazan 420029,  
Russian Federation

<sup>2</sup> Kazan State Power Engineering University, Kazan 420066, Russian Federation

Lead chalcogenides PbS, PbSe and PbTe (AIVBVI) have the rocksalt structure with a strong ionic character of the bonds and belong to the family of narrow gap semiconductors. They are characterized by high static dielectric constants and by large free carrier mobility. Their direct band gap is located at the L point in the Brillouin zone. Physical characteristics of the lead chalcogenides have important applications in infrared and thermoelectric devices. Modern investigations on various heterostructures, films, quantum wires, quantum dots and wells attract much attention to the physical properties of the lead chalcogenides, especially, to magnetic properties of these semiconductors doped by paramagnetic impurities such as gadolinium, europium, manganese, and so on.

We report here the EPR data on deep  $\text{Gd}^{3+}$  centers in  $\text{Pb}_{1-x}\text{Gd}_x\text{Te}$  ( $0.002 \leq x \leq 0.02$ ). X-band EPR measurements were performed on single crystals  $\text{Pb}_{1-x}\text{Mn}_x\text{Te}$  grown by Bridgman method in quartz crucibles. Temperature gradient near crystallization zone was in the range  $25 \leq dT/dz \leq 250$  deg/cm. To study the angular dependencies of the EPR line positions in an (110) crystallographic plane, the samples were mounted in a two-circle goniometer. The measurements were carried out at liquid helium temperature (4.2 K). Taking into account a tendency of gadolinium impurities to clusterization [2], we studied by EPR method the samples

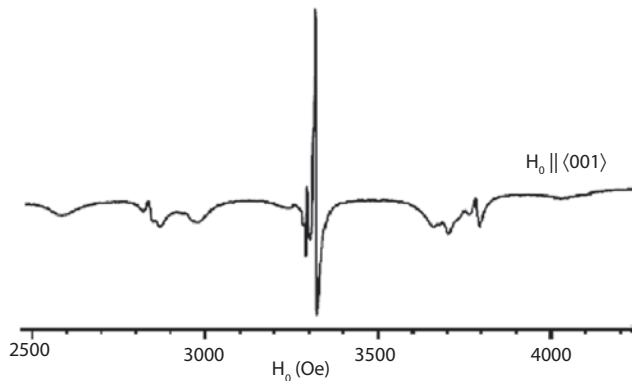


**Fig. 1.** EPR spectrum of monocrystalline  $\text{Pb}_{1-x}\text{Gd}_x\text{Te}$  sample ( $x = 0.02$ ;  $T = 4.2$  K;  $H_0 \parallel \langle 001 \rangle$ ;  $f = 9342$  MHz).

$\text{Pb}_{1-x}\text{Gd}_x\text{Te}$  ( $x = 0.02$ ) grown with  $dT/dz \approx 30$  deg/cm. The EPR spectrum of such sample recorded at 4.2 K in orientation is represented in Fig. 1. In the figure one can see three groups of EPR lines which belong to three paramagnetic centers formed by  $\text{Gd}^{3+}$  ions. First of them corresponds to cubic  $\text{Gd}^{3+}$  centers studied earlier by authors of the work [2]. Second and third groups of EPR lines arise due to  $[\text{Cd}^{3+}\text{-Gd}^{2+}]$  pair centers with tetragonal symmetry of magnetic properties. Analysis of the Dysonian profiles of the EPR lines drive to the conclusion that the latest two groups of centers correspond to the  $[\text{Cd}^{3+}\text{-Gd}^{2+}]$  pairs located at the crystal body regions with different concentrations of the gadolinium impurities. Really, X-ray measurements showed that the gadolinium impurities distribution in the  $\text{Pb}_{1-x}\text{Gd}_x\text{Te}$  samples was highly non-uniform.

1. Zayachuk D.M., Ivanchuk D.D., Ivanchuk R.D., Maslyanchuk S.S., Mikityuk V.I.: Phys. Stat. Sol. (a), **119**, 2015 (1990)
2. Bartkowski N., Northcott D.J., Park J.M.: Solid State Commun. **56**, 659 (1985)

## Research-Class Bench-Top EPR-Spectrometer Bruker EMXnano

S. Lyubanova<sup>1</sup>, P. Hofer<sup>1</sup>, and D. Kuznetsov<sup>2</sup>

<sup>1</sup> Bruker BioSpin Corp., Rheinstetten 76287, Germany

<sup>2</sup> Bruker Ltd., Moscow 119017, Russian Federation,  
denis.kuznetsov@bruker.com

Extending Bruker's renowned EMX spectrometer family to the bench-top class, the EMXnano is a completely new development featuring the latest digital and microwave technologies. Combined with a new generation of magnet system with field range from  $-1$  to  $+6$  kG and a highly efficient microwave resonator, this state-of-the-art bench-top instrument is superior in sensitivity and stability, making it ideal for a comprehensive range of analysis and teaching applications.

Basic specifications of EMXnano:

|                                      |                       |
|--------------------------------------|-----------------------|
| Operating frequency                  | X-band                |
| Microwave power                      | 100 mW                |
| Concentration sensitivity            | 50 pM                 |
| Field sweep range                    | $-1000 \dots +6000$ G |
| Field resolution                     | 4 $\mu$ G             |
| Field homogeneity over sample volume | 50 mG                 |
| Field stability                      | 10 mG/h               |
| Sweep resolution (field or time)     | up to 250.000 points  |

The new dedicated bench-top instrument requires minimal infrastructure with a low cost of ownership, making it suitable for a wide range of laboratory types. Now any laboratory can confidently add or enhance its research potential with advanced CW-EPR methods.

No matter what the focus of your application is, the crucial required strengths of an EPR spectrometer are sensitivity and stability. The latest generation magnet and microwave technology delivers class-leading performance, enabling EMXnano to combine ease of use with highest quality of EPR data. Moreover, in addition



Fig. 1. Tabletop EPR-spectrometer EMXnano.

to its superior technical characteristics, EMXnano offers the following features and functionality:

- Integrated frequency counter
- Integrated amplitude and g-factor marker
- Quantitative EPR by reference-free spin counting
- Spin-trap library
- Spectrum fitting
- Remote diagnostics
- Variable Temperature Control (optional)
- UV irradiation system (optional)
- Wide range of ampoules and cells for specific sample types

EMXnano is supplied with Linux-based professional EPR-software Xenon, providing the wide range of Bruker' unique software routines for fast and convenient spectral processing and analysis, including microwave saturation analysis, reference-free quantitative analysis and many more.

As a good example of EMXnano highest efficiency and performance, one could mention modern application field of EPR-spectroscopy – development of paramagnetic polarizing agents for currently very popular Dynamic Nuclear Polarization (DNP) method. In this case, EPR-spectroscopy is the only method allowing direct measurement of the most important characteristics of a polarizing agent, directly related to its efficiency: microwave saturation, real concentration of paramagnetic centers in the sample and dipolar splitting in biradical-type agents. Reliable information about these properties is essential for understanding and improving the efficiency of a polarizing agent.

With convenient user-friendly graphical interface and Bruker' patented software procedures one can carry out a prompt, accurate and comprehensive study of the object of interest. It makes EMXnano the essential part of any laboratory using DNP methods.

---

## SECTION 3

# LOW-DIMENSIONAL SYSTEMS AND NANO-SYSTEMS

## Spin Probes for EPR and Overhauser-Enhanced Magnetic Resonance Imaging

G. Audran, P. Brémont, and S. Marque

Aix-Marseille University, 13397 Marseille Cedex 20, France, sylvain.marque@univ-amu.fr

This talk is divided in two parts. The first part deals with the development of a nitroxides sensitive to non-radical enzymatic activity, and their application as probes for Overhauser-enhanced Magnetic Resonance Imaging. Hence, a  $\beta$ -phosphorylated nitroxide substrate prototype exhibiting keto-enol equilibrium upon enzymatic activity has been prepared. Upon enzymatic hydrolysis, a large variation of  $a_p$  ( $\Delta a_p = 4$  G) was observed. The enzymatic activities of several enzymes were conveniently monitored by Electronic Paramagnetic Resonance (EPR). Using a 0.2 T MRI machine, *in vitro* and *in vivo* OMRI experiments were successfully performed affording *in vitro* a 1200% enhanced MRI signal and a 600% enhanced signal *in vivo* [1]. These results nicely highlight the enhanced imaging potential of these nitroxides upon specific enzymatic substrate-to-product conversion and must be gauged at the light of the 50% increased of MRI signal when  $Gd^{3+}$ -derivatives are used as contrast agents in conventional MRI.

The second part is devoted to the development of new nitroxides highly sensitive to the polarity of the solvent [2]. Hence, for decades, the nitrogen hyperfine coupling constant  $a_N$  of nitroxides has been applied to probe their environment using EPR. However, the small changes observed ( $\approx 2$  G from *n*-pentane to water) with the solvent polarity allow only a qualitative discussion. A stable  $\beta$ -phosphorylated nitroxide exhibiting a small change in  $a_N$  ( $\approx 3$  G from *n*-pentane to water) and a striking change in  $a_p$  ( $\approx 25$  G from *n*-pentane to water) with the polarity of solvent was prepared and used to develop the first procedure for the titration of water in THF by EPR, down to 0.1% v/v.

1. Audran G., Bosco L., Brémont P., Franconi J.-M., Koonjoo N., Marque S.R.A., Massot P., Mellet P., Parzy E., Thiaudière E.: *Angew. Chem. Int. Ed.* (2015) ASAP.
2. Audran G., Bosco L., Brémont P., Butscher T., Marque S.R.A.: *Anal. Chem.* (2015) sub.

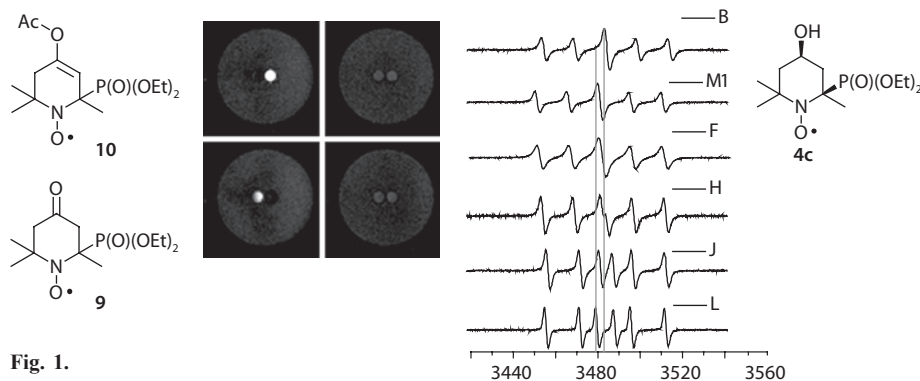


Fig. 1.



## Magnetic Resonance of Spinons in $S = 1/2$ Antiferromagnetic Spin Chains

**A. I. Smirnov<sup>1</sup>, T. A. Soldatov<sup>1</sup>, and K. Yu. Povarov<sup>2</sup>**

<sup>1</sup> P. L. Kapitza Institute for Physical Problems RAS, Moscow, Russian Federation, smirnov@kapitza.ras.ru

<sup>2</sup> Neutron Scattering and Magnetism, ETH Zürich, Switzerland

One-dimensional  $S = 1/2$  antiferromagnets demonstrate a variety of collective quantum effects, such as a spin-liquid behavior at zero temperature and fractionalized spin excitations (spinons), which result, e.g., in a two-particle continuum of excitations [1]. In a magnetic field the continuum splits into two branches of transverse and longitudinal fluctuations and develops a fine structure. A fine structure of longitudinal spin fluctuations near a Brillouin zone boundary was observed by neutron scattering [2]. Typically, the continuum structure is undetectable by the electron spin resonance (ESR) probing strictly zero wave vector ( $\mathbf{q} = 0$ ) excitations. We address now to a fine structure of the two-spinon continuum, appearing at  $\mathbf{q} = 0$  in spin chains with the so-called *uniform* Dzyaloshinskii-Moriya interaction (DMI). In contrast to a conventional *staggered* DMI, causing a tilting of magnetic sublattices in a classical antiferromagnet, the *uniform* DMI interaction would stabilize a spiral spin structure. In case of a quantum spin chain, which has a disordered ground state, DMI was predicted to shift the spinon continuum in  $\mathbf{q}$ -space by a wavevector  $q_{\text{DM}} = D/(Ja)$  (here  $D$  is a value of DMI vector,  $J$  is the exchange integral and  $a$  - interspin distance) [3]. As a result, in a magnetic field  $\mathbf{H} \parallel \mathbf{D}$ , the ESR line should split into a doublet with the frequencies at the upper and lower boundaries of the unshifted transversal continuum at the wavevector  $q_{\text{DM}}$ .

We describe ESR experiments on  $S = 1/2$  quasi-1D antiferromagnets  $\text{K}_2\text{CuSO}_4\text{Br}_2$ , and  $\text{Cs}_2\text{CuCl}_4$ , allowing uniform DMI. We observe and study the spinon doublet ESR in a frequency range 0.5–300 GHz, rising from sub- $D$  to over- $J$  domains. In particular, we observe at low temperatures a soft mode at a magnetic field  $H_D = D/(g\mu_B)$  and a collapse of the spinon doublet in a high magnetic field, suppressing zero point spin fluctuations.

1. Tennant D.A. *et al.*: Rev. B **52**, 13368 (1995)
2. Dender D.C. *et al.*: Phys. Rev. Lett. **79**, 1750 (1997)
3. Gangadharaiah S., Sun J., Starykh O.A.: Phys. Rev. B **78**, 054436 (2008)

## NMR of $^3\text{He}$ in Porous Media

**A. V. Klochkov, E. M. Alakshin, R. R. Gazizulin, V. V. Kuzmin,  
K. R. Safiullin, and M. S. Tagirov**

Kazan Federal University, Kazan 420008, Russian Federation

Nuclear magnetic resonance (NMR) of  $^3\text{He}$  in porous media is a method of obtaining rich information about structure and properties of the porous substrates. The NMR characteristics of normal liquid  $^3\text{He}$  strongly depend on size of volume where  $^3\text{He}$  is located. The main reason for that is highly effective spin diffusion, which allows seeing space restriction starting from several mm sizes. Usually, the nuclear magnetic relaxation of liquid  $^3\text{He}$  (both  $T_1$  and  $T_2$ ) takes place by means of fast spin diffusion from liquid  $^3\text{He}$  to adsorbed  $^3\text{He}$  and further effective surface relaxation in adsorbed layer of  $^3\text{He}$  [1–5]. Thus, the  $^3\text{He}$  spin kinetics and the spectral characteristics are strongly dependable on size of geometry filled by liquid  $^3\text{He}$ . Additionally, the study of spin kinetics of  $^3\text{He}$  in porous media at low temperatures is in the matter of interest due to direct magnetic coupling between  $^3\text{He}$  and solid state substrate [2, 6, 7].

The main subject of the present work is the study of spin kinetics of  $^3\text{He}$  in contact with different types of silica aerogels, charcoals, inverse opals, clay minerals and nanosized crystal powders of Van Vleck paramagnet  $\text{PrF}_3$ . The experimental results, obtained in Kazan Federal University in the last 10 years are published in [4, 8–11].

This work is partially supported according to the Russian Government Program of Competitive Growth of Kazan Federal University.

1. Naletov V.V., Tagirov M.S., Tayurskii D.A., Teplov M.A.: JETP **81**, 311 (1995)
2. Friedman L.J., Millet P.J., Richardson R.C.: Phys. Rev. Lett. **47**, 1078 (1981)
3. Friedman L.J., Gramila T.J., Richardson R.C.: J. Low Temp. Phys. **55**, 83 (1984)
4. Klochkov A.V. *et al.*: JETP Letters **88**, 823 (2008)
5. Cowan B.P.: J. Low Temp. Phys. **50**, 135 (1983)
6. Egorov A.V. *et al.*: JETP Letters **39**, 584 (1984)
7. Egorov A.V. *et al.*: JETP Letters **86**, 416 (2007)
8. Alakshin E.M. *et al.*: JETP Letters **93**, 223 (2011)
9. Gazizulin R.R. *et al.*: Appl. Magn. Res. **38**, 271 (2010)
10. Tagirov M.S. *et al.*: J. Low. Temp. Phys. **162**, 645 (2011)
11. Alakshin E.M. *et al.*: JETP Letters **97**, 579 (2013)

## Silicon-Based Hybrid Nanostructures: Magnetic State and Magneto-Dependent Charge Transport

**N. V. Volkov<sup>1,2</sup>, A. S. Tarasov<sup>1</sup>, M. V. Rautskii<sup>1</sup>, S. N. Varnakov<sup>1,2</sup>,  
and S. G. Ovchinnikov<sup>1</sup>**

<sup>1</sup> Kirensky Institute of Physics SB RAS, Krasnoyarsk 660036, Russian Federation  
volk@iph.krasn.ru

<sup>2</sup> Siberian State Aerospace University, Krasnoyarsk 660014, Russian Federation

The giant magnetoresistance (MR) effects in hybrid nanostructures attract much attention of researchers because they initiate nontrivial fundamental physical problems and offer the opportunity of integrating the MR functionalities in electronic devices. We demonstrate that the devices based on the metal/insulator/semiconductor hybrid structures can exhibit specific magnetotransport properties [1–2]. For back-to-back Schottky diodes fabricated on base of the Fe/SiO<sub>2</sub>/p(n)-Si structure, dc MR was found. The MR ratio does not exceed 20% at 9 T. More strong influence of magnetic field is observed in case of ac transport properties. Magnetoimpedance ratio at 1 T exceeds 600% in frequency range of 10 Hz – 1 MHz. In addition, we found the giant dc MR effect induced by laser irradiation in the planar Fe/SiO<sub>2</sub>/p(n)-Si-based devices. The MR ratio in this case attained 10<sup>5</sup>%. The value and sign of all MR effects can be effectively controlled by a bias voltage on the devices.

We suggested some mechanisms which allow explaining the origin of the MR effects. At the same time, the role of the magnetic state of the metal electrode in the manifestation of these effects is still inexplicit. To clarify this question, we studied the correlation between magnetic state and magnetotransport properties in the devices fabricated from M/SiO<sub>2</sub>/p(n)-Si structures, where M is Fe<sub>3</sub>Si, FeNi, Fe<sub>3</sub>O<sub>4</sub> and Mn. Magnetic properties were studied by using static and resonance methods. In addition, we used method combined magnetic resonance and the methods for measuring of the transport properties. Such approach allows studying the interplay between spin dynamics and spin-dependent electron transport. That is very important both for understanding of the nature of spin-dependent phenomena and for search of the novel ways to generate spin current and to control spin-dependent current in the hybrid structures.

1. Volkov N.V., Tarasov A.S., Smolyakov D.A. *et al.*: Appl. Phys. Lett. **104**, 222406 (2014)
2. Volkov N.V., Tarasov A.S., Smolyakov D. A. *et al.*: JMMM **383**, 69 (2015)

## Electronic and Magnetic Structures of Nanographites and Their Changes Influenced by Adsorbed Molecules: EMR and MS Studies

A. M. Ziatdinov

Institute of Chemistry, Far Eastern Branch of the RAS, Vladivostok 690022, Russian Federation, ziatdinov@ich.dvo.ru

The effect of the surface and edge atoms on electronic structure increases with decreasing sizes of particles and depends on the geometry of the positions of the peripheral atoms [1]. According to calculations [2], the specific  $\pi$ -electronic band forms near the zigzag edges of honeycomb carbon networks, which can significantly affect their electronic structure near the Fermi level in nanoscale samples. In this paper, the results of ESR, conduction ESR (CESR) and magnetic susceptibility (MS) investigations of multilayer graphene nanoclusters (nanographites) with an emphasis on their atomic pattern and features of electronic structure near the Fermi level and changes in these states at the interaction of nanographites with some acceptor molecules are presented.

The graphite particles forming a disordered network in polyacrylonitrile-based activated carbon fibers (ACFs) with specific surface area  $\approx 2000$  m<sup>2</sup>/g have been chosen as the object of this study. The data of X-ray diffraction, X-ray small-angle scattering and Raman spectroscopy for chosen ACFs indicate the presence of disordered system of turbostratic nanographites separated from each other by nanoscale pores and/or sp<sup>3</sup>-carbon amorphous phase. Due to turbostratic packing of nanographenes, the average distance between them ( $\approx 0.366$  nm) is

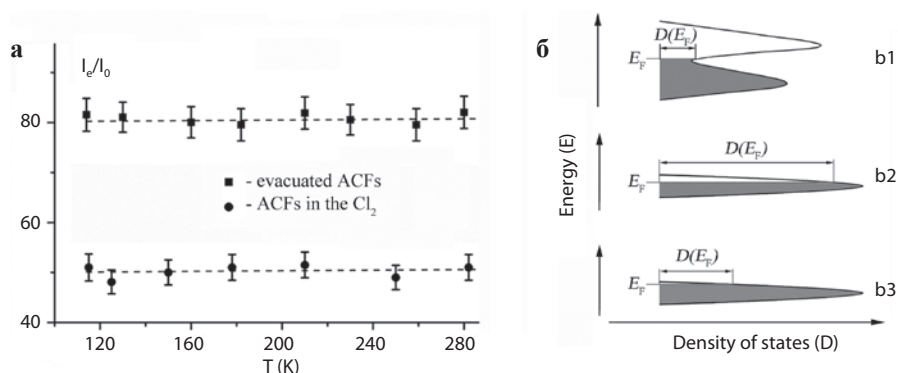


**Fig. 1.** The change of  $D(E_F)$  during adsorption of chlorine molecules by nanographites (a) and a schematic explanation of this phenomenon (b). b1, b2 and b3 correspond to the edge  $\pi$ -electronic band before and after adsorption of molecules by nanographites and subsequent spin splitting of this band.  $I_0$  – the intensity of the CESR signal of reference sample Li:LiF.

significantly larger than the distance between the carbon layers in the macroscopic ordered graphite.

Regardless of vacuum degree the ESR spectrum of ACFs consists of two signals, which have different widths but the same value of  $g$ -factor ( $=2.0027 \pm 0.0001$ ). With decreasing temperature, the integral intensity of broad spectrum component is invariable, while that of narrow component varies approximately according to the Curie law. On this basis, the broad signal can be attributed to spin resonance on conduction electrons and the narrow one can be regarded as spin resonance on the localized magnetic moments. According to the CESR and MS data of nanographites, the density of states  $D(E_F)$  of current carriers at the Fermi level  $E_F$  significantly exceeds the corresponding values for the macroscopic graphite. This result suggests the existence of edge  $\pi$ -electronic states in nanographites.

The data of magnetic research methods show that the values of  $D(E_F)$ , concentration of localized spins  $N_s$  and spin relaxation rate of current carriers for nanographites in the chlorine and oxygen atmospheres differ significantly from the values of these parameters for initial sample (Fig. 1a). It is shown that the change in  $D(E_F)$  can be attributed to the spin splitting of edge  $\pi$ -electronic states induced by increasing of electron-electron interactions due to enhancement of  $D(E_F)$  while a part of the electron density is transferred from nanographites to chlorine or oxygen adatoms (Fig. 1b). It has been shown that mentioned point of view on the nature of considered phenomenon does not contradict the results of other physical methods of investigations of edge  $\pi$ -electronic states, including scanning probe microscopy [3, 4]. The decrease of  $N_s$  during the interaction of nanographites with chlorine indicates pairing of the electron spins on uncoupled (“dangling”)  $\sigma$ -orbitals of nanographite edge atoms with the electron spins on 3p-orbitals of chlorine atoms, that is the formation of edge covalent compound of nanographites with chlorine. The changes in the spin-relaxation characteristics of the current carriers during chlorination of samples are also consistent with the above model of interaction of nanographites with chlorine.

1. Poole C.P., Owens F.J.: Introduction to Nanotechnology, New Jersey (USA). Wiley 2003, 475 p.
2. Nakada K. *et al.*: Phys. Rev. B **54**, 17954 (1996)
3. Ziatdinov M.A. *et al.*: Phys. Rev. B. **87**, No. 115427 (2013)
4. Ohtsuka M. *et al.*: ACSNano **7**, 6868 (2013)

## Investigation of Magnetoelastic Effect in Permalloy Microparticles by Ferromagnetic Resonance and Magnetic Force Microscopy Techniques

**D. A. Biziyaev<sup>1</sup>, A. A. Bukharaev<sup>1,2</sup>, Yu. E. Kandrashkin<sup>1</sup>, R. V. Gorev<sup>3</sup>,  
L. V. Mingalieva<sup>1</sup>, V. L. Mironov<sup>3,4</sup>, N. I. Nurgazizov<sup>1</sup>,  
and T. F. Khanipov<sup>1</sup>**

<sup>1</sup>Zavoisky Physical-Technical Institute, Russian Academy of Sciences, Kazan 420029,  
Russian Federation

<sup>2</sup>Kazan Federal University, Kazan 420008, Russian Federation

<sup>3</sup>Institute for Physics of Microstructures of the RAS, Nizhny Novgorod 603950, Russian Federation

<sup>4</sup>Lobachevsky State University of Nizhny Novgorod, Nizhny Novgorod 603950, Russian Federation

The remagnetization processes initiated by magnetoelastic interaction in heterogeneous ferromagnetic nanostructures is the subject of intensive investigations motivated by perspective applications in magnetic data processing systems with the electric field controlling [1]. Obvious advantage of the electric field record is associated with a considerable decrease in energy consumption per one magnetic bit in comparison with the magnetic field recording. One of the simplest methods to create an elastic tension in magnetic material is the deposition of the thin film on the mechanically curved elastic substrate. This method enables the formation of the uniaxial magnetoelastic anisotropy in magnetic films [2].

Here we present the study of the magnetoelastic phenomena in the ordered array of permalloy ( $\text{Ni}_{75}\text{Fe}_{25}$ ) micro squares with the sizes  $22 \times 22 \times 0.02 \mu\text{m}^3$  (the separation between squares is  $7 \mu\text{m}$ ) by ferromagnetic resonance (FMR) and magnetic force microscopy (MFM) techniques. The array of the squares was formed by deposition of  $\text{Ni}_{75}\text{Fe}_{25}$  in UHV on glass substrate through the metallic grating (with  $22 \times 22 \mu\text{m}^2$  cells) as the mask. The elastic stresses were created along the axis parallel to the side of the square similarly to the method described in [2]. The FMR measurements were performed with Bruker EMX Plus electron paramagnetic resonance spectrometer using dc external magnetic field ( $H_{\text{ex}}$ ) up to 1.4 T. The microwave magnetic field  $H_{\text{mw}}$  with the frequency 9.8 GHz was perpendicular to the  $H_{\text{ex}}$ . The samples were driven through the resonance by sweeping the  $H_{\text{ex}}$ . Additionally, the microwave absorption in the micro squares was studied by the computer micromagnetic modeling based on the numerical solution of Landau-Lifshitz-Gilbert equation using the modified object oriented micromagnetic framework (OOMMF) code [3]. The calculations were performed for the typical permalloy parameters: the saturation magnetization was  $M_{\text{S}} = 9.4 \cdot 10^5 \text{ A/m}$ , the exchange stiffness was  $A = 1.3 \cdot 10^{-11} \text{ J/m}$ , and the damping constant was 0.01.

The atomic force microscope (AFM) image of the micro square array is presented in Fig. 1a. The resonance field dependence on the sample orientation investigated by FMR is shown in Fig. 1b, c. These data allowed us to estimate the effective anisotropy field and the magnetization saturation parameters, which

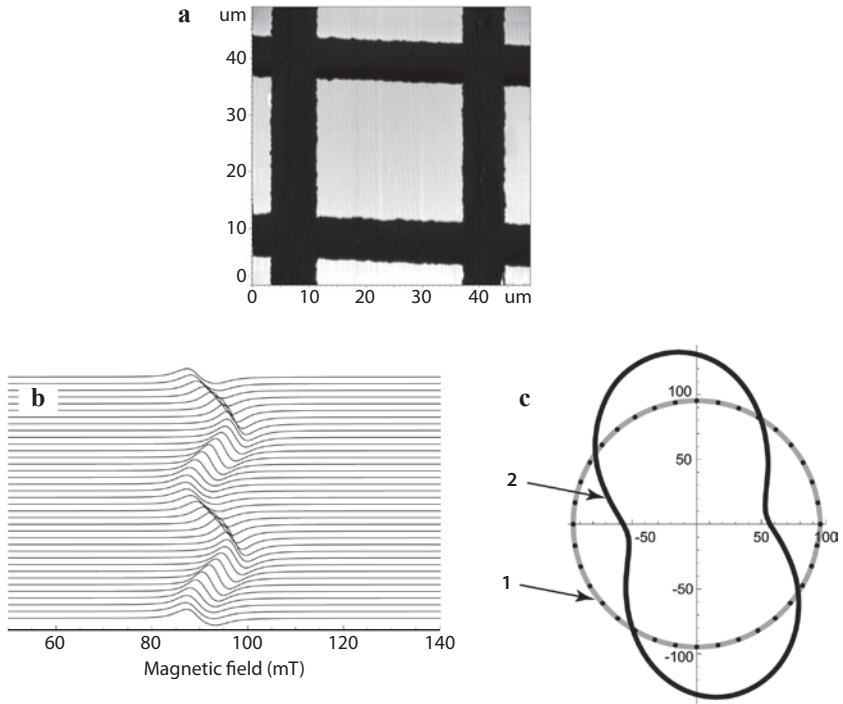


**Fig. 1.** The AFM image of the micro square array (a). The dependence of the FMR spectra on the angle  $\theta$  between the axis along the one of side of the square particles and the direction of the external magnetic field: b the FRM spectra for the angles  $\theta$  varied in the range  $0-360^\circ$  (from bottom to top); c the polar plot of the resonance condition as a function of the angle  $\theta$ . The mutual shift of the resonance condition relative to the mean resonance condition has been enlarged by 10 times. The curves 1 and 2 correspond to the interpolation functions derived from the experimental data of the unstressed and stressed samples, correspondingly.

were supplied to the micromagnetic simulations of the domain structure and the FMR spectra changes, induced by the elastic compression. The simulated MFM pictures of the domain structure are in good agreement with the experimentally observed MFM images and the simulated FMR spectra coincide well with the experimental data.

This work was partly supported by RFBR (grants 15-02-02728 and 15-02-04462) and programs of the Presidium of the RAS.

1. Morosov A.I.: *Physics of the Solid State* **56**, 865 (2014)
2. Belyaev B.A., Izotov A.V.: *Physics of the Solid State* **49**, 1731 (2007)
3. Donahue M.J., Porter D.G.: OOMMF (<http://math.nist.gov/oommf/>)

## Features of Ferromagnetic Resonance and Exchange Interaction in Structures CoPt with not Collinear Magnetizations

A. A. Fraerman<sup>1,2</sup>, N. S. Gusev<sup>1</sup>, V. L. Mironov<sup>1,2</sup>, E. S. Demidov<sup>2</sup>,  
and L. I. Budarin<sup>2</sup>

<sup>1</sup> Institute for Physics of Microstructures RAS, Nizhny Novgorod 603950, Russian Federation

<sup>2</sup> Lobachevsky State University of Nizhny Novgorod, Nizhny Novgorod 603950,  
Russian Federation, demidov@phys.unn.ru

In recent years the attention of many groups was focused on the investigations of magnetic structures with non-collinear magnetization (SNCM). In particular, the challenge problem is the realization of the special localized spin configurations – skyrmions, which are very perspective for the application in new spintronics structures [1, 2]. In the present work we report on the investigation of ferromagnetic resonance (FMR) and exchange interaction (EI) in SNCM  $(\text{Co}(d)\text{Pt}(t))_5/\text{Co}(D)/\text{Si}$  with the layer thicknesses  $d = (0.7-0.9)$  nm,  $t = 1.5$  nm and  $D = 10$  nm, which is similar to the structures described in [2]. The SNCM were fabricated by DC magnetron deposition of metal multilayers on Si substrates [2]. The spectra FMR were registered in 3 cm Bruker EMX spectrometer at 293 K. The angular dependences of resonant lines  $H_r(\theta_H)$  position were investigated at the sample rotation with the plane parallel to the direction of magnetic component of microwave field. For comparison we measured the FMR of five-layers  $(\text{Co}(d)\text{Pt}(t))_5/\text{Si}$  and thick layers  $\text{Co}(D)/\text{Si}$ . The numerical simulation of FMR spectra was performed on the basis of Landau-Lifshitz-Gilbert equations with rank of a matrix of coefficients up to  $12 \times 12$  for six-layer SNCM  $(\text{Co}(d)\text{Pt}(t))_5/\text{Co}(D)/\text{Si}$ . The equilibrium directions of magnetization of layers were found from the minimum of the free energy. In the case of single layer  $\text{Co}(10 \text{ nm})$  the calculated angular dependence  $H_r(\theta_H)$  (Fig. 1) is well described by the following parameters corresponding to the

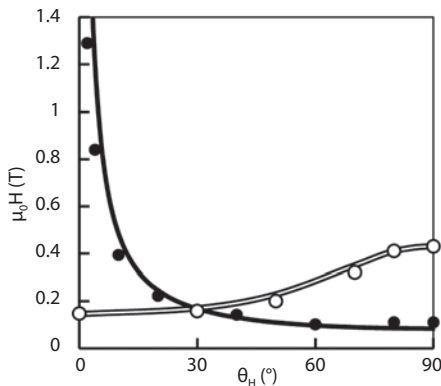


**Fig. 1.** The experimental and simulated angular dependences of position of resonant peak of FMR  $H_r(\theta_H)$  for sample  $\text{Co}(10)/\text{Si}$  (the black points and black curve), the same for structure  $(\text{Co}(0.9)\text{Pt}(1.5))_5/\text{Si}$  (light points and double curve).



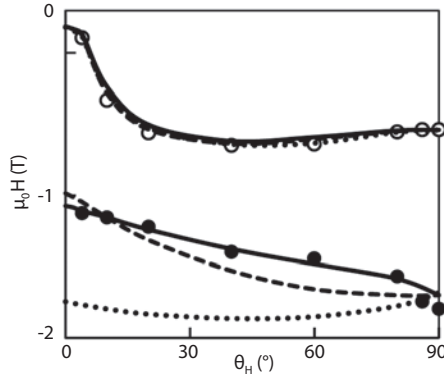


**Fig. 2.** The experimental dependences of  $H_r(\theta_H)$  acoustic (light points) and optical (black points) of modes for six-layer  $(\text{Co}(0.9)\text{Pt}(1.5))_5/\text{Co}(10)/\text{Si}$ . The dot curves were calculated for the scalar EI, the dotted with addition of the biquadratic EI, the continuous with addition of the Dzyaloshinskii- Moriya EI.

lateral equilibrium magnetization at  $H = 0$ : the factor of spectroscopic splitting  $g = 2.02$ ; the saturation magnetization  $M_s = 1.42 \cdot 10^6$  A/m and the constant of uniaxial anisotropy  $K_2 = 4.6 \cdot 10^5$  J/m<sup>3</sup>. The five-layer structure  $(\text{Co}(d)\text{Pt}(t))_5$  in accordance with experimental data and calculation presented in Fig. 1 shows the perpendicular orientation of equilibrium magnetization at  $H = 0$  with parameters  $H_r(\theta_H)$   $g = 2.07$ ,  $M_s = 1.42 \cdot 10^6$  A/m and  $K_2 = 1.396 \cdot 10^6$  J/m<sup>3</sup>. For the  $(\text{Co}(0.9)\text{Pt}(1.5))_5/\text{Co}(10)/\text{Si}$  structure the experimental and computed FMR spectra comprised two lines of  $H_r(\theta_H)$  corresponding to the high-field acoustic and low-field optical modes of the spin precession with the ferromagnetic EI of subsystems  $(\text{Co}(0.9)\text{Pt}(1.5))_5$  and  $\text{Co}(10)$ . The corresponding dependences of  $H_r(\theta_H)$  are presented in Fig. 2. The simulation of FMR spectra with the same parameter of EI  $j = 2.4$  mJ/m<sup>2</sup> between all magnetic layers has allowed us to receive the good consent of  $H_r(\theta_H)$  only for acoustic FMR line. The better consent for optical mode (Fig. 2) can be reached with following parameters EI:  $j_1 = 1.14$  mJ/m<sup>2</sup> between layers of five-layer  $(\text{Co}(d)\text{Pt}(t))_5$ ,  $j_2 = 0.436$  mJ/m<sup>2</sup> between this five-layer and the layer of  $\text{Co}(10$  nm) and with inclusion of biquadratic EI  $j_b = 1.14$  mJ/m<sup>2</sup>.

The best consent for both modes of spin precession (Fig. 2) have been received with parameters  $j_1 = 2.5$  mJ/m<sup>2</sup>,  $j_2 = 1.5$  mJ/m<sup>2</sup> and inclusion of the Dzyaloshinskii-Moriya EI  $\text{EDM} = j_{\text{DM}}(\mathbf{M}_1 \times \mathbf{M}_2)_x / M_1 M_2$  with  $j_{\text{DM}} = 0.1$  mJ/m<sup>2</sup>. Thus, the possibility of essential manifestation of the Dzyaloshinskii-Moriya EI between ferromagnetic layers with non-collinear magnetization was shown.

This work was supported by Russian Foundation for Basic Research and Ministry of Education and Science of RF (Agreement 02.B.49.21.0003).

1. Nagaosa N., Tokura Y.: Nature Nanotechnol **8**, 899–911 (2013)
2. Fraerman A.A., Ermolaeva O.L., Skorohodov E.V., Gusev N.S., Mironov V.L., Vdovichev S.N., Demidov E.S.: JMMM **393**, 452–456 (2015)

## Ferromagnetic Resonance in Permalloy Microstripes

**E. Skorohodov<sup>1,2</sup>, R. Gorev<sup>1</sup>, R. Yakubov<sup>2</sup>, Yu. Khivintzev<sup>3</sup>, Yu. Filimonov<sup>3</sup>,  
E. Demidov<sup>2</sup>, and V. Mironov<sup>1,2</sup>**

<sup>1</sup> Institute for Physics of Microstructures, Nizhny Novgorod 603950, Russian Federation, [evgeny@ipmras.ru](mailto:evgeny@ipmras.ru)

<sup>2</sup> Lobachevsky State University, Nizhny Novgorod 603950, Russian Federation

<sup>3</sup> Kotel'nikov Institute of Radio-Engineering and Electronics RAS, Saratov branch, Saratov 410019, Russian Federation

The microwave properties of the ferromagnetic planar patterned structures (PPS) is the subject of the recent intensive investigations stimulated by perspective applications in magnetoelectronics, spintronics and data processing [1]. In particular, the PPS consisting of ferromagnetic elements with different shape and spatial arrangement are considered as the effective tuned filters for the ultra high frequency (UHF) electromagnetic radiation [2]. The ferromagnetic resonance (FMR) and spin wave resonances (SWR) in PPS strongly depend on the internal fields connected with the shape anisotropy, exchange and magnetostatic interaction. As a result the absorption spectrum of PPS is defined by the different geometric factors, such as shape and size of elements, spatial configuration of elements in PPS. This opens the wide opportunities for tuning of UHF absorption spectrum by changing the architecture of PPS using the nanolithography methods. The array of permalloy ( $\text{Ni}_{80}\text{Fe}_{20}$ ) rectangular stripes  $3000 \times 500 \times 30 \text{ nm}^3$  (the separation between stripes is  $3 \mu\text{m}$ ) were fabricated by electron-beam lithography and lift-off process. The FMR measurements were performed with Bruker EMX Plus-10/12 electron paramagnetic resonance spectrometer using a  $\text{TE}_{102}$  resonant cavity and dc magnetic field ( $H_{\text{ex}}$ ) up to 2 T. The polarized microwave magnetic field  $h_{\text{mw}}$  with frequency 9.8 GHz was perpendicular to the  $H_{\text{ex}}$ . The samples were driven through the resonance by sweeping the  $H_{\text{ex}}$ .

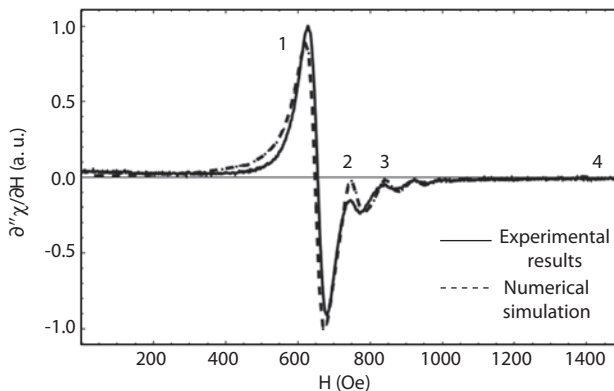


**Fig. 1.** The experimental and calculated FMR spectra for isolated microstripes. Magnetic field was applied along the long axis of the stripe.

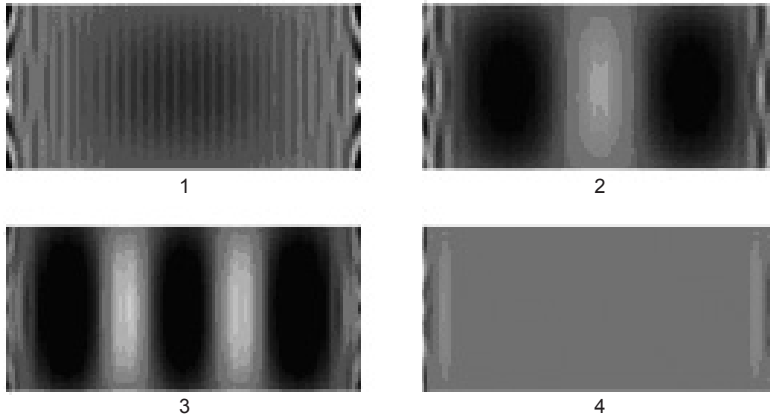


**Fig. 2.** The modes of magnetization oscillations in microstrip for different resonant fields corresponding to the picks indicated in Fig. 1.

Theoretically, the microwave absorption in microstrip was studied by computer micromagnetic modeling based on numerical solution of Landau-Lifshitz-Gilbert equation using the standard object oriented micromagnetic framework (OOMMF) code [3]. The calculations were performed for the typical permalloy parameters: the saturation magnetization was  $M_s = 8 \cdot 10^5$  A/m, the exchange stiffness was  $A = 1.3 \cdot 10^{-11}$  J/m, and the damping constant was 0.01. We omitted magnetocrystalline anisotropy, assuming a polycrystalline structure of our samples. In calculations the microstrip  $3000 \times 500 \times 30$  nm<sup>3</sup> was discretized into rectangular parallelepipeds with a square base of size  $\delta = 10$  nm in the  $x,y$  plane and height  $h = 30$  nm.

We investigated the dependencies of UHF absorption power on the magnitude of swept  $H_{ex}$ . For this purpose, we calculated the time dependencies of magnetization forced oscillations under  $h_{mw}$  with the frequency of 9.8 GHz for the different values of  $H_{ex}$ . As the example, Fig. 1 shows the experimental and calculated FMR spectra for isolated microstrips with magnetic field applied along the long axis of the stripe. In addition, to visualize the modes of magnetization oscillations we calculated the time dependencies of spatial distributions for different magnetization components. The Fig. 2 presents the images of different resonant modes, corresponding to the resonant picks indicated in Fig. 1. The peculiarities of the FMR spectra and mode structures for different sample orientations in external dc and microwave magnetic fields are discussed.

This work was supported by Russian Foundation for Basic Research (grant # 15-02-04462).

1. Zhang H., Hoffmann A., Divan R., Wang P.: Appl. Phys. Lett. **95**, 232503 (2009).
2. Wismayer M.P., Southern B.W., Fan X.L., Gui Y.S., Camley R.E., Hu C.-M.: Phys. Rev. B **85**, 064411 (2012)
3. Donahue M.J., Porter D.G.: Interagency Report No. NISTIR 6376, National Institute of Standards and Technology, Gaithersburg, (<http://math.nist.gov/oommf/>)

## Magnetic Resonance Studies of Ion-Beam Implanted Single Crystal Oxides

**B. Rameev<sup>1,2</sup> and R. Khaibullin<sup>2</sup>**

<sup>1</sup> Department of Physics, Gebze Technical University, Gebze-Kocaeli 41400, Turkey, rameev@gtu.edu.tr

<sup>2</sup> Zavoisky Physical-Technical Institute, Russian Academy of Sciences, Kazan 420029, Russian Federation, rik@kfti.knc.ru

An interest to the studies of spintronic (magneto-electronic) materials are driven by their high value with point of view of both fundamental science and potential technology applications. Magnetic resonance has been proven as one of the most effective methods to probe various properties of magnetic materials, such as the local magnetic anisotropy, exchange interaction energies, dynamic damping parameters, crystal electric field, etc.

In this work we review our advances in electron magnetic resonance studies of various magnetic nanomaterials produced by ion-beam implantation of magnetic 3d-ions into oxide semiconductors and semi-metals (TiO<sub>2</sub>, ZnO, ITO). The results of both Electron Paramagnetic Resonance (EPR) studies of diluted ions in the single crystal host material and FerroMagnetic Resonance (FMR) studies of ferromagnetic layer formed by high fluence implantation of 3d-ions in the single crystal substrate are presented.

Our investigations demonstrate that magnetic resonance is very effective technique to study the local structural and magnetic properties of 3d-ion implanted oxides. EPR signals of Mn<sup>4+</sup>, Cr<sup>3+</sup>, Fe<sup>3+</sup>, Co<sup>2+</sup>, and other paramagnetic ions have been observed in single crystal TiO<sub>2</sub> (ZnO) substrates implanted and/or subsequently annealed at high temperatures. It has been shown that post-annealing procedure favours the 3d-ions to enter substitutionally into Ti<sup>4+</sup> (Zn<sup>2+</sup>) lattice positions of the host crystal structure. The room-temperature anisotropic ferromagnetism in the non-annealed oxides, implanted with transition metals (e.g. Co, Fe, Ni), have been also observed. We have also shown that the anisotropic ferromagnetism in the as-implanted TiO<sub>2</sub>, ZnO, ITO thin films/plates is mainly related to the formation of Co, Ni, Fe-rich phases of magnetic nanoparticles in the implanted layer.

This work is supported by the TÜBİTAK/RFBR joint project programme, No. 213M524/14-02-91374\_CT-a.

## One-Third Magnetization Plateau and Spin Dynamics in Low-Dimensional Magnet $\text{NaFe}_3(\text{HPO}_3)_2(\text{H}_2\text{PO}_3)_6$

**E. A. Zvereva<sup>1</sup>, I. Munao<sup>2</sup>, P. Lightfoot<sup>2</sup>, A. A. Tsirlin<sup>3</sup>, Y. A. Ovchencov<sup>1</sup>, O. S. Volkova<sup>1</sup>, C. Koo<sup>4</sup>, R. Klingeler<sup>4</sup>, and A. N. Vasiliev<sup>1</sup>**

<sup>1</sup> Low Temperature Physics and Superconductivity Department, Faculty of Physics, M. V. Lomonosov Moscow State University, Moscow 119991, Russian Federation  
zvereva@mig.phys.msu.ru

<sup>2</sup> School of Chemistry, University of St Andrews, St Andrews, Fife KY16 9ST, UK

<sup>3</sup> National Institute of Chemical Physics and Biophysics, Tallinn 12618, Estonia

<sup>4</sup> Kirchhoff Institute for Physics, Heidelberg University, Heidelberg 69120, Germany

We report on static and dynamic magnetic properties of new low-dimensional magnet  $\text{NaFe}_3(\text{HPO}_3)_2(\text{H}_2\text{PO}_3)_6$ . The compound has triclinic crystal structure, space group P1 and characterized by non-trivial magnetic topology with two different

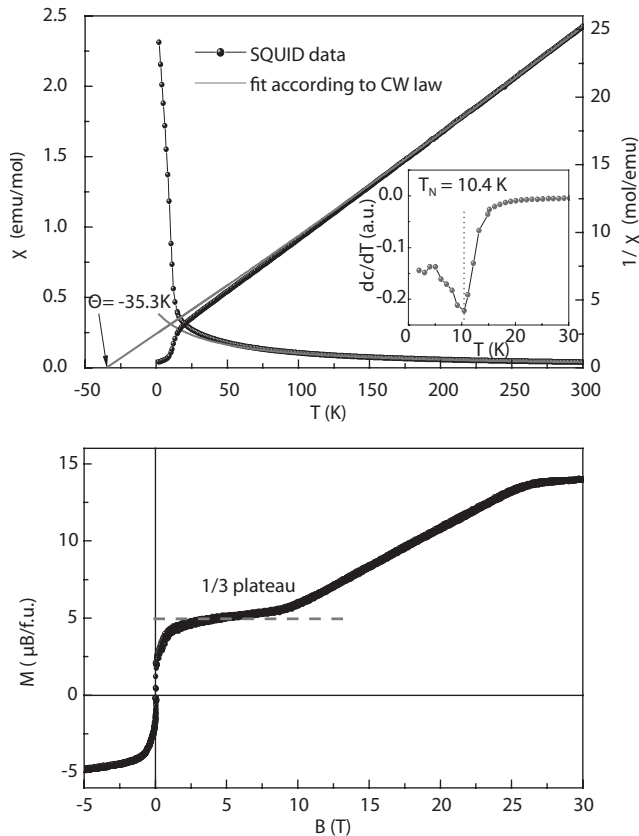


**Fig. 1.** Temperature dependence of the magnetic susceptibility at  $B = 0.1$  T (upper panel) and field dependence of the magnetization at  $T = 2.4$  K (lower panel) for  $\text{NaFe}_3(\text{HPO}_3)_2(\text{H}_2\text{PO}_3)_6$ .

magnetic subsystems corresponding to two crystallographic positions for  $\text{Fe}^{3+}$  ions. The Fe(1) ions form dimers coupled via two phosphate groups  $\text{HPO}_3$  in the structure, while Fe(2) ions bridge the dimers into 3D magnetic network via  $\text{H}_2\text{PO}_3$  phosphate groups. The  $\text{NaFe}_3(\text{HPO}_3)_2(\text{H}_2\text{PO}_3)_6$  demonstrates a long-range antiferromagnetic order at about 10 K and reveals plateau on the magnetization curve on one-third of the saturation field (Fig. 1). ESR data corroborate very well with the picture yielded from the structural and static magnetization data. An accurate quantitative analysis of the ESR lineshape requires the usage of sum of two Lorentzian functions for proper description of the experimental data. It means that two different resonance modes  $L_1$  and  $L_2$  may be distinguished in the spectrum, which are characterized by isotropic effective  $g$ -factors  $g_1 = 1.99(1)$  and  $g_2 = 1.99(3)$ , typical of high spin  $\text{Fe}^{3+}$  ( $S = 5/2$ ) in octahedral oxygen coordination. The difference in origin of two resonance modes is most obvious from the behavior of the integral ESR intensity  $\chi_{\text{ESR}}$  which is proportional to the number of magnetic spins (Fig. 2). It was estimated by double integration of the experimental first derivative ESR spectrum for each temperature. The integral ESR intensity  $\chi_{\text{ESR}2}$  for  $L_2$  mode demonstrates Curie-Weiss-like growth down to  $\sim 30$  K, then passes through maximum and decreases non-monotonically.

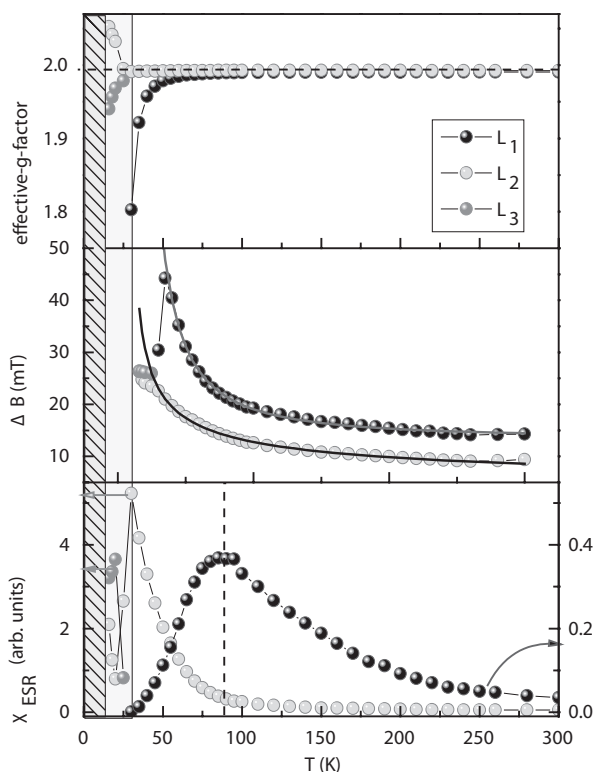


**Fig. 2.** The temperature dependence of the effective  $g$ -factor, the ESR linewidth and ESR integral intensity for two resolved components of ESR spectra for  $\text{NaFe}_3(\text{HPO}_3)_2(\text{H}_2\text{PO}_3)_6$ .

In contrast  $\chi_{\text{csr1}}$  passes through a broad maximum at about 90 K resembling the behavior of the low-dimensional spin-gapped system. Taking into account that the Fe(1) ions form dimers one can expect that  $L_1$  mode corresponds to the signal from this dimer magnetic sublattice, while  $L_2$  mode can be related to the signal from Fe(2) ions, which bridge the dimers into 3D magnetic network. At  $T^* \sim 30$  K the  $L_1$  signal vanishes and cannot be detected at  $T < T^*$ . Instead of it at lower temperature another resonance mode  $L_3$  was revealed and related to AFMR mode arising upon approaching the long-range ordering transition from above. The possible spin-configuration model for new compound was proposed based on theoretical density functional calculations.

The financial support of the Foundation for Basic Research (grant 14-02-00245), (grant 14-02-00111) and the Excellence Initiative of the German Federal Government and States is gratefully acknowledged.

---



---

## SECTION 4

# THEORY OF MAGNETIC RESONANCE

## Distance Measurements by Peldor Spectroscopy in Systems Containing Photoexcited Triplet States and Nitroxides

**D. Carbonera, M. Di Valentin, M. Albertini, E. Zurlo, and M. Gobbo**

Dipartimento di Scienze Chimiche, Università di Padova, Padova 35131, Italy

Pulsed electron–electron double resonance (PELDOR) is a well-established technique for measuring nanometer distances in spin-labeled systems. Conventionally, PELDOR is performed on nitroxide spin labels. In recent years, numerous efforts have been devoted to the development of alternative spin labels, featuring more attractive properties. The orthogonal labeling approach, based on the use of non-identical labels, which can be addressed selectively in the EPR experiment, has proved to be very promising for the Gd(III)-nitroxide pair. Further development of orthogonal labeling approaches is essential to broaden the applicability of the technique. In this context, we have explored the possible advantage of using a photoexcited triplet state ( $S = 1$ ), as an orthogonal spin label to be coupled to the nitroxide radical. The triplet state has distinctive properties compared to metal centers, since the large anisotropy due to the zero-field splitting tensor is accompanied by a strong spin polarization.

Among organic chromophores, porphyrins have been widely studied by EPR spectroscopy, due to their high triplet yields, strong spin polarization, non extreme relaxation times, and moderate spectral anisotropy. To verify the feasibility of measuring nitroxide-porphyrin triplet state interspin distances, we have designed a ruler based on bis-labeled model peptides with well-defined, predictable separations between a porphyrin moiety and the 4-amino-1-oxyl-2,2,6,6-tetramethylpiperidine-4-carboxylic acid (TOAC) nitroxide. The peptide

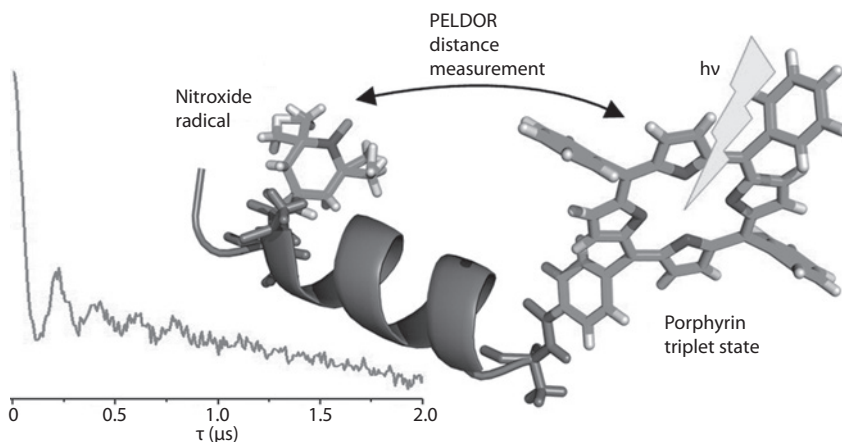


Fig. 1.

bridge connecting the paramagnetic probes consists of alternating L-alanine (Ala) and  $\alpha$ -aminoisobutyric acid (Aib) residues, known to promote the  $\alpha$ -helix conformation and consequently a well-defined geometry in terms of distance, relative orientation, and restricted conformational flexibility. The PELDOR traces of these systems show deep envelope modulation induced by electron-electron dipole interaction between the partners in the pair, providing an accurate distance measurement.

This new labeling approach has a high potential for measuring nanometer distances in more complex biological systems due to the sensitivity acquired from the spin polarization of the photoexcited triplet state spectrum. We used the technique to measure distance between the carotenoid triplet state populated under photoexcitation in the light harvesting protein PCP (peridinin chlorophyll protein) and a nitroxide, introduced in the protein by site directed spin labeling. The measured distance is in agreement with our previous assignment of the photo-protective site of PCP.

1. Di Valentin M., Albertini M., Zurlo E., Gobbo M., Carbonera D.: *J. Am. Chem. Soc.* **136**, 6582 (2014)

## Applications of Information Geometry to Saturated Spectra

**K. A. Earle** and **T. Broderick**

Physics Department, University at Albany, Albany, NY 12222, USA,  
kearle@albany.edu, tbroderick@albany.edu

We have shown in previous work that magnetic resonance spectra may be profitably analyzed by using concepts derived from information geometry [1, 2]. That analysis was restricted to the linear response regime where constraints, in the form of sum rules for example, induced a geometry on the line shape function treated as a probability density function (PDF). The conditions that a line shape function must satisfy for it to be considered as a member of a family of PDF's have also been described [1]. Although careful analysis of the linear response line shape is a useful tool for quantifying important details of molecular structure and dynamics, complementary information is available from the non-linear response line shape which is often sensitive to processes on longer time scales than the transient coherences probed in the linear regime. The non-linear response of a system satisfies constraints that do not allow for a direct interpretation in terms of a PDF, as the non-linear response may have absorptive and emissive character and thus cannot be constrained to be non-negative. Nevertheless, entropic methods and concepts from information geometry may be used to compare simulated and measured non-linear spectra in order to infer appropriate model parameter values. We demonstrate how this can be achieved for a model system described by the Zeeman interaction of a magnetic moiety with an applied magnetic field modulated by stochastic processes such as rotational diffusion. For the case of Electron Paramagnetic Resonance (EPR), we will show how the methods presented here may be extended to include hyperfine interactions which arise due to couplings of the electron magnetic moment with nearby nuclei.

1. Earle K. *et al.*: Appl. Magn. Reson. **37**, 865 (2010)
2. Earle K., Hock K.: Appl. Magn. Reson. **45**, 859 (2014)

## Investigation of Quantum Correlations and Quantum Computations with NMR Methods

**E. B. Fel'dman**

Institute of Problems of Chemical Physics of Russian Academy of Sciences,  
Chernogolovka 142432, Russian Federation, efeldman@icp.ac.ru

Recently the model of deterministic quantum calculations with one qubit (DQC1) [1] was suggested. This model considers a system of one polarized qubit and several qubits in the maximal mixed state. It was shown [1] that this simple model yields exponential speed-up in calculations of the traces of unitary matrices. It was also shown [2] that simple NMR experiments in solids (free induction decay, electron-nuclear spin echo, etc.) can realize the DQC1 model and obtain speed-up in quantum calculations. It is very significant that there is no entanglement in this system. The quantum correlations which are responsible for speed-up can be characterized by quantum discord [1].

We suggested a many-qubit spin model [3, 4], analogous to the one in [1]. Our model allows the investigation of quantum correlations and an analytical calculation of quantum discord. We consider a ring of nuclear spins ( $I = 1/2$ ), coupled by the dipole-dipole interactions in a strong external magnetic field. We call it subsystem A. The distances between spins of subsystem A are not necessarily the same. Subsystem A interacts with the impurity spin  $S$ , which is in the center of the ring (subsystem B). We calculate quantum discord analytically at different relations between the Larmor frequencies of the ring spins and the impurity spin. Such calculations are possible only in the high temperature approximation [3, 4]. We developed a method which allows us to find the contributions of different parts of the spin-spin interactions to quantum correlations [3, 4].

We have also found a method, different from DQC1, for the calculation of different sums with an exponential speed-up.

Our work is supported by the Russian Foundation for Basic Research (Grant No.13-03-00017) and the Program of the Presidium of RAS No.32 "Electron spin resonance, spin-dependent electron effects and spin technologies".

1. Datta A., Shaji A., Caves C.M.: Phys. Rev. Lett. **100**, 050502 (2008)
2. Zobov V.E.: JETP **119**, 817 (2014)
3. Doronin S.I., Fel'dman E.B., Kuznetsova E.I.: Phys. Scr. **164**, 015008 (2015)
4. Doronin S.I., Fel'dman E.B., Kuznetsova E.I.: Quantum Inf. Processing (accepted)

## Resonance Line Shape and Orthogonal Two-Spin Correlation Functions in Magnetically Disordered Systems

**F. S. Dzheparov**

RC KI, FSBI SSC RF ITEP, Moscow 117218, Russian Federation, dzheparov@itep.ru

Homonuclear spin systems randomly distributed over crystal sites are considered. Spins of  $^{29}\text{Si}$  in silicon and  $^{13}\text{C}$  in diamond can be regarded as typical examples. Recently new theory of two-spin correlation functions in similar systems was developed, which indicates common ways to treat uniformly crystals with high ( $c = 1$ ) and small ( $c \ll 1$ ) concentration  $c$  of magnetic spins  $I = 1/2$  [1–3]. Main assumptions of the theory are analyzed and modernized to find a way for a treatment of the problem at arbitrary  $c$  and  $I$ .

1. Dzheparov F.S., Lvov D.V., Veretennikov M.A.: JETP Lett **98**, 484 (2013)
2. Dzheparov F.S., Lvov D.V., Veretennikov M.A.: Low Temperature Physics **41**, 9 (2015)
3. Dzheparov F.S.: Spin Dynamics in Disordered Solids. In “Encyclopedia of Complexity and Systems Science” (R. Meyer, ed.). New York: Springer 2015. DOI 10.1007/978-3-642-27737-5\_513-3

## Exploiting the Concept of Avoided Level Crossings for Analysing Magnetic Field Dependence of Solid-State CIDNP

**D. Sosnovsky<sup>1,2</sup>, J. Matysik<sup>3</sup>, G. Jeschke<sup>4</sup>, and K. Ivanov<sup>1,2</sup>**

<sup>1</sup> International Tomography Centre of SB RAS, Novosibirsk 630090, Russian Federation, denis.sosnovsky@tomo.nsc.ru

<sup>2</sup> Physics Department, Novosibirsk State University, Novosibirsk 630090, Russian Federation

<sup>3</sup> Institut für Analytische Chemie, Universität Leipzig, Leipzig D-04103, Germany

<sup>4</sup> Institut für Physikalische Chemie, ETH Zürich, Zürich CH-8093, Switzerland

Chemically Induced Dynamic Nuclear Polarization (CIDNP) is a method of creating non-thermal polarization of nuclear spins by using chemical reactions, which have radical pairs as intermediates. The CIDNP effect originates from (i) electron spin-selective recombination of radical pairs and (ii) dependence of the inter-system crossing rate in radical pairs on the state of magnetic nuclei [1]. The CIDNP effect can be investigated by using Nuclear Magnetic Resonance (NMR) methods. The gain from CIDNP is two-fold: it allows one to obtain considerable amplification of NMR signals; furthermore, CIDNP is a very useful tool for investigating elusive radicals and radical pairs.

While the mechanisms of the CIDNP effect in liquids are well established and understood, CIDNP mechanisms in solid state are still not fully clear. Difficulties in understanding the spin dynamics underpinning the CIDNP effect in the solid-state case are caused by the presence of anisotropic spin interactions, which result in the complex evolution of the spin system; the importance of such interactions for solid-state CIDNP has been discussed in previous works [2–4]. However, complete analysis of CIDNP in solid state is a challenging theoretical problem.

Previously, it has been demonstrated that the description based on level crossings is very useful for unravelling otherwise complex dynamics of nuclear spin systems with non-thermal polarization [5]. LCs and LACs provide a similar simplification in the CIDNP case as well. All features of liquid-state CIDNP can be interpreted in terms of LCs and LACs. The same holds for the solid-state case where anisotropic interactions play a significant role in CIDNP formation. In solids, all features arise from LACs (and never from LCs), since anisotropic couplings always result in perturbations, which turn all LCs into LACs. We have interpreted the CIDNP mechanisms in terms of the LAC concept and have formulated sign rules for polarization. Besides this, kinetic traces of CIDNP were calculated revealing contributions of different mechanisms in CIDNP formation.

This work has been supported by the Russian Foundation for Basic Research (project 14-03-00397) and the CPRF Grant MD-3279.2014.2.

1. Salikhov K.M., Molin Y.N., Sagdeev R.Z., Buchachenko A.L.: “Spin Polarization and Magnetic Effects in Chemical Reactions”, Elsevier, Amsterdam 1984.
2. Jeschke G.: *J. Am. Chem. Soc.* **120**, 4425 (1998)
3. Jeschke G., Matysik J.: *Chem. Phys.* **294**, 239 (2003)
4. Bode B.E., Thamarath S.S., Gupta K.B.S.S., Alia A., Jeschke G., Matysik J.: *Top. Curr. Chem.* **2013**, **339**, 105
5. Pravdivtsev A.N., Yurkovskaya A.V., Vieth H.-M., Ivanov K.L., Kaptein R.: *ChemPhysChem.* **14**, 3327 2013

## Intrinsic Gilbert Damping in Polycrystalline Multilayer Structures with Exchange Bias NiFe/Cu/NiFe/IrMn

A. N. Orlova, A. Y. Zubin, and G. S. Kupriyanova

Immanuel Kant Baltic Federal University, Kaliningrad, Russian Federation, galkupr@yandex.ru

Ferromagnetic resonance (FMR) method is widely used as a method for studying and determining the quality of the nanostructures, the diagnosis of their functional properties, since the resonant frequency is sensitive to the internal magnetic fields to a field anisotropy, the quality of the structure. Data FMR can be used to study transport properties of multilayer structures, in view of the connection of these properties with the Gilbert damping constant [1, 2].

Of particular interest is the definition of internal Hilbert constants in structures with exchange bias, establishing a relationship between a constant and exchange bias field. In the literature there are conflicting data on the relationship between internal constant Hilbert and the field of the exchange bias [3].

From this point of view an important task is to identify the contributions due to the magnetic internal damping to determine the exact value of the Gilbert constant, as well as the elucidation of the mechanism of interaction between the layers. These characteristics can be extracted from the line width FMR, the angular dependence of the resonance frequency and line width when the sample is rotated relative to the magnetic field and from the frequency dependence of the resonant field. However, the extraction of these parameters becomes problematic in multilayer polycrystalline structures in the presence of due to magnetic inhomogeneous. Some problems arise because of the overlap of the resonance lines of each layer, and the broadening of the resonance lines, caused by the interaction between the layers, the spread of the resonance fields in crystals. In this work three-layers structures FM/NM/FM with different thickness of NM interface and the structures with exchange bias field Si/Ta/NiFe/Cu/NiFe/IrMn/Ta were investigated by FMR [2, 3]. The out-of-plane and in-plane angular dependences of the resonance field and line width were registered. Landau-Lifshitz-Gilbert (LLG) equation was used for modeling of experiment results and extracted spectral parameters for each line. It was found that the line shape in some structures do not described by Lorentz function due to magnetic inhomogeneous. To take into account effect of magnetic inhomogeneous we suppose that the line shape is set by Gaussian and Lorents convolution. Our approach gives us possibility to extract homogeneities contributions for calculation of magnetic internal damping (Gilbert constant), the parameters of interlayer exchange coupling.

1. Platow W., Anisimov A.N., Dunifer G.L., Farle M., Baberschke K.: Phys. Rev. B, **58**, no. 9, 5611–5621 (1998)
2. Zubin A.Y., Astashenok A.V., Kupriyanova G.S. Vestnik I.K.: BFU **4**, 43–51 (2013)
3. Kupriyanova G., Rodionova V., Chechenin N., Dzhun I., Ay F., Rameev B.: Book of Abstracts. MISM Moscow 29 June–2 July, 2014, p. 612.
4. Song H.S., Lee K.-D., You C.-Y., Yang S.-H., Parkin S., Park B.-G., Sohn J.-W., Hong J.-I., Shin S.-C.: Appl. Phys. Express **8**, 053002 (2015)



---

## SECTION 5

MODERN METHODS OF MAGNETIC RESONANCE.  
OTHER APPLICATIONS OF MAGNETIC  
RESONANCE

## RF-SABRE and PH-INEPT Sequences Make High Field SABRE Feasible

**A. N. Pravdivtsev,<sup>1,2</sup> A. V. Yurkovskaya<sup>1,2</sup>, H.-M. Vieth<sup>1,3</sup>,  
and K. L. Ivanov<sup>1,2</sup>**

<sup>1</sup> International Tomography Center, Siberian Branch of the Russian Academy of Science,  
Novosibirsk 630090, Russian Federation, a.n.true@tomo.nsc.ru

<sup>2</sup> Novosibirsk State University, Novosibirsk, 630090, Russian Federation

<sup>3</sup> Freie Universität Berlin, Berlin D-14195, Germany

We present a method of hyper-polarizing protons ( $^1\text{H}$ ) and “insensitive” NMR nuclei (here,  $^{15}\text{N}$ ) by exploiting the SABRE (Signal Amplification By Reversible Exchange) technique and transferring spin order from protons originating from parahydrogen. We demonstrate that hyperpolarization transfer due to a coherent mechanism operative not only at low (1 mT) and ultralow ( $\sim 1\ \mu\text{T}$ ) magnetic field but also at the high field of an NMR spectrometer in the presence of a suitable RF-excitation scheme: for protons we developed a method named  $^1\text{H}$ -RF-SABRE and for heteronuclei (e.g.  $^{15}\text{N}$ ) we used the following techniques:  $^{15}\text{N}$ -RF-SABRE, PH-INEPT, PH-INEPT+ or PH-INEPT++.

High-field SABRE techniques are particularly important for solving the sensitivity issue in NMR: they dramatically enhance NMR signals and avoid technically demanding field-cycling. Thus, the proposed method can serve as a new robust and sensitive tool in NMR. Furthermore, the reported SABRE experiments make feasible continuous re-hyperpolarization of substrates in high-field experiments. Polarization can be quickly restored to the maximal level within only a few seconds with the polarization levels staying constant over at least several hundred experiments.

This work has been supported by the Russian Foundation for Basic Research (projects No. 13-03-00437, 14-03-00397 and 15-33-20716), the CPRF grant MD-3279.2014.2 and the Alexander von Humboldt Foundation.

## Electron Paramagnetic Resonance Study of Color Centers in Silicon Carbide. From Identification to Quantum Applications

**V. Soltamov<sup>1</sup>, B. Yavkin<sup>2</sup>, G. Astakhov<sup>3</sup>, V. Dyakonov<sup>3</sup>, H. Kraus<sup>3</sup>,  
F. Fuchs<sup>3</sup>, S. B. Orlinskii<sup>2</sup>, and P. G. Baranov<sup>1</sup>**

<sup>1</sup> Ioffe Institute, Saint-Petersburg 194021, Russian Federation, victor\_soltamov@mail.ru

<sup>2</sup> Kazan Federal University, Kazan 420008, Russian Federation, boris.yavkin@gmail.com

<sup>3</sup> Julius-Maximilian University of Würzburg, Würzburg 97074, Germany,  
astakhov@physik.uniuerzburg.de

Detection and manipulation of the spin states in solids at room temperature is a basis of the emerging fields of quantum information processing and spintronics. The first system on which such manipulations were realized at room temperature was the nitrogen-vacancy (NV) center in diamond. Owing to its unique optical excitation cycle that leads to the optical alignment of triplet sublevels of the defect ground state, the NV center can be easily initialized, manipulated, and readout by means of optically detected magnetic resonance (ODMR) [1, 2]. A search for systems possessing unique quantum properties of the NV defect in diamond that can extend the functionality of such systems seems to be a very promising objective.

In the recent few years, the big progress in this field has been achieved on color centers in silicon carbide (SiC). Particularly the spin properties of these centers have been shown to be applicable for creation of high sensitive quantum magnetometers with optical pumping, room temperature operated masers and single spin quantum bits [3–5].

To use the color centers in active devices better understanding of the impact of external and internal environment as well as the microscopic model of the centers is required. How the properties of the centers are altered by optical excitation? What are the effects of external magnetic and microwave fields? What role play the ambient temperature, isotopic composition of the host material and the position of the centers in the crystal lattice? Alteration of these parameters drastically changes the behavior of the system, providing many degrees of freedom to play with, but also to account for.

Here we would like to show how the Electron paramagnetic resonance and related methods, such as time resolved EPR spectroscopy, ODMR and High frequency ENDOR could answer the questions mentioned above thus showing the SiC as the most perspective material for spintronic applications.

1. Gruber A., Drabenstedt A., Tietz C., Fleury L., Wrachtrup J., von Borczyskowski C.: *Science* **276**, 2012 (1997)
2. Koehl W.F., Buckley B.B., Heremans F.J., Calusine G., Awschalom D.D.: *Nature (London)* **479**, 84 (2011)
3. Kraus H., Soltamov V.A., Riedel D., Vath S., Fuchs F., Sperlich A., Baranov P.G., Dyakonov V., Astakhov G.V.: *Nature Phys.* **10**, 157–162 (2014)
4. Kraus H., Soltamov V.A., Fuchs F., Simin D., Sperlich A., Baranov P.G., Astakhov G.V., Dyakonov V.: *Sci. Rep.* **4**, 5303 (2014)
5. Widmann M., Lee S.-Y., Rendler T., Son N.T., Fedder H., Paik S., Yang L.-P., Zhao N., Yang S., Booker I., Denisenko A., Jamali M., Momenzadeh S.A., Gerhardt I., Ohshima T., Gali A., Janzen E., Wrachtrup J.: *Nat. Mater.* **14**, 164–168 (2015)

---

---

## POSTERS

## NMR Studies of the Solution of Mechanically Activated Calcium Gluconate

**M. M. Akhmetov<sup>1</sup>, G. G. Gumarov<sup>1</sup>, V. Yu. Petukhov<sup>1</sup>, G. N. Konygin<sup>2</sup>,  
D. S. Rybin<sup>2</sup>, and A. B. Konov<sup>1</sup>**

<sup>1</sup> Zavoiisky Physical-Technical Institute, Russian Academy of Sciences, Kazan 420029,  
Russian Federation, mansik86@mail.ru

<sup>2</sup> Physical-Technical Institute Ural Branch of RAS, Izhevsk, Russian Federation, dsrybin@mail.ru

The interaction of carboxyl- and hydroxyl-containing sugar acids with metal ions is a very interesting subject in the biochemistry of metals associated with ecological and toxicological problems [1]. <sup>1</sup>H and <sup>13</sup>C NMR, and two-dimensional NMR were used for studying the solution and powder of the calcium salt of gluconic acid C<sub>12</sub>H<sub>22</sub>CaO<sub>14</sub> · H<sub>2</sub>O subjected to mechanical activation. Conclusions were made about the structure of the molecule on the basis of spectroscopic measurements and simulation using ACD 10.0.

NMR spectra of solutions in D<sub>2</sub>O were recorded on a Bruker Avance 400 spectrometer with a superconducting magnet 9.5 T at room temperature at the resonant frequency of the <sup>13</sup>C nuclei at 100 MHz and <sup>1</sup>H nuclei at 400 MHz.

Figure 1 shows the <sup>1</sup>H NMR spectrum of the 8.3 mMol D<sub>2</sub>O solution of calcium gluconate of the initial and mechanically activated samples. It can be concluded that no changes take place in the proton environment of the molecule. Solid-state <sup>13</sup>C NMR spectroscopy shows changes in the structure of the spectra, broadening and redistribution of the intensities of the resonance lines. Solid phase spectra of mechanically activated samples with the activation time from 10 min to 3 h are almost identical but differ from the spectrum of the original

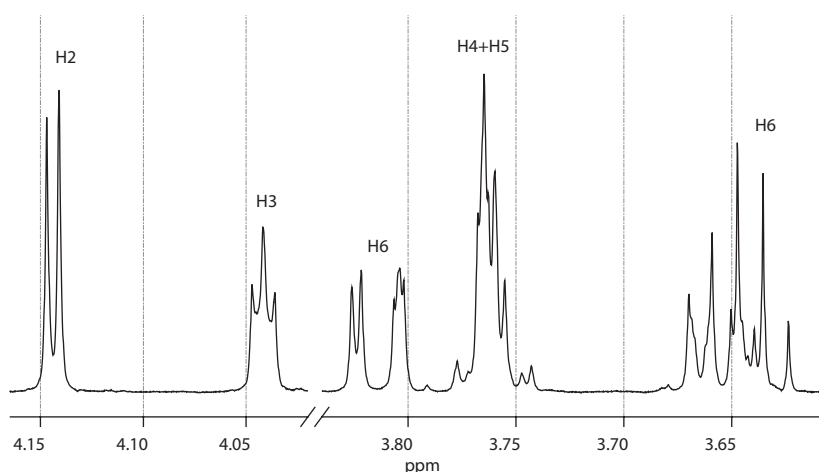


**Fig. 1.** <sup>1</sup>H NMR spectrum of the D<sub>2</sub>O solution of calcium gluconate.

sample. Main changes in the NMR spectrum are associated with the formation of a broad band in the region of lines with the values of the chemical shifts of 73 and 74 ppm, which corresponds to the positions of the carbon atoms C2 and C3 [2] associated with calcium-coordinated oxygen atoms of hydroxyl groups. Thus, it is possible to assume that in the process of mechanical activation of calcium gluconate carbons C4-C6 mainly occupy positions equivalent to the carbon atoms C2 and C3, and the number of oxygen atoms of the alcohol groups coordinated by calcium ions increases. The increase in the coordination number of the calcium ion is indicated by the shift of the center of gravity of the band C1 to the region of large values of the chemical shift as it occurs during the formation of intra-coordination compounds of gluconic acid.

In the  $^{13}\text{C}$  NMR spectra of  $\text{D}_2\text{O}$  solutions of calcium gluconate in the mode of the suppression of the signal from protons there are six lines, each of which corresponds to a certain position of the carbon atom in the molecule of calcium gluconate. The spectrum shows a slight change of the chemical shift of the line C1 on the order of 0.1 ppm, which is in good agreement with data of solid-state NMR spectroscopy. It was found that no breakage of the C-C bond, as previously assumed, takes place. Also, using the program ACD 10.0 and two-dimensional NMR spectroscopy it was found that the off-diagonal cross-peaks COSY are symmetrical and correspond to the region of the interaction of two close hydrogen atoms.

Thus, it can be concluded the shape of the molecule is zigzag-like (elongated).

1. Escandar M.G. *et al.*: Polyhedron **15**, 2251 (1996)
2. Tajmir-Riahi H.A.: Can. J. Chem. **67**, 651 (1989)

## Influence of Uniaxial Compression on EPR Spectra of Nickel Chloride with 3-Amino-4-Ethoxycarbonylpyrazol Compound

A. S. Berezin<sup>1,2</sup>, V. A. Nadoliny<sup>1</sup>, and L. G. Lavrenova<sup>1,2</sup>

<sup>1</sup> Nikolaev Institute of Inorganic Chemistry, Novosibirsk 630090, Russian Federation, berezin-1991@ngs.ru

<sup>2</sup> Novosibirsk State University, Novosibirsk 630090, Russian Federation

Investigation of properties of nickel complexes is of great interest, since these complexes are used in various fields of life. In recent decades, based on the availability of stable paramagnetic compounds of  $\text{Ni}^{2+}$  and  $\text{Ni}^{3+}$  ions, nickel has been considered as a potential complexing agent for producing molecular magnets. Moreover, their properties strongly depend on nature of complex former and its nearest environment. To change magnetic properties of such compounds is possible for example by impacting.

The present study is a continuation of research [1] on the influence of pressure on compounds of 3d-metal halides with 3-amino-4-ethoxycarbonyl-pyrazole ( $\text{ML}_2\text{X}_2$ ) as a ligand.  $\text{NiL}_2\text{Cl}_2$  compound [2] has been investigated. X-band EPR spectrum of initial polycrystalline  $\text{NiL}_2\text{Cl}_2$  is absent. Compacting of the sample in a titanium mold under pressure of about 1,000 atmospheres leads to arising EPR spectrum at room temperature with following parameters in X-band:  $S = 1$ ,  $g_{\perp} = 2.72(3)$ ,  $g_{\parallel} = 2.55(5)$ ,  $D = 1230(100)$  G and  $E = 0$ . To determine the correct  $g$ -tensor, EPR spectrum in Q-band, where the  $h\nu = g\beta H \gg D$  condition is valid, were recorded. This spectrum is described by a spin Hamiltonian with

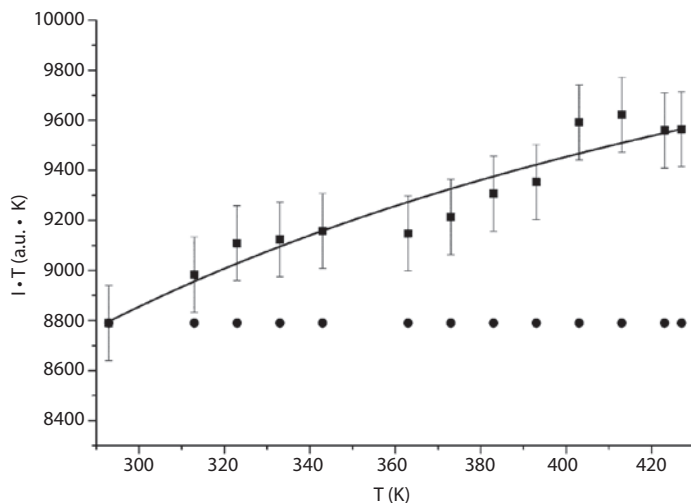


**Fig. 1.** Temperature dependence of the EPR spectrum integrated intensity multiply by temperature for the reference  $\text{CuSO}_4 \cdot 5\text{H}_2\text{O}$  sample (●) and a  $\text{NiL}_2\text{Cl}_2$  sample (■).



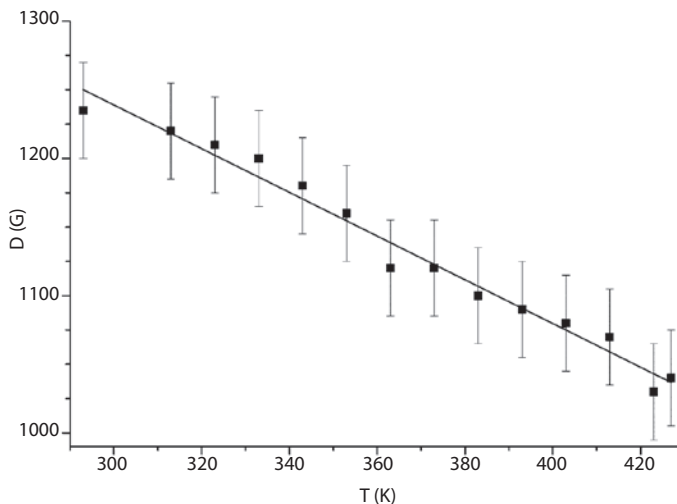


**Fig. 2.** Temperature dependence of the  $D$  parameter for a uniaxially compressed polycrystalline  $\text{NiL}_2\text{Cl}_2$  sample.

the following parameters:  $S = 1$ ,  $g_{\parallel} = 2.18(1)$ ,  $g_{\perp} = 2.17(2)$ ,  $D = 1300(100)$  G and  $E = 0$ . The concentration of paramagnetic centers observed in a sample after uniaxial compression was found by EPR to be about  $\sim 3\%$ . A low concentration of nickel ion states observed in the EPR spectra is due to a statistical distribution of microcrystal orientations with respect to the direction of uniaxial compression, the influence of which leads to the irreversible changes.

Temperature dependence of EPR spectra was recorded in X-band from 293 to 425 K. Intensity of EPR spectra changes according to  $I \sim (1 - \exp(-2h\nu/kT))/(1 + \exp(-h\nu/kT) + \exp(-2h\nu/kT) + \exp(\Delta E/kT))$  [3] with  $\Delta E = 0.018$  eV (Fig. 1). Thus, the states are the low-lying singlet and high-lying triplet with  $\Delta E$  splitting. Parameter of ZFS also depends on temperature according to  $\Delta D/\Delta T = -1.6$  G/K (Fig. 2) pointing out to the crystal field changes.

The XRD analysis showed that the all reflections position for sample subjected to uniaxial compression is the same as for the original sample [2]. The only difference is the appearance of a broad line  $21^\circ 2\theta$  with the width of  $\sim 10^\circ 2\theta$  in the diffraction pattern, which may indicate the emergence of an amorphous phase in the sample after uniaxial compression. In this phase, the nickel ground state  $3d^8$  has the electronic state with spin  $S = 0$ . This electronic state may result from lowering the symmetry of the nickel ion environment due to the tetrahedral distortion.

This research was financially supported by the Russian Foundation for Basic Research (Grants No. 15-03-00878 a).

1. Berezin A.S., Nadolinny V.A., Lavrenova L.G.: *JOSC* **28**, 1007 (2015)
2. Lavrenova L.G., Zhilin A.S., Bogomyakov A.S. *et al.*: *J. Struct. Chem.* **54**, 4, 713 (2013)
3. Poole C.P.: *Electron Spin Resonance: A Comprehensive Treatise on Experimental Techniques/* edited by Dekabrun. USSR. 1970. -559.

## Development of the Method of Indirect Registration of D<sub>2</sub>O Involved in a Chemical Exchange

**A. Bogaychuk<sup>1</sup>, G. Kupriyanova<sup>2</sup>, N. Sinyavsky<sup>3</sup>, and A. Gorkin**

<sup>1</sup> Immanuel Kant Baltic Federal University, Kaliningrad 236041, Russian Federation, aleksandr.bogaychuk@gmail.com

<sup>2</sup> Immanuel Kant Baltic Federal University, Kaliningrad 236041, Russian Federation, galkupr@yandex.ru

<sup>3</sup> Baltic State Academy, Kaliningrad 236029, Russian Federation, n\_sinyavsky@mail.ru

One parameter of the organism, as measured by MRI is the level of tissue perfusion. Back in 1987, Ackerman, Ewy, Becker and Shalwitz assessed the level of tissue perfusion rat deuterium signal of D<sub>2</sub>O [1]. However, the direct registration of deuterium signal has a range of well-known shortcomings in comparison with direct detection of protons. As one of the solutions to this problem, there is the idea of indirect registration deuterium concentration by proton signals. In particular, it has repeatedly conducted the study changes the relaxation times of water, depending on the concentration of deuterium, as for example in the work Vasilyev and Kashaev [2].

In this work, as a first approximation to the biological samples fat, studied glycerol with deuterated water (concentration of 10, 15, 20, 30, 40, 50%). Relaxation measurements were performed on a Varian 400 MHz at the frequency of protons, with and without affecting at the frequency of deuterium nuclei.

Also been produced multicomponent decomposition relaxation curves by using inverse Laplace transform. The algorithm of this treatment was based on the program RILT, presented in Iari-Gabriel Marino [3].

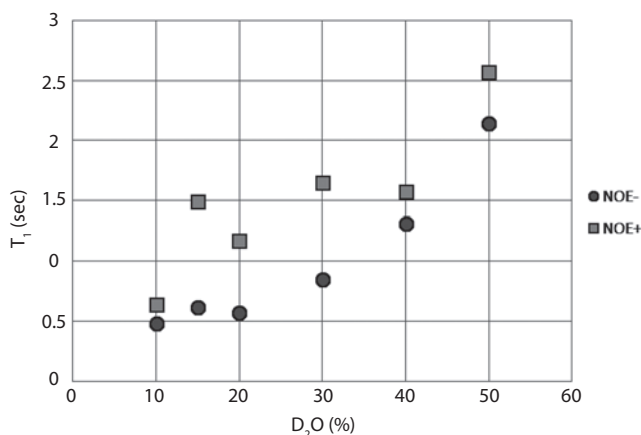


**Fig. 1.**  $T_1$  relaxation times signal by water in samples Glycerol with any D<sub>2</sub>O concentrations.

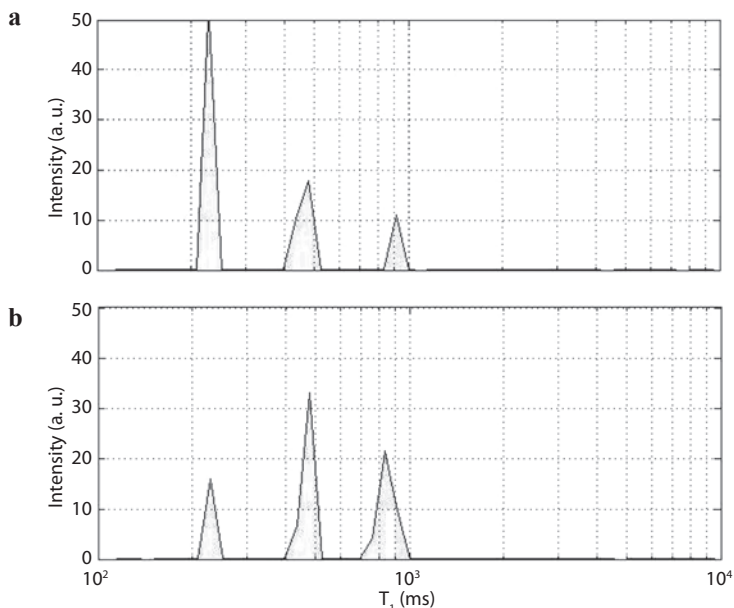


**Fig. 2.** Distributions of relaxation times  $T_1$  signal by water Glycerol with  $D_2O$  (1:1) without (a) and with (b) NOE.

Preliminary results indicated that with increasing concentrations of deuterated water, processes of exchange with water affect OH-groups, while the CH- and  $CH_2$ -groups are practically not used.

In order to indirect register deuterium has proposed a method of comparison of the spin-lattice relaxation times  $T_1$  with and without impact on the frequency of the deuterium in the moments of relaxation delay.

Figure 1 shows the dependence of the spin-lattice relaxation time of the test solutions with and without affecting frequency of deuterium in a concentration-dependent  $D_2O$ . Worth noting not only the growth of the relaxation times, but they increase when exposed to deuterium nuclei.

For a more detailed study this effect was made decomposition of the spin-lattice relaxation using inverse Laplace transform. Figure 2 shows a decomposition for 50% glycerol solution with  $D_2O$ . This decomposition illustrates a significant increase slowly decaying component is relatively short at influence on deuterium.

In this work it was proposed and tested system makes it possible to identify the contribution of deuterated water in the chemical exchange processes, as well as the possibility to estimate the concentration of the heavy water.

1. Ackerman J.J., Ewy C.S., Becker N.N., Shalwitz R.A.: Proc. Natl. Acad. Sci. USA **84**(12) 4099–4102 (1987)
2. Vasilyev S., Kashaev NMR research into  $H_2O$ - $H_2O_2$ - $D_2O$  system. Book of Abstracts NMRCM 2014. Saint Petersburg, Russia 2014. p. 68.
3. Iari-Gabriel Marino, Regularized Inverse Laplace. –<http://www.mathworks.com/matlabcentral/fileexchange/6523-rilt/content/rilt.m>

## Photo- and Thermo-Active Magnetic Properties of Iron-Containing Dendrimers

**N. Domracheva<sup>1</sup>, V. Vorobeva<sup>1</sup>, M. Gruzdev<sup>2</sup>, U. Chervonova<sup>2</sup>,  
A. Kolker<sup>2</sup>, and A. Pyataev<sup>3</sup>**

<sup>1</sup> Zavoiisky Physical-Technical Institute, Russian Academy of Sciences, Kazan 420029, Russian Federation, ndomracheva@gmail.com

<sup>2</sup> G. A. Krestov Institute of Solution Chemistry, Ivanovo 153045, Russian Federation, gms@isc-ras.ru

<sup>3</sup> Kazan Federal University, Kazan 420008, Russian Federation, 151eu@mail.ru

Photo- and thermo-active magnetic properties of two novel iron-containing dendrimeric systems – liquid-crystalline poly (propylene imine) (PPI) dendrimer with  $\gamma$ -Fe<sub>2</sub>O<sub>3</sub> nanoparticles (NPs) and spin-crossover ( $S = 1/2 \leftrightarrow 5/2$ ) iron(III) dendrimeric complex have been studied for the first time. Electron paramagnetic resonance (EPR) investigation of the first system has shown that  $\gamma$ -Fe<sub>2</sub>O<sub>3</sub> NPs fabricated in PPI-dendrimer have the average diameter  $\sim 2.5$  nm, magnetic moment about 350 Bohr magnetons, possess uniaxial magnetic anisotropy and “core/shell” structure [1]. A temperature-driven transition from superparamagnetic to ferrimagnetic state was observed for the sample with blocking temperature  $\sim 18$  K. The influence of pulsed laser irradiation on the superparamagnetic properties of  $\gamma$ -Fe<sub>2</sub>O<sub>3</sub> NPs was studied by EPR spectroscopy [2]. It has been shown that irradiation of the sample held in vacuum and cooled in zero magnetic field to 6.9 K leads to the appearance of a new EPR signal, which decays immediately after the irradiation is stopped (Fig. 1). The appearance and disappearance of this new signal can be repeated many times at 6.9 K when we turn on/turn off the laser. We suppose that

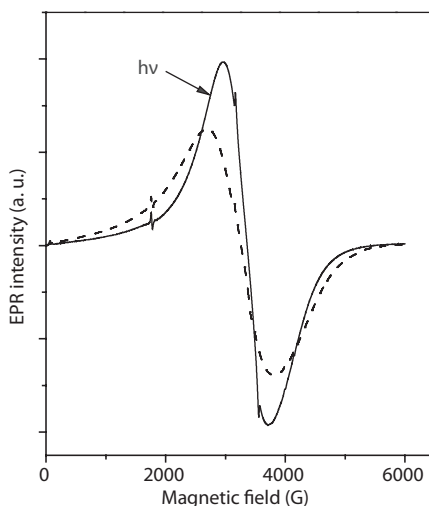


**Fig. 1.** Changes in the EPR signal during laser irradiation with a wavelength of  $\lambda = 266$  nm at 6.9 K for FC-sample held in vacuo.

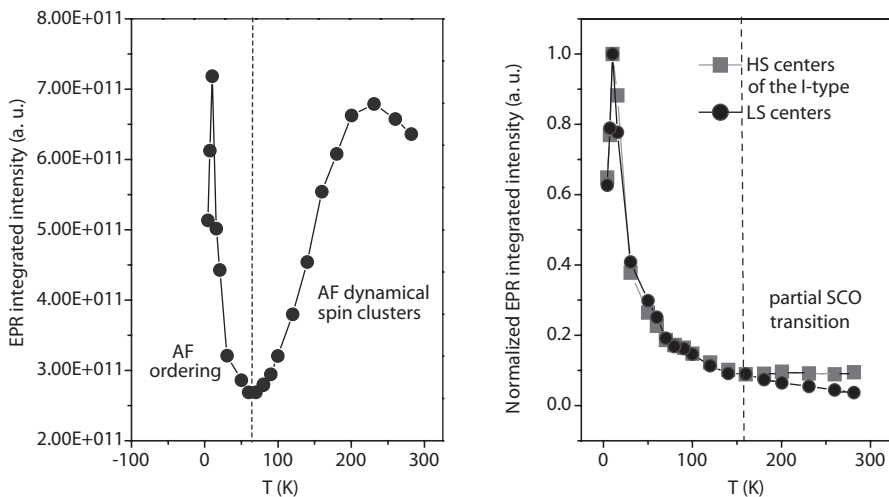


**Fig. 2.** The temperature dependence of the EPR lines integrated intensity of the whole EPR spectrum and the temperature dependence of the EPR normalized integrated intensity of the LS and HS centers of the I-type.

the generation of conduction band electrons by irradiation into the band gap of the semiconductor  $\gamma$ -Fe<sub>2</sub>O<sub>3</sub> NPs changes the superparamagnetic properties of NPs.

Thermo-active magnetic properties have been studied for the second system – dendrimeric spin crossover Fe(III) complex of formula [Fe(L)<sub>2</sub>]<sup>+</sup>PF<sub>6</sub><sup>-</sup>, where L = 3,5-di(3,4,5-tris(tetra-decyloxy)benzoyloxy)benzoyl-4-oxy-salicylidene-N'-ethyl-N-ethylenediamine. It has been shown that this system contains three types of magnetically active iron centers: one  $S = 1/2$  low-spin (LS) and two  $S = 5/2$  high-spin (HS) centers with strong ( $D = 0.421 \text{ cm}^{-1}$ ,  $E = 0.109 \text{ cm}^{-1}$ ) low-symmetry and weak ( $0.02 \text{ cm}^{-1} < |D| < 0.03 \text{ cm}^{-1}$ ) distorted octahedral environments. EPR spectroscopy revealed that the compound is magnetically inhomogeneous, consists of two magnetic sub-lattices, displays a partial spin crossover ( $S = 5/2 \Leftrightarrow 1/2$ ) of ~25% of the Fe(III) molecules above 160 K and undergoes antiferromagnetic (AF) ordering below 10 K (Fig. 2). The HS Fe(III) centers with weakly distorted octahedral environment most probably form chains in layers. The dimeric molecules formed from LS-LS centers and HS-HS centers with strongly distorted octahedral environment are likely located between the layers and are involved in the spin crossover. EPR has shown the presence of AF dynamical spin clusters in the high temperature (70–300 K) range, which are visible in the short time scale ( $10^{-10}$  s) and could not be registered in the static magnetic measurements. Mössbauer spectroscopy confirms the concept of dynamical spin clusters.

This work was supported by RAS Presidium program No. 24 and in part by the RFBR, project No. 11-03-01028.

1. Domracheva N., Pyataev A., Manapov R., Gruzdev M.: ChemPhysChem. **12**, 3009 (2011)
2. Domracheva N., Vorobeveva V., Gruzdev M., Pyataev A.: J. Nanopart. Res. **17**, 83 (2015)

## Ferromagnetic Resonance of Deposited from Laser Plasma Nanosized Layers of the Diamond-Like Diluted Magnetic Semiconductor on the Basis of Si, Doped by Mn

**E. S. Demidov, V. V. Podol'skii, V. P. Lesnikov, V. V. Karzanov,  
A. A. Tronov, and L. I. Budarin**

Lobachevsky State University of Nizhny Novgorod, Nizhny Novgorod 603950, Russian Federation,  
demidov@phys.unn.ru

The diluted magnetic semiconductors (DMS) on the basis of the diamond-like semiconductors doped by iron group 3d-impurities represent the big interest for development of new devices of spintronics [1]. The highest temperature diluted magnetic semiconductors on the basis of diamond-like semiconductors were synthesized in our laboratory by pulse deposition from a laser plasma [1–5]. It was demonstrated that such strongly nonequilibrium technology can be used to synthesize thin (30–200 nm) GaSb:Mn and InSb:Mn layers with the Curie temperature  $T_C$  above 500 K and Ge:Mn, Si:Mn, and Si:Fe layers with the Curie temperatures of 400, 500, and 250 K, respectively, on single-crystal GaAs, Se, and sapphire ( $\text{Al}_2\text{O}_3$ ) substrates. Especially attractive DMS are on the basis of elementary semiconductor Si in connection with compatibility with the most widespread silicon technology. The most studied diluted magnetic semiconductor Si:Mn with 10–15% Mn has the highest mobility of the current

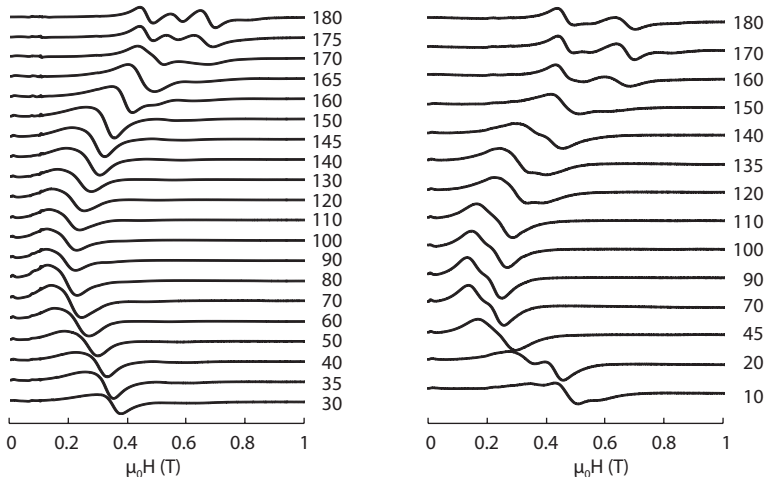


**Fig. 1.** FMR spectra at 293 K of 50 nm layer of DMS Si:15%Mn on GaAs (100) at rotation of the sample round  $\langle 110 \rangle$  axis at the left and  $\langle 010 \rangle$  on the right. Figures on the right are angles in degrees.

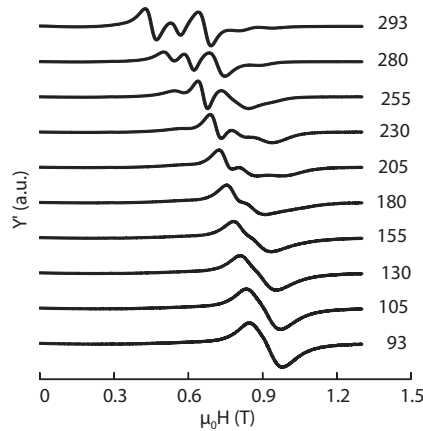


**Fig. 2.** Temperature dependence of FMR of layer of DMS Si:15%Mn on GaAs (100).

carriers. The Mn impurity in it has the high electric and magnetic activity. The direct evidence of the ordered structure of the layers of the diluted magnetic semiconductor Si:Mn/GaAs was presented earlier [4, 5], which was obtained using high-resolution transmission electron microscopy (HRTEM) and local electron diffraction (LED). The self-organized formation of the superlattice structure with the period of the triple distance between the nearest atomic layers (110) and the interval between layers (110) doped with Mn atoms and oriented along the growth direction of the Si:Mn film was found. The layers Si:15% Mn (or  $\text{Si}_{2.5}\text{Mn}_{0.5}$ ) consist of 15- to 50-nm blocks with the mutually perpendicular orientations of the superlattice modulations. Manganese atoms in the (110) layers doped with this impurity are located in the form of single-atom stripes, which alternate with the silicon single-atom stripes. With such nanosized structure of this DMS we relate the complicated FMR spectrum of the DMS Si:Mn earlier observed by us [3]. In the present work the analysis of experimental, recorded on Bruker EMX spectrometer, of such FMR spectra is carried out at temperatures 77–300 K and in fields up to 1.5 T (Fig. 1, 2). The numerical simulation of FMR spectra was performed on the basis of Landau-Lifshitz-Gilbert equations with rank of a matrix of coefficients  $8 \times 18$  with the account of four possible variants of anisotropy in agreement with the HRTEM and LED data. Equilibrium directions of magnetizations of each type of blocks were defined from a minimum of free energy. Difference of our approach from known calculations for layered structures consists in the account of exchange interaction of each block with three other blocks with other orientations of Mn strips. The calculated spectra well agree with experiment with corresponding adjustments of constants of uniaxial magnetic anisotropy for different blocks and with growth of scalar exchange interaction parameter up to  $0.3 \text{ mJ/m}^2$  at decrease of temperature to 93 K. Thus, it is shown that

FMR data for DMS  $\text{Si}_{2.5}\text{Mn}_{0.5}$  are in accordance with established by HRTEM and LED nanosized structure of this ferromagnetic material.

The financial support of the Education and Science of RF (Agreement 02.B.49.21.0003) is gratefully acknowledged.

1. Danilov Yu.A., Demidov E.S., Drosdov Yu.N. *et al.*: JMMM, et al., e24 (2006)
2. Demidov E.S., Podolskii V.V., Lesnikov V.P. *et al.*: JETP, **106**, 110 (2008)
3. Demidov E.S., Aronzon B.A., Gusev S.N. *et al.*: JMMM, **321**, 690 (2009)
4. Demidov E.S., Pavlova E.D., Bobrov A.I., JETP Lett.: **96**, 706 (2012)
5. Demidov E.S., Podolskii V.V., Lesnikov V.P. *et al.*: JETP Lett.: **100**, 818 (2014)



## Synthesis and ESR Investigations of $Gd_{1-x}Sr_xMnO_3$

R. M. Eremina<sup>1</sup>, T. Maiti<sup>2</sup>, and A. K. Shukla<sup>3</sup>

<sup>1</sup> Zavoisky Physical-Technical Institute, Russian Academy of Sciences, Kazan 420029,  
Russian Federation [reremina@ya.ru](mailto:reremina@ya.ru)

<sup>2</sup> Department of Materials Science and Engineering, Indian Institute of Technology, Kanpur 208016,  
India, [tmaiti@iitk.ac.in](mailto:tmaiti@iitk.ac.in)

<sup>3</sup> Physics Department, Ewing Christian College, Allahabad 211003, India, [drkshukla@gmail.com](mailto:drkshukla@gmail.com)

Multiferroic materials with expected possibilities of potential coupling between distinct ferroic orders are important for new device applications. Therefore, understanding coupling mechanisms has attracted the scientific community in materials science. Perovskite type manganites  $R_{1-x}A_xMnO_3$  (where R is a trivalent rare-earth ion and A is divalent alkali earth ion) are of primary interest in this area because their properties are sensitive to external parameters like doping and temperature, hence offering opportunity to tailor spin-spin and spin-lattice interactions [1]. Investigation of the complex magnetic state in manganites requires a technique, sensitive to various interactions such as spin-spin interactions, spin-lattice interactions, spin-orbit interactions, crystal field interactions and the magnetic environment of the spins. Electron Spin Resonance (ESR) spectroscopy which allows to directly access the spin of interest can be suitably employed as a tool for these studies [2-5].

This talk reflects our attempt to investigate the nature of interplay between spin & charge degrees of freedom and temperature evolution of magnetically ordered phases in  $Gd_{1-x}Sr_xMnO_3$  ( $x = 0.5, 0.6$  and  $0.7$ ) using the temperature dependence of various ESR parameters, such as the resonance field, peak-to-peak line width and resonance intensity.

1. Fontcuberta J.: C. R. Physique **16**, 204 (2015)
2. Deisenhofer J., Eremin M.V., Zakharov D.V., Ivanshin V.A., Eremina R.M., Krug von Nidda H.-A., Mukhin A.A., Balbashov A.M., Loidl A.: Phys. Rev. B **65**, 104440 (2002)
3. Deisenhofer J., Braak D., Krug von Nidda H.-A., Hemberger J., Eremina R.M., Ivanshin V.A., Balbashov A.M., Jug G., Loidl A., Kimura T., Tokura Y.: Phys. Rev. Lett. **95**, 257202 (2005)
4. Eremina R.M., Fazlizhanov I.I., Yatsyk I.V., Sharipov K.R., Pyataev A.V., Krug von Nidda H.-A., Pascher N., Loidl A., Glazyrin K.V., Mukovskii Ya.M.: Phys. Rev. B **84**, 064410 (2011)
5. Nig'matullina I.I., Parfenov V.V., Rodionov A.A., Ibragimov Sh.Z., Eremina R.M.: Phys. Solid State **54**, 1996 (2012)

## AFM-PM Phase Transitions in Nano-Composite Materials (SrFe<sub>12</sub>O<sub>19</sub>)<sub>x</sub>(CaCu<sub>3</sub>Ti<sub>4</sub>O<sub>12</sub>)<sub>1-x</sub>

R. M. Eremina<sup>1,2</sup>, K. R. Sharipov<sup>1</sup>, I. V. Yatsyk<sup>1,2</sup>, N. M. Lyadov<sup>1</sup>,  
T. P. Gavrilova<sup>1,2</sup>, I. F. Gilmudinov<sup>2</sup>, A. G. Kiyamov<sup>2</sup>, Yu. V. Kabirov<sup>3</sup>,  
V. G. Gavrilyachenko<sup>3</sup>, and T. I. Chupakhina<sup>4</sup>

<sup>1</sup> Zavoisky Physical-Technical Institute, Russian Academy of Sciences, Kazan 420029,  
Russian Federation, reregina@yandex.ru

<sup>2</sup> Kazan Federal University, Kazan 420008, Russian Federation

<sup>3</sup> Southern Federal University, Rostov-on-Don 344006, Russian Federation

<sup>4</sup> Institute of Solid State Chemistry RAS, Yekaterinburg 620990, Russian Federation

Nano-composite materials are multi-constituent combinations of nano-dimensional phases with distinct differences in structures and physical properties, which can be used in variety of applications. These materials typically consist of two or more inorganic phases in some combination and possess unique combinations of magnetic, dielectric, electrical, and other properties compared to those of each individual constituent. Nano-composite dielectrics are promising materials for technical applications such as microelectronics, capacitors, and energy storage systems because they combine the good processability and high breakdown field strength of metal oxides with the high permittivity of ABO<sub>3</sub> type oxides.

One of the components of the composite material that is studied in this work is CaCu<sub>3</sub>Ti<sub>4</sub>O<sub>12</sub> (CCTO). The dielectric behavior of calcium copper titanate (CCTO) exhibits an extraordinary high dielectric constant ( $\epsilon_r \sim 10^4$ – $10^5$ ) and shows good thermal stability in a wide temperature range (100–600 K) [1]. Due to the high dielectric constant, it is widely utilized to manufacture electronic components. The only limitation, which restricts the broader applications of this compound, is the dielectric loss. But recently, Singh et al. reported about improvement in both the dielectric constant ( $\epsilon_r \sim 7007$ ) and dielectric loss ( $\tan \delta \sim 0.2$ ) at 1 kHz, at room temperature for 0.5 · Bi<sub>0.5</sub>Na<sub>0.5</sub>TiO<sub>3</sub> · 0.5CaCu<sub>3</sub>Ti<sub>4</sub>O<sub>12</sub> nano-composite material [2]. This fact stimulated us to study composite materials based on CCTO. As the second component of the composite material besides CCTO we chose the strontium hexaferrite SrFe<sub>12</sub>O<sub>19</sub> (SFO) to modulate the magnetic properties of the composite to get multiferroic material.

The magnetic microstructure of (SrFe<sub>12</sub>O<sub>19</sub>)<sub>x</sub>(CaCu<sub>3</sub>Ti<sub>4</sub>O<sub>12</sub>)<sub>1-x</sub> were investigated by the ESR method. ESR measurements of ceramic samples (SrFe<sub>12</sub>O<sub>19</sub>)<sub>x</sub>(CaCu<sub>3</sub>Ti<sub>4</sub>O<sub>12</sub>)<sub>1-x</sub> ( $x = 0, 0.05, 0.9, 1$ ) were carried out in the temperature range of 20–300 K at the frequency of 9.48 GHz. Some interesting results were obtained for concentration of the strontium hexaferrite  $x = 0.05$ .

ESR spectrum of (SrFe<sub>12</sub>O<sub>19</sub>)<sub>0.05</sub>(CaCu<sub>3</sub>Ti<sub>4</sub>O<sub>12</sub>)<sub>0.95</sub> consists of one superparamagnetic resonance line at room temperature (Fig. 1a), because the ferromagnetic core of SrFe<sub>12</sub>O<sub>19</sub> polarizes the paramagnetic matrix CaCu<sub>3</sub>Ti<sub>4</sub>O<sub>12</sub> forming superparamagnetic particle. With decreasing the temperature one of the sublattices of iron ions in SrFe<sub>12</sub>O<sub>19</sub> orders antiferromagnetically and fer-

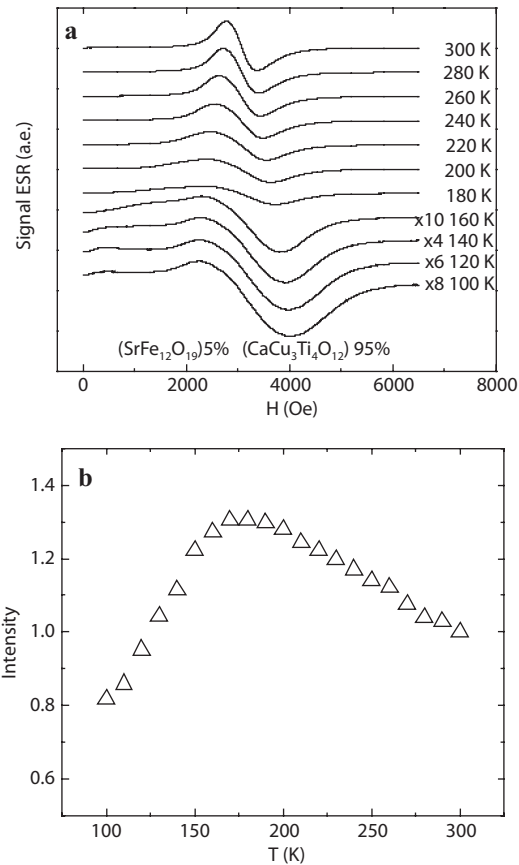


**Fig. 1.** Temperature dependence of the ESR spectrum (a) and integral intensity (b) in  $(\text{SrFe}_{12}\text{O}_{19})_{0.05} \times (\text{CaCu}_3\text{Ti}_4\text{O}_{12})_{0.95}$ .

romagnetic correlations between CCTO and SFO destroy. Thus we observe the phase transition to the phase-separated state in  $(\text{SrFe}_{12}\text{O}_{19})_{0.05}(\text{CaCu}_3\text{Ti}_4\text{O}_{12})_{0.95}$  at  $T = 175$  K. This state is characterized by the presence of paramagnetic (CCTO) and ferrimagnetic phases (SFO) that results to the two lines in the ESR spectrum (Fig. 1a). The temperature of the phase transition corresponds to the maximum of the temperature dependence of the integral intensity of the ESR spectrum in  $(\text{SrFe}_{12}\text{O}_{19})_{0.05}(\text{CaCu}_3\text{Ti}_4\text{O}_{12})_{0.95}$  (Fig. 1b). Below  $T = 25$  K system CCTO is ordered antiferromagnetically. These results are confirmed by the magnetic susceptibility measurements.

1. Subramanian M.A., Li D., Duan N., Reisner B.A., Sleight A.W.: J. Solid State Chem. **151**, 323 (2000)
2. Singh L., Kim I.W., Cheol Sin B., Ullah A., Woo S.K., Lee Y.: Materials Science in Semiconductor Processing **31**, 386 (2015)

## Electron Paramagnetic Resonance Study of $\text{Yb}^{3+}$ in Hexagonal Perovskite $\text{RbMgF}_3$ Crystal

**M. L. Falin<sup>1</sup>, V. A. Latypov<sup>1</sup>, and S. V. Petrov<sup>2</sup>**

<sup>1</sup> Zavoisky Physical-Technical Institute of the RAS, Kazan 420029, Russian Federation  
falin@kfti.knc.ru

<sup>2</sup> Kapitza Institute for Physical Problems of the RAS, Moscow 119334, Russian Federation

Fluoroperovskite  $\text{RbMgF}_3$  doped with transition metal ions attract attention due to their application in optical stimulated luminescence and usage as radiation detectors [1, 2]. Only crystals activated with iron group ions were studied by electron paramagnetic resonance (EPR) and to the best of our knowledge, the studies of rare-earth ions in this crystal are absent.  $\text{RbMgF}_3$  has the hexagonal structure and the space group  $P63/mmc^3$ . The crystal has two different crystallographic 6-fold  $\text{Mg}^{2+}$  positions. One of them,  $\text{Mg}^{2+}$  (I – 2a position), has the local symmetry  $D_{3d}$ , the other,  $\text{Mg}^{2+}$  (II – 4f position) the symmetry  $C_{3v}$ . Analogously, there are two different crystallographic 12-fold  $\text{Rb}^+$  position. This report is concerned with investigation of the impurity paramagnetic centers formed by  $\text{Yb}^{3+}$  ions in  $\text{RbMgF}_3$  single crystal.

The crystals were grown using the Bridgman method. EPR experiments was carried out using an X-band spectrometer ERS-231 (Germany) at  $T = 4.2$  K.

The parameters of the corresponding spin Hamiltonians, the ground states and their wave functions were determined. On the basis of the comparison of valence states and ion radii of  $\text{Rb}^+$ ,  $\text{Mg}^{2+}$  and  $\text{Yb}^{3+4}$  ions it is assumed that  $\text{Yb}^{3+}$  occupies one of  $\text{Mg}^{2+}$  states.

This study was supported by the grant of the Presidium of the Russian Academy of Sciences no. 32 “Electron spin resonance, spin-dependent electron effects and spin technologies” and President of the Russian Federation “Leading Scientific Schools” (NSh-4653.2014.2).

1. Dotzler C., Williams G.V.M., Rieser U., Robinson J.: Appl. Phys. **105**, 023107 (2009)
2. Dotzler C., Williams G.V.M., Edgar A.: Curr. Appl. Phys. **8**, 447 (2008)
3. Dance J.M., Kerkouri N., Tressaud A.: Mat. Res. Bull. **14**, 869 (1979)
4. Shannon, R.D.: Acta Crystallogr. A **32**, 751 (1976)

## CIDNP Study of Biradicals from Nucleotide-Photosensitizer and Amino Acid-Photosensitizer Conjugates

**N. Fishman<sup>1</sup>, A. Kiryutin<sup>1</sup>, O. Morozova<sup>1</sup>, M. Panov<sup>1,2</sup>,  
T. Abramova<sup>3</sup>, and A. Yurkovskaya<sup>1,2</sup>**

<sup>1</sup> International Tomography Center, Novosibirsk 630090, Russian Federation

<sup>2</sup> Novosibirsk State University, Pirogova 2, Novosibirsk 630090, Russian Federation

<sup>3</sup> Institute of Chemical Biology and Fundamental Medicine, SB RAS, Novosibirsk 630090, Russian Federation, mike.p@tomo.nsc.ru

Recently in addition to the enzymatic DNA repair, a new repair mechanism was discovered. This repair mechanism refers to the removal of transient products of the DNA damage like short-lived DNA radicals, with a very high reaction rate by endogenous natural and synthetic compounds (so called “chemical way” of DNA repair). Our previous studies revealed a great potential of the time-resolved CIDNP technique for the investigation of electron transfer between oxidized DNA nuclear bases and amino acids or small peptides. The further development of this work implies the investigation of the electron transfer processes and the detection of elusive radicals in biomolecules using model compounds, where key participants of the reaction (dye, amino acid, and nucleoside) are spatially drawn together mimicking the biologically important DNA repair processes. To start this investigation we have constructed dyads (Fig. 1) that contain a photosensitizer (4-carboxy-benzophenone, 4CBP) as an acceptor of  $e^-$  or  $H^\cdot$  and guanosine mono-phosphate (BLG) or amino acid tyrosine (BTyr) or tryptophan (BLTrp) as a donor of  $e^-$  or  $H^\cdot$  connected by a linker (L) of variable length.

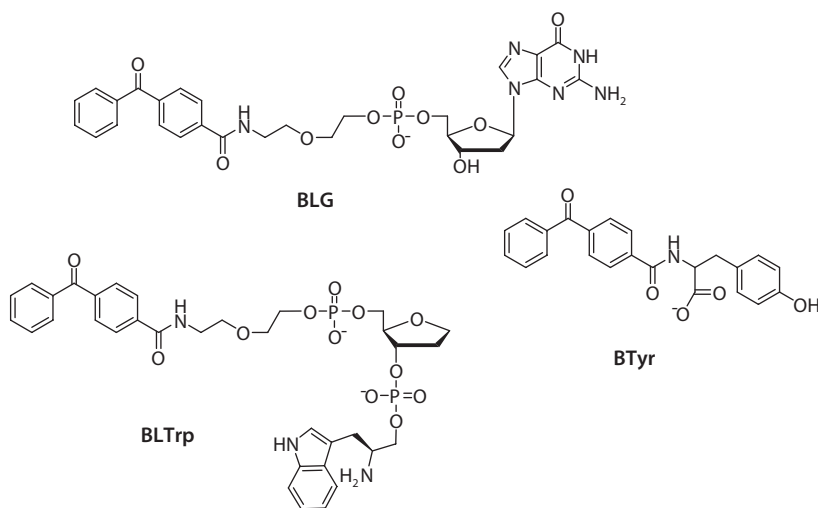


Fig. 1. Structures of dyads.

All these relatively simple systems, which are flexible biradicals formed under UV-light excitation, are shown to produce very strong CIDNP effects in liquids. For BLG dyad system the pH dependence of the CIDNP intensity was revealed and explained in terms of  $pK_a$ 's of reactants and reaction mechanisms. A complementary study of CIDNP field dependencies for BLG system and for the system containing non-linked 4-CBP and guanosine-5'-monophosphate at different pH values enabled us to get information on electronic spin-spin exchange interaction in BLG biradical within a large pH range.

The financial support by the program of RFBR (Projects No. 14-03-31563, No. 14-03-00453), RScF (Project No. 15-13-20035).

## The Modes of the Superconducting Triplet Spin-Valve and Distribution of Condensate Functions

**R. R. Gaifullin<sup>1</sup>, R. G. Deminov<sup>1</sup>, L. R. Tagirov<sup>1</sup>, T. Yu. Karminskaya<sup>2</sup>,  
M. Yu. Kupriyanov<sup>2,3,1</sup>, Ya. V. Fominov<sup>4,3</sup>, and A. A. Golubov<sup>5,3</sup>**

<sup>1</sup> Kazan Federal University, Kazan 420008, Russian Federation  
gaifullin.rashid@gmail.com

<sup>2</sup> Skobeltsyn Institute of Nuclear Physics, Moscow State University, Moscow 119992,  
Russian Federation

<sup>3</sup> Moscow Institute of Physics and Technology, Dolgoprudny 141700, Russian Federation

<sup>4</sup> L. D. Landau Institute for Theoretical Physics RAS, Chernogolovka 142432, Russian Federation

<sup>5</sup> Faculty of Science and Technology and MESA+ Institute of Nanotechnology, University of Twente,  
Enschede 7500 AE, The Netherlands

We investigate the critical temperature  $T_c$  of F2F1S trilayers (S is a singlet superconductor, Fi is a ferromagnetic metal), where the long-range triplet superconducting component is generated at noncollinear magnetizations of the F layers [1]. An asymptotically exact numerical method [2] is employed to calculate  $T_c$  as a function of the trilayer parameters. Earlier we demonstrated that  $T_c$  in the structures can be a non-monotonic function of the angle  $\alpha$  between magnetizations of the two F layers [3], contrary to the monotonic  $T_c(\alpha)$  behavior calculated for the FSF superconducting spin-valve design [4]. We examine the spin-singlet and spin-triplet pairing distributions and amplitudes as a function of the layers thicknesses under different values of the angle  $\alpha$  in the F2F1S and F2SF1 superconducting spin-valve designs to clarify which one and why may show maximum spin-triplet pairing impact on the superconducting  $T_c$ .

The support in parts by RFBR (grants No. 14-02-00793-a, 14-02-31002-mol\_a, 15-32-20362-bel\_a\_ved) is gratefully acknowledged.

1. Bergeret F.S., Volkov A.F., Efetov K.B.: Rev. Mod. Phys. **77**, 1321–1373 (2005)
2. Fominov Ya.V., Chitchev N.M., Golubov A.A.: Phys. Rev. B. **66**, 014507(13) (2002)
3. Fominov Ya.V., Golubov A.A., Karminskaya T.Yu., Kupriyanov M.Yu., Deminov R.G., Tagirov L.R.: JETP Lett. **91**, 308–313 (2010)
4. Fominov Ya.V., Golubov A.A., Kupriyanov M.Yu.: JETP Lett. **77**, 510–515 (2003)

## EPR Study of Nitric Oxide Production in Brain, Heart and Liver of Rats after Hemorrhagic Insult Modeling

**Kh. L. Gainutdinov<sup>1,2</sup>, V. V. Andrianov<sup>1,2</sup>, V. S. Iyudin<sup>1</sup>, G. G. Yafarova<sup>1,2</sup>,  
A. A. Denisov<sup>3</sup>, M. O. Khotyanovich<sup>3</sup>, S. G. Pashkevich<sup>3</sup>,  
and V. A. Kulchitchkii<sup>3</sup>**

<sup>1</sup> Zavoiisky Physical-Technical Institute, Russian Academy of Sciences, Kazan 420029,  
Russian Federation, kh\_gainutdinov@mail.ru

<sup>2</sup> Kazan Federal University, Kazan 420008, Russian Federation

<sup>3</sup> Institute of Physiology of Nat. Acad. of Sci. of Belarus, Minsk, Belarus

The functioning of the bodies tissues depends on several factors. One of such factors is the necessity for the oxidizing processes of a sufficient amount of oxygen that is supplied with the blood. The lack of oxygen leads to pathological processes in the body, the precursor of which is hypoxia. Hypoxia is a pathological process that occurs when there is insufficient supply of tissues with oxygen, or disruption of its utilization in the process of biological oxidation (the state of oxygen deficits as the whole body and separate organs and tissues); this is an important component of the pathogenesis of many diseases [1]. During disruption of cerebral circulation, leading to lack of oxygen supply of parts of the brain, there is the brain ischemia which can culminate by insult fail defined as acute damage of brain tissue, a violation of its functions due to the difficulty or cessation of blood flow to a brain areas.

The role of nitric oxide (NO) in the functioning of nervous and cardiac systems is very important [2]. The literature provides evidence of two opposing modes of NO influence on the physiology of various tissues: (1) positive, stimulatory, versus (2) toxic, damaging action that may lead to cell death. Hence it can be asserted that the “sign” of effect depends on the amount of NO, yet it is not clear what amounts should be regarded as low, normal, or elevated. It is

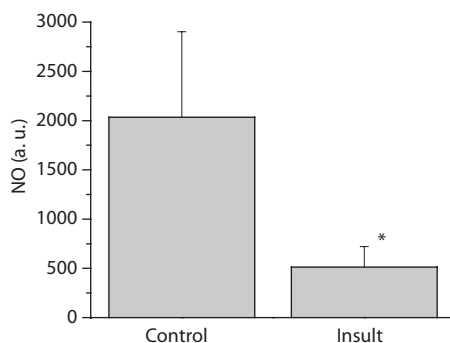


**Fig. 1.** Intensity of EPR signal of spin trap (DETC)<sub>2</sub>-Fe<sup>2+</sup>-NO from hippocampus (insult and noninsult areas) of control (K) and rats after hemorrhagic insult.



shown that the change of the NO production in the tissues can result in various pathologies. Early by method of EPR spectroscopy we studied the changes of intensity of NO production after modeling of insult to rats through analyses of quality of NO containing paramagnetic complexes in tissues of brain. It was found that in the ischemic part of the left hemisphere in 5 h after modeling the ischemic stroke, the NO content in the spin trap and R-conformer compositions decreases by 5 times and 30%, respectively. This decrease in the NO content is kept in 9 and 24 h after the stroke [3]. Therefore, we carried out a study of the dynamics of changes in the levels of NO in the tissues of brain, heart and liver of rats after hemorrhagic insult using EPR spectroscopy.

This series of experiments were performed on rats weighing an average of 200 gr. During EPR samples preparation the spin traps method has been used (prof. Vanin A.F.) [4]. As a spin traps were applied the complex of  $\text{Fe}^{2+}$  with diethyldithiocarbamate (DETC) –  $(\text{DETC})_2\text{-Fe}^{2+}\text{-NO}$ .

Experimental analysis of NO content by method of EPR spectroscopy showed that as when modeling hemorrhagic stroke is a decrease of NO production in the hippocampus in 2–3 times in 5 hours after ischemia and this decrease is stored for 72 hours (Fig. 1). The same picture is observed in the heart and liver tissues after 24 and 72 hours after hemorrhagic stroke. Thus, it was found that the level of NO production to third day after hemorrhagic stroke in the hippocampus is decreased. Surprising for us was data showing a decrease of NO production in heart and liver, although no direct effect on them should not be in the case of cerebral ischemia. We can assume that this result is a consequence of the significant influence of the central nervous system on the regulation of NO production in the body.

1. Koshelev V.B. in: "Selected lectures on modern physiology". Kazan, GOETAR, 178–194 (2010)
2. Boehning D., Snyder S.H.: *Annu. Rev. Neurosci.* **26**, 105 (2003)
3. Gainutdinov Kh.L., Andrianov V.V., Iyudin V.S. *et al.*: *Biophysics* **58**, No. 2, 203–205 (2013)
4. Mikoyan V.D., Kubrina L.N., Serezhenkov V.A. *et al.*: *Biochim. Biophys. Acta* **1336**, No. 2, 225–234 (1997)

## **Effect of Levels Anticrossing on the EPR Spectra and the Dynamic Susceptibility**

**R. T. Galeev**

Zavoisky Physical-Technical Institute, Russian Academy of Sciences, Kazan 420029,  
Russian Federation, galeev@kfti.knc.ru

In this study a model system of two coupled spins  $S = 1/2$  with the strong anisotropic g-factors was considered. The problem we were interested in a vicinity of levels anticrossing and its manifestations in the EPR spectra and the dynamic susceptibility.

This research was supported in part by the Russian Foundation for Basic Research (project no. 13-02-01157) and the President of the Russian Federation (grant no. NSh-4653.2014.2)

## ESR Study of Electron Beam Irradiated Calcium Gluconate

**I. A. Goenko<sup>1</sup>, V. Yu. Petukhov<sup>1</sup>, I. V. Yatzyk<sup>1</sup>, G. G. Gumarov<sup>1</sup>,  
M. M. Akhmetov<sup>1</sup>, and G. N. Konygin<sup>2</sup>**

<sup>1</sup> Zavoisky Physical-Technical Institute, Russian Academy of Sciences, Kazan 420029,  
Russian Federation, ilya.goenko@mail.ru

<sup>2</sup> Physical-Technical Institute Ural Branch of RAS, Izhevsk, Russian Federation,  
konygin@fhms.udm.ru

Calcium gluconate is one of the commonly used pharmacological preparations for the therapy of diseases associated with hypocalcaemia. It is known that mechanical activation of calcium gluconate results in the increased bioavailability and efficacy of therapy [1]. It is assumed that the increase in the therapeutic efficacy is associated with the change in the stereochemical structure of the molecule [2]. At the same time, it was found that mechanochemical treatment of calcium gluconate is accompanied by the appearance of paramagnetic centers, which may affect the enhancement the biological activity of the drug [3]. In this work we attempted to obtain paramagnetic centers using the ionizing radiation.

In the experiments, we used calcium gluconate monohydrate as a powder. A beam of electrons with the energy of 9 Mev obtained on a linear accelerator Elekta Synergy® S was used as the ionizing radiation. The samples were irradiated with the dose of 100 Gy. ESR spectra were measured on an EMX Plus spectrometer at the frequency of 9.3 GHz at room temperature.

Fig. 1, curve A shows the EPR spectrum of calcium gluconate after the electron beam irradiation. The spectrum has a complex shape due to the superposition of some lines. Fig. 1, curve B is represented by the well-known ESR spectrum of mechanoactivated calcium gluconate (MACG) with  $g = 2.0051$  [3]. The spectrum (curve A) most probably contains the line from MACG.

The paramagnetic centers produced by the electron beam irradiation are long-lived. The nature of the new additional paramagnetic centers is not yet

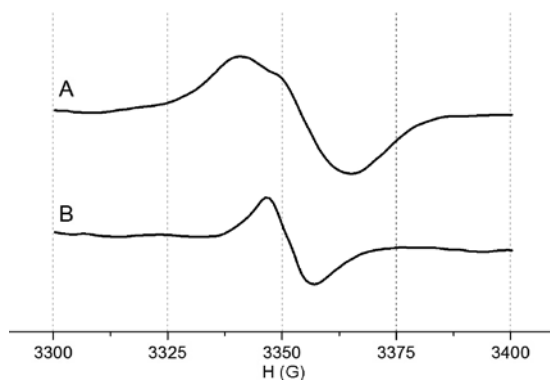


**Fig. 1.** EPR spectra: A – electron beam irradiated calcium gluconate, B – MACG.

clear but according to the Franck-Rabinovich concept in the radiolysis of organic compounds [4], the breakage of the C-H bonds and the removal of the hydrogen atom from lattice are the most probable origins .

Thus, the electron-beam irradiation leads to the appearance of some EPR lines, one of which coincides with the signal from MACG, and the others are unidentified signals.

1. Konygin G.N. *et al.*: Patent of Russia № 2373185 (2009)
2. Konygin G.N. *et al.*: Conference materials “Actual questions of pediatric surgery”, ISMA, Izhevsk, **56** (2003)
3. Gumarov G.G. *et al.*: Journal of Physical Chemistry, **87**, 1578 (2013)
4. Blumenfeld L.A. *et al.*: EPR applications in chemistry (1962)

## Electron Spin Resonance in 1-2-2 Pnictides $\text{EuCd}_2\text{As}_2$ and Influence Substitutions on its Parameters

**Yu. Goryunov<sup>1</sup> and A. Nateprov<sup>2</sup>**

<sup>1</sup> Zavoisky Physical-Technical Institute, Russian Academy of Sciences, Kazan 420029, Russian Federation, goryunov@kfti.knc.ru

<sup>2</sup> Institute of Applied Physics of ASM, Kishinev, 2028, Moldova, nateprov@phys.asm.md

We performed the X band ESR measurements of powder samples 1-2-2 pnictide  $\text{EuCd}_2\text{As}_2$  [1] with structural type  $\text{CaAl}_2\text{Si}_2$  (space group P3.m1) at temperatures 10–300 K. This structural type, also as structural type  $\text{ThCr}_2\text{Si}_2$  (space group I4/mmm), is characterized by alternating single layers of  $\text{Eu}^{2+}$ , in which ions are located at the nodes of a plane square lattice.  $\text{EuFe}_2\text{As}_2$  [2] is a parent compound for known 1-2-2 superconductors based on iron pnictides and well known member of this structure type. At the same time, the complete substitution europium by cadmium  $\text{Eu}_x\text{Cd}_{3-x}\text{As}_2$  is resulting to form the compound  $\text{Cd}_3\text{As}_2$  [3, 4] with another structure the centrosymmetric I41/acd space group. At recent the compound  $\text{Cd}_3\text{As}_2$  is known as 3D Dirac semimetal that demonstrates properties of topological insulator.

As in the past for others 1-2-2 europium compounds with structure type  $\text{CaAl}_2\text{Si}_2$ , it was observed almost symmetric Lorentzian resonance line. At high temperature  $g$ -factor for this compound was 2.03 and pic-to-pic linewidth was 900 Oe. The temperature dependences of the resonance field and linewidth were of the type  $\sim(T - T_c)^{-1/2}$ , which is indicative of spin fluctuations associated with the phase transition temperature  $T_c$ . Also at high temperatures was observed Curie-like temperature dependence of the inverse the ESR intensity with positive temperature Curie Weiss  $\theta_{\text{cw}} = 16$  K, which does not coincide with  $T_c = T_N \sim 7$  K.

A comparative analysis of the  $\text{Eu}^{2+}$  ion  $g$ -factors deviations for different Eu pnictides from its value for the free electron, which corresponds to a pure spin state of the ion Eu, was made. It was found that the anion pnictides substitution effect on the  $g$ -factor of the  $\text{Eu}^{2+}$  is negligible (smaller 0.5%). Lattice constant is proportional to the radius of the anion  $\text{Pn}^{3-}$  pnictides with accuracy better than 1%. However, the substitution of the transition metal  $\text{M}^{2+}$  ion leads to a strong increase of the ion  $\text{Eu}^{2+}$   $g$ -factor despite sameness of configuration of external electronic shells. Obviously, this is related to the size and distribution of the electron density remaining after filling p-orbitals of pnictides due to electrons of the Eu and the transition metal. It should be emphasized that the substitution of  $\text{Cd}^{2+}$  to  $\text{Fe}^{2+}$  in  $\text{EuM}_2\text{As}_2$  changes the behavior of the  $\text{Eu}^{2+}$  ions layers: of adjacent europium layers are compressed and shifted by half a period along their surfaces and thus doubles the period of the structure of the ions along  $c$ -axis. The consequence of this is the metallization of the Eu layers, which is manifested in significant reduction of the  $g$ -factor to smaller 2.0 and the temperature contribution in the linewidth. The full inverse picture is observed for  $\text{Eu}_x\text{Cd}_{3-x}\text{As}_2$  compound.

Thus, at the temperature decreasing well before the antiferromagnetic ordering temperature  $T_N$  we have observed an increasing of linewidth and a decreasing of the resonance fields, which in our case very good described by Landau's theory of magnetic fluctuations. The paramagnetic temperature  $\theta_{cw}$  of the antiferromagnetic  $\text{EuCd}_2\text{As}_2$  compounds has the positive sign. We believe such behaviour of  $\theta_{cw}$  is connected with critical spin fluctuation and critical spin fluctuation the relevant topologic instability of electronic structures of compound.

1. Schellenberg I, Pfannenschmidt U., Eul M. , Schwickert C., Poettgen R.: *Z. Anorg. Allg. Chem.* **637**, 1863 (2011)
2. Oleaga A., Salazar A., Thamizhavel A, Dhar S.: *Journal of Alloys and Compounds* **617**, 534 (2014)
3. Liu Z., Jiang J, Zhou B., Wang Z, Zhang Y, Weng H., Prabhakaran D., Mo S., Peng H, Dudin P., Kim T., Hoesch M, Fang Z, X. Dai, Shen Z., Feng D., Hussain Z., Chen Y.: *Nature Materials* **13**, 677 (2014)
4. Mazhar N. Ali, Quinn Gibson, Sangjun Jeon, Brian B. Zhou, Ali Yazdani, R. J. Cava: arXiv:1312.7576v2 (2014)

## Spin Dynamics in the Frustrated System $\text{CoAl}_2\text{O}_4$

**M. Iakovleva<sup>1</sup>, E. Vavilova<sup>1</sup>, H.-J. Grafe<sup>2</sup>, S. Zimmermann<sup>2,3</sup>,  
A. Alfonsov<sup>2</sup>, H. Luetkens<sup>4</sup>, H.-H. Klauss<sup>3</sup>, A. Maljuk<sup>2</sup>, S. Wurmehl<sup>2</sup>,  
B. Büchner<sup>2,3</sup>, and V. Kataev<sup>1,2</sup>**

<sup>1</sup>Zavoisky Physical-Technical Institute, Russian Academy of Sciences, Kazan 420029,  
ymf.physics@gmail.com

<sup>2</sup>Leibniz Institute for Solid State and Materials Research IFW Dresden, Dresden 01069, Germany

<sup>3</sup>Institute for Solid State Physics, TU Dresden, Dresden 01069, Germany

<sup>4</sup>Laboratory for Muon-Spin Spectroscopy Paul Scherrer Institut CH-5232 Villigen PSI, 5232,  
Switzerland

The competition of exchange interactions or to the specific geometry of the lattice yields the frustration in the strongly correlated electron systems. In the systems with frustration of magnetic interactions classical order is prohibited and different exotic ground states can occur (for instance spin-spiral structures, spin glasses and spin liquid states, etc.).

In this work the dynamic and static magnetic properties of a single crystal of the frustrated spin magnet  $\text{CoAl}_2\text{O}_4$  investigated by local spin probe methods are performed. We have found that the frustration of the spin interactions and Co/Al site disorder strongly affect the spin dynamics. Inhomogeneous broadening of ESR and NMR lines at temperatures below 30–50 K indicates the growth of short-range spin correlations. The analysis of the relaxation rates evidences a critical slowing down of spin fluctuations at characteristic temperature  $T^* = 8$  K which suggests the inset of a quasi-static order at this temperature.

## Abnormal Absorption Lines in ESR Spectra of Sportsmen Serum Samples

**M. I. Ibragimova<sup>1</sup>, A. I. Chushnikov<sup>1</sup>, G. V. Cherepnev<sup>2</sup>, V. Yu. Petukhov<sup>1</sup>,  
and I. V. Yatsyk<sup>1</sup>**

<sup>1</sup> Zavoisky Physical-Technical Institute, Russian Academy of Sciences, Kazan 420029,  
Russian Federation, ibragimova@kfti.knc.ru

<sup>2</sup> Tatarstan Republic Clinical Hospital №2, Kazan 420043, Russian Federation, rkb2\_rt@mail.ru

Recently we reported on an appearance of new absorption lines in ESR spectra (X-band, 77 K) of serum samples collected from professional sportsmen [1]. The significant portion of new signals we assigned to Fe and Cu ions incorporated into cytochrome-*c*-oxidase. In the present study we extend ESR measurements to lower temperature range 5–80 K.

Serum samples were collected from 22 Continental Hockey League professional players and 3 control male volunteers. Nearly all ESR spectra recorded at 5 K showed a combination of two new signals at  $g = 5.85$  and  $8.6$  and regular absorption lines from  $\text{Fe}^{3+}$  in transferrin ( $g_{\perp} = 4.21$ ) and  $\text{Cu}^{2+}$  in ceruloplasmin ( $g_{\perp} = 2.058$ ) (Fig. 1). Importantly, the amplitude of these new signals was rather small and slightly distinguishable but in some cases ( $n = 5$ ) the intensity of the line at  $g = 5.85$  was significantly higher, the ratio of line intensities increasing up to 12:1. The value of  $g$ -factor and unchangeable shape of the lines one may assign to high-spin  $\text{Fe}^{3+}$  ( $S = 5/2$ ) in heme. The inverse temperature-dependent pattern of signal intensities in the range of 5–40 K (decrease up to zero at 40

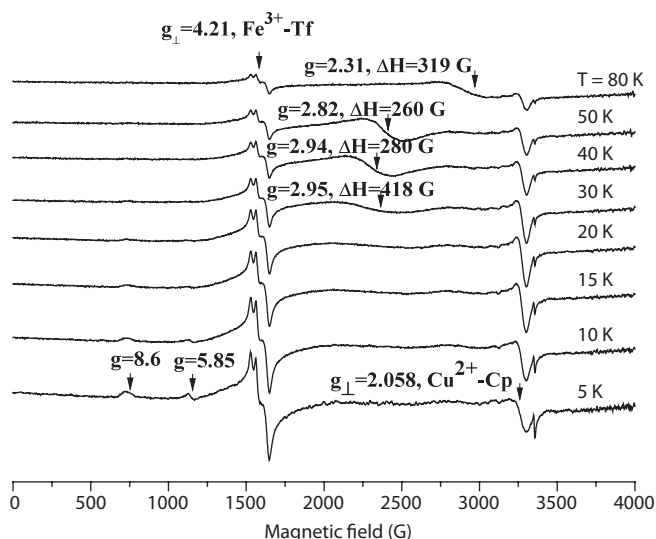


**Fig. 1.** ESR spectra of sportsman serum blood recorded at temperature range of 5–80 K.



K) is characteristic of cytochromes, more likely cytochrome *c*. At the same time such rhombic distortion of cytochrome *c* heme was not observed earlier, while lines at  $g \sim 8$  and 8.52 were assigned to high-spin ferric form of cytochrome *P*-450 and rhombically distorted heme of bovine liver catalase, respectively [2, 3]. Hence, two different explanations are possible: either they correspond to 2 different centers (with nearly tetragonal iron environment) or to rhombically distorted  $\text{Fe}^{3+}$ -heme.

In two sportsmen's serum ESP spectra showing relatively low signals at  $g = 5.85$  and 8.6 there was a new more intensive absorption line at  $g = 3.15$  with specific for cytochrome temperature-dependent pattern. This signal we assigned to low spin heme  $\text{Fe}^{3+}$ .

Noteworthy are unexpected results obtained for two serum blood ESR spectra (see Fig. 1). The intensive broad unresolved absorption line at temperature range of 30–80 K was registered. Unusual features of this signal are the shift of  $g$ -factor value proportional to the temperature increase (from  $g = 2.95$  at 30 K to 2.31 at 80 K) and line width changes. Somewhat similar was observed in solids, namely, in chain-polymer complex including triple-spin exchange-coupled systems in temperature range of 70–220 K [4]. This phenomenon was explained by spin exchange between the different multiplet triple-spin systems.

One study subject presented with well-resolved triplet with  $g_1 = 2.037$ ;  $g_2 = 2.008$  and  $g_3 = 1.980$  recorded at 80 K. To identify this spectrum the serum sample was supplemented with industrial nitroxyl spin label TEMPO. Again, the similar triplet was found with  $g_1 = 2.017$ ;  $g_2 = 2.002$ ; and  $g_3 = 1.982$  from nitroxyl radical. The reason for nitroxyl complex formation in serum blood of sportsmen is not yet clear. Routine serum plasma chemistry tests in study subjects showed no significant deviations from the normal range.

1. Ibragimova M.I. *et al.*: *Biofisika* **59**, 520–526 (2014)
2. Shergill J.K. *et al.*: *Biochem. J.* **307**, 719–728 (1995)
3. Williams-Smith D.L., Patel K.: *Biochim.Biophys Acta* **405**, 243–252 (1975)
4. Veber S.: Author's abstract of dissertation, Novosibirsk, 2009.

## In-Plane Magnetic Anisotropy Constants of Thin Films from Angular FMR Dependence

**A. V. Izotov<sup>1,2</sup> and B. A. Belyaev<sup>1,2,3</sup>**

<sup>1</sup> Siberian Federal University, Krasnoyarsk 660041, Russian Federation, iztv@mail.ru

<sup>2</sup> Kirensky Institute of Physics SB RAS, Krasnoyarsk 660036, Russian Federation, belyaev@iph.krasn.ru

<sup>3</sup> Siberian State Aerospace University, Krasnoyarsk 660014, Russian Federation

Accurate determination of the different magnetic anisotropy contributions from angular dependence of ferromagnetic resonance (FMR) field is very difficult problem for complex magnetic structures with mixed anisotropy [1]. In such cases, experimental data are analysed with the help of a numerical procedure to fit theoretical dependence to experimental data. At realisation of this procedure in practice have to deal with two major difficulties that directly affect the accuracy and reliability of the results.

The first problem is related to the implementation of the algorithm of joint solutions of coupled nonlinear equations of equilibrium and FMR conditions. If we are dealing with a small number of unknown parameters of the theoretical model, this problem is easily solved by using modern mathematical packages. However, in the study of complex thin film structures with mixed magnetic anisotropy this approach not only leads to an increase in calculation time, but does not guarantee the accuracy and reliability of the results. The second problem is associated with a form of the theoretical representation of the magnetic anisotropy energy. It is a quite common, that the magnetic anisotropy energy of a magnetically saturated sample is expressed as a function of the direction cosines of the magnetization vector relative to the reference axes through a polynomial series expansion. From a theoretical point of view the disadvantage of using these underlying functions is the fact that they are nonorthogonal. As a result, anisotropy constants mix anisotropy contributions of different order, which complicates the mathematical handling and physical interpretation of the anisotropy constants.

In this work, we have developed a general approach for the analysis and interpretation of the angular dependence of FMR in thin magnetic films with in-plane orientation of the magnetic moment. The approach is far from the above-mentioned drawbacks. It allows using a universal technique for finding effective parameters of the planar magnetic anisotropy with an arbitrary number of anisotropy constants.

## Orientational Self-Ordering of Spin-Labeled Cholesterol Analog in Lipid Bilayers

**M. E. Kardash** and **S. A. Dzuba**

Voevodsky Institute of Chemical Kinetics and Combustion,  
and Novosibirsk State University, Novosibirsk 630090, Russian Federation,  
kardash.marya@gmail.com

Cholesterol and lipids in cell membranes are distributed heterogeneously forming the so-called lipid rafts. Rafts are important participants of various membrane processes. In this work, electron spin echo (ESE) spectroscopy was used for investigation of spin-labeled analog of cholesterol, 3 $\beta$ -doxyl-5 $\alpha$ -cholestane (CHL), in lipid bilayers consisted of equimolecular mixture of 1,2-dipalmitoyl-sn-glycero-3-phosphocholine (DPPC) and 1,2-dioleoyl-sn-glycero-3-phosphocholine (DOPC) [1]. Figure 1 shows echo-detected EPR spectra with different time delay  $\tau$  between microwave pulses. Spectra for convenience of visualization are normalized by the maximal amplitude of the left shoulder. The observed line-shape changes with  $\tau$  arise because of so-called “instantaneous diffusion” effect in ESE. Surprisingly, for the CHL system under study (a) spectral changes are stopped at large  $\tau$ . Meanwhile, for the reference system of spin-labeled stearic

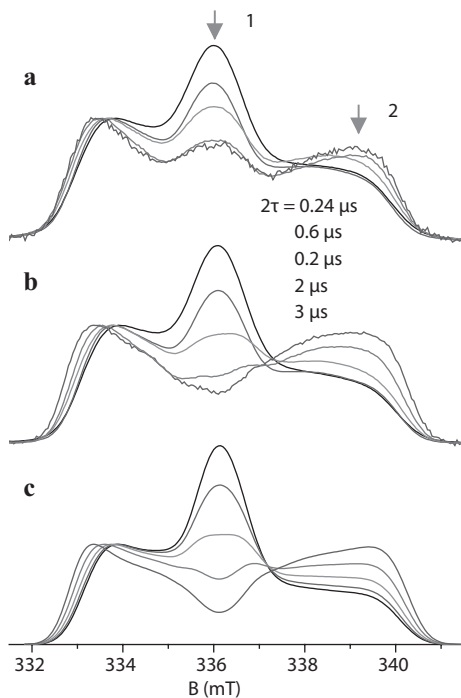
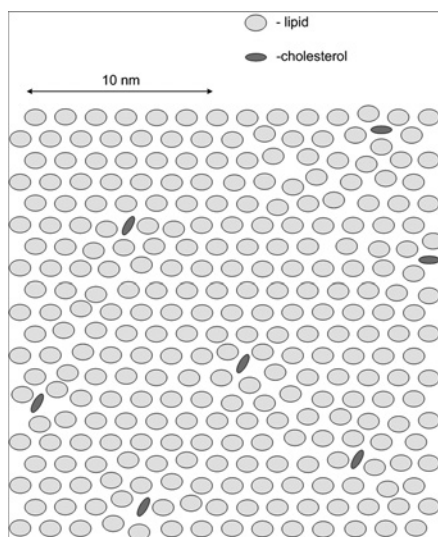


Fig. 1.



**Fig. 2.**

acid (b) spectral changes occur in agreement with theoretical prediction (c) for uniform distribution of spin labels. The abnormal behavior of CHL system may be explained assuming formation of domains in which CHL molecules are equally oriented (Fig. 2). As CHL molecules are located at distances about several nanometers, the found effect may imply long-range interactions between molecules in biological membranes.

1. Kardash M.E., Dzuba S.A.: *J. Chem. Phys.* **141**, 211101 (2014)

## Development of Four-Pulse ELDOR Theory for the Case of Overlapping EPR Spectra and Overlapping Excitation Bands Taking into Account Nonsecular Part of the Dipole-Dipole Interaction

**I. T. Khairuzhdinov and K. M. Salikhov**

Zavoisky Physical-Technical Institute, Russian Academy of Sciences, Kazan 420029,  
Russian Federation, semak-olic@mail.ru

The current theory of the four-pulse electron double resonance (PELDOR) has been extended to take into account two effects: (1) overlapping of the electron paramagnetic resonance (EPR) spectra of paramagnetic spin 1/2 particles (spin labels) in pairs and (2) overlapping of the excitation bands by the pump and echo forming pulses [1]. In our theoretical calculations nonsecular part of the dipole-dipole interaction has been taken into account. It has been shown that the PELDOR signal contains additional terms in contrast to the situation considered in the current theory, when the EPR spectra of the spin labels in the pairs and the excitation bands do not overlap [2]. The largest additional terms originates from the fact that both spins in pairs can be excited by the echo forming pulses when the EPR spectra of the partners in pairs do essentially overlap. When the difference of Zeeman frequencies greater than the spin-spin interaction all terms oscillate with the same frequency, which is the characteristic dipolar interaction frequency. In a situation where the difference of Zeeman frequencies becomes comparable with the value of the spin-spin interaction new oscillation frequencies appear in the PELDOR signal. The results of the numerical calculations, which illustrate the possible scale of the effect of these additional terms and additional frequencies on the PELDOR signal are presented.

1. Salikhov K.M., Khairuzhdinov I.T.: Appl. Magn. Reson. **46**, 67–83 (2015)
2. Salikhov K.M., Khairuzhdinov I.T., Zaripov R.B.: Appl. Magn. Reson. **45**, 573–620 (2014)

## Spin-Dependent Transport in Bismuth Doped Silicon

**A. V. Koroleva<sup>1</sup>, A. V. Soukhorukov<sup>1</sup>, D. V. Guseinov<sup>1</sup>, A. V. Kudrin<sup>1</sup>,  
S. A. Popkov<sup>1</sup>, A. A. Detochenko<sup>1</sup>, A. A. Ezhevskii<sup>1</sup>, A. A. Konakov<sup>1</sup>,  
N. V. Abrosimov<sup>2</sup>, and H. Riemann<sup>2</sup>**

<sup>1</sup>Lobachevsky State University of Nizhni Novgorod, Nizhniy Novgorod, Russian Federation, [dalika@inbox.ru](mailto:dalika@inbox.ru)

<sup>2</sup>Leibniz Institute for Crystal Growth, Berlin D-12489, Germany

In recent years, actively being sought semiconductor materials for spintronics applications. These materials must possess high spin relaxation time, and be compatible with the base component / of modern microelectronics. Silicon meets these requirements. However, the weak spin-orbit interaction in silicon impedes the effective spin polarization. The use of silicon doped with heavy Group V donors, such as antimony or bismuth, can solve this problem. These impurities lead to strong spin-dependent scattering, which could under certain conditions contribute to the orientation of the spin currents.

The paper considers the spin relaxation of conduction electrons in bismuth-doped silicon with concentrations of  $1.1 \cdot 10^{13}$ – $2.5 \cdot 10^{14}$  cm<sup>-3</sup>. Excessive concentration of conduction electrons in the samples was achieved by additional doping with lithium at a concentration of  $\sim 10^{16}$  cm<sup>-3</sup>. Spin relaxation was determined on the basis of electron paramagnetic resonance (EPR). It revealed a significant broadening of the EPR line at a concentration of bismuth  $\sim 2.5 \cdot 10^{14}$  cm<sup>-3</sup>, which is a consequence of the strong spin relaxation occurring Elliott-Yafet mechanism induced by bismuth centers [1, 2].

Since the samples were doped with two kinds of impurities contribution of each impurity in the spin-orbit coupling (SOC) was estimated. In [3] was represented SOC constant for Bi of the order 1 meV. To determine the SOC constant of Li the method of saturation of the EPR line was used. Considering that for electrons localized on centers Li, characteristic Blum-Orbach relaxation mechanism, SOC constant of Li is about  $10^{-6}$  meV. From a comparison of the SOC constants it can be concluded that contribution of lithium to the spin-orbit interaction is small compared with bismuth.

Magneto-transport properties of samples <sup>28</sup>Si doped Bi with concentrations  $1.1 \cdot 10^{13}$ – $7.7 \cdot 10^{15}$  cm<sup>-3</sup> were studied by Hall spectroscopy. In the temperature range 10–80 K observed deviation from the linear dependence of the Hall resistance with temperature, which is a manifestation of the anomalous Hall effect. The contribution of the anomalous Hall component to the total resistance decreases with increasing temperature and with decreasing concentration of Bi. When studying sample magnetoresistance <sup>28</sup>Si:Bi at a concentration  $7.7 \cdot 10^{15}$  cm<sup>-3</sup> has been found that with increasing current magnetoresistance can vary from positive to negative. The results can be explained based on ideas about spin-dependent scattering.

1. Elliott R.J.: Phys. Rev.: **96**, 266 (1954)
2. Yafet, in Solid State Physics, edited by F. Seitz and D. Turnbull, **14**, 1 (1963)
3. Castner T.G.: Phys. Rev. **155**, 816–825 (1967)

## NMR Bottle Scanner

**A. B. Konov, M. F. Sadykov, and A. Tirkiya**

Zavoisky Physical-Technical Institute, Russian Academy of Sciences, Kazan 420029,  
Russian Federation, [andrew.konov@gmail.com](mailto:andrew.konov@gmail.com)

There is a problem of security in crowded places, such as airports. Several methods were developed for detecting illicit materials (e.g., explosive or narcotic substances) using X-ray diffraction and NQR. However, those methods are used for detection of solids only. At the same time, there are no widely used methods for scanning of liquids that could be met in luggage.

In this paper, we report results of our development of a prototype instrument for the identification of explosives by using nuclear magnetic resonance phenomena. The main idea of the liquid identification is measuring the longitudinal relaxation time  $T_1$ , transverse relaxation time  $T_2$  and molecular diffusion coefficient  $D$  of each liquid.

We have created a prototype. By computer simulation, we designed and optimized the size and shape of the exciting coil. As a part of this work, we designed a power amplifier for excitation pulses. We used an electromagnet from an EPR spectrometer with a magnetic field up to 1500 Oe. For the purposes of noise reduction, we used a gradiometric receiving coil. This allows us to reduce external noise signals. The system was also placed in a shielded box to reduce noise from external sources of signals.

## Investigation of the $T_1$ and $T_2$ Relaxation of Polyamides NMR in the Low Magnetic Field

**G. S. Kupriyanova<sup>1</sup>, V. V. Molchanov<sup>1</sup>, E. A. Severin<sup>1</sup>,  
and G. V. Mozzhukhin<sup>2</sup>**

<sup>1</sup> Immanuel Kant Baltic Federal University, Kaliningrad 236041, Russian Federation  
wi-m@yandex.ru

<sup>2</sup> Gebze Institute of Technology, Gebze-Kocaeli 41400, Turkey

Thermoresistant polymers which include synthetic high molecular compound of an amide group (CO-NH or CO-NH<sub>2</sub>) were called polyamides. An amide bond as part of the polymer macromolecules is repeated from two to ten times. All polyamides are rigid materials. They have high strength due to crystallization. Their density is generally in the range from 1.01 to 1.235 g/cc. The polyamides have many applications from the machine tool industry to the food industry and medicine, so aging of polyamides is an important issue, especially the influence of mechanical stress. NMR being non-destructive method of investigation, is a better tool for inspection and defect detection, which is indistinguishable by external examination [1]. Modern mobile NMR spectrometers allow to obtain data about investigated sample in the place of its location. The main idea of this

**Table 1.** Values of the relaxation times  $T_1$  and  $T_2$ .

| Sample                  | $T_1$ (ms) | $T_2$ (ms) |
|-------------------------|------------|------------|
| Kestamid (yellow)       | 66.6       | 8.7        |
| Kestamid HS (dark blue) | 41.5       | 11.7       |
| Kestlub (red)           | 63.8       | 12.2       |

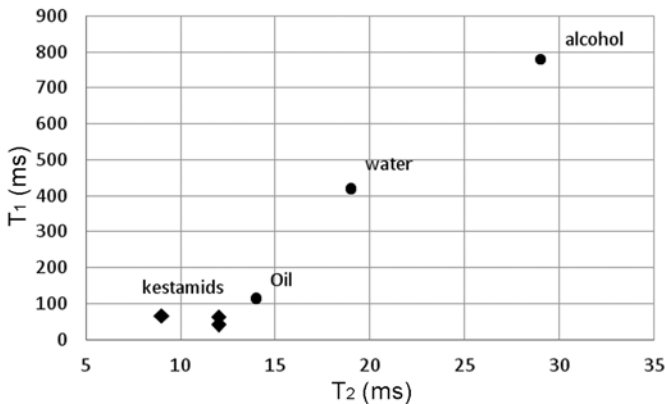


**Fig. 1.** Correlation  $T_1$ - $T_2$  map for same samples.



work is the measurement of relaxation times  $T_1$  and  $T_2$  in the solid polymers using a weak magnetic field and the possibility of using NMR techniques for fixing the mechanical action on the polymers. As samples were taken polyamides produced by POLIKIM Turkey. As samples were taken polyamides produced by POLIKIM Turkey, which are called kestamids. The main difficulty of measurement of relaxation times in these conditions is a weak, inhomogeneous magnetic field of the permanent magnet and the absence of temperature stabilization [2]. Measurement of relaxation times performed on NMR/NQR spectrometer Tecmag Apollo with permanent magnet  $B = 314$  mT. Table 1 shows the average values of the relaxation times obtained for several polyamide samples. The samples were triturated into small shavings before measurement. Fig. 1 shows a correlation map of relaxation times  $T_1$ - $T_2$  for a group of polyamides with background of another samples. Using such a correlation map is possible to distinguish the type of polyamide.

1. Slonim I.Y., Lyubimov A.N.: Nuclear Magnetic Resonance in the Polymer, "Chemistry" Moscow 1966.
2. Kupriyanova G.S., Molchanov V.V., Severin E.A., Mershev I.G.: Composite Pulses in Inhomogeneous Fields NMR, NATO Science for Peace and Security Series B: Physics and Biophysics, 137–147 (2012)

## Pulse and CW EPR Study of Triarylmethyl Radicals at Room Temperature

**A. A. Kuzhelev<sup>1,2</sup>, O. A. Krumkacheva<sup>3,1</sup>, D. V. Trukhin<sup>2</sup>,  
O. Yu. Rogozhnikova<sup>2</sup>, T. I. Troitskaya<sup>2</sup>, V. M. Tormyshev<sup>2,1</sup>,  
M. V. Fedin<sup>3,1</sup>, and E. G. Bagryanskaya<sup>2,1</sup>**

<sup>1</sup> Novosibirsk State University, Novosibirsk 630090, Russian Federation

<sup>2</sup> N. N. Vorozhtsov Novosibirsk Institute of Organic Chemistry SB RAS, Novosibirsk 630090, Russian Federation

<sup>3</sup> International Tomography Center SB RAS, Novosibirsk 630090, Russian Federation, [kuzhelev@nioch.nsc.ru](mailto:kuzhelev@nioch.nsc.ru)

Triarylmethyl (trityl) radicals represent a relatively new class of spin labels having long  $T_m$  on the order of microseconds in liquids at room temperature. This profoundly long relaxation makes trityls a promising alternative for nitroxide spin labels. Recently we demonstrated first distance measurement of  $\sim 4.6$  nm at physiological temperature 310 K (37 °C) in model DNA duplex [1]. The development of this research area implies further improvement of trityl-based labels in order to achieve longer phase memory time  $T_m$  and identification of the factors affecting the  $T_m$  for trityl radicals at 298 K.

In this work we studied the spectroscopic properties of mono-, di-, tri-ester and triamide derivatives of trityl radicals by CW and pulse EPR. We observed the clear dependence of phase memory time ( $T_m$ ) on the magnetic field: room-temperature  $T_m$  values are  $\sim 1.5$ – $2.5$  times smaller at the Q-band (34 GHz, 1.2 T) than at the X-band (9 GHz, 0.3 T). This trend is ascribed to the contribution from  $g$ -anisotropy that is negligible at lower magnetic fields but comes into play at the Q-band. In agreement with this, the difference between  $T_1$  and  $T_m$  becomes more pronounced at the Q-band than at the X-band due to increased contributions from incomplete motional averaging of  $g$ -anisotropy. Linear dependence of  $(1/T_m - 1/T_1)$  on viscosity implies that  $g$ -anisotropy is modulated by rotational motion of the trityl radical. On the basis of the analysis of previous data and results of the our work, we conclude that, in the general situation where the spin label is at least partly mobile, the X-band is most suitable for application of trityls for room-temperature pulsed EPR distance measurements [2].

The financial support of the Russian Foundation for Basic Research (No. 14-03-31839, 13-04-00680) and Russian Science Foundation (No. 14-14-00922).

1. Shevelev G.Y., Krumkacheva O.A., Lomzov A.A., Kuzhelev A.A., Rogozhnikova O.Y., Trukhin D.V., Troitskaya T.I., Tormyshev V.M., Fedin M.V., Pyshnyi D.V., Bagryanskaya E.G.: J. Am. Chem. Soc. **136**, 9874 (2014)
2. Kuzhelev A.A., Trukhin D.V., Krumkacheva O.A., Strizhakov R.K., Rogozhnikova O.Y., Troitskaya T.I., Fedin, M.V., Tormyshev V.M. Bagryanskaya E.G.: J. Phys. Chem. B, DOI: 10.1021/acs.jpcc.5b03027 (2015)

## Electron Paramagnetic Resonance of $Ce^{3+}$ Ions in $KZnF_3$ Single Crystal

**V. A. Latypov<sup>1</sup>, M. L. Falin<sup>1</sup>, and S. L. Korableva<sup>2</sup>**

<sup>1</sup> Zavoisky Physical-Technical Institute, Russian Academy of Sciences, Kazan 420029,  
Russian Federation, vlad@kfti.knc.ru

<sup>2</sup> Kazan Federal University, Kazan 420008, Russian Federation

Double fluoride crystals with perovskite structure  $ABF_3$  are very interesting because they are convenient model systems for studying the magneto - optical properties of impurity dopant ions. In these matrices it is possible to substitute two various cations being inequivalent positions. This enables one to carry out investigations of impurity dopant ions in sixfold or uncommon twelfold coordinations. The physical properties of rare-earth ions in last coordination are not sufficiently studied. The introduction of three-charge rare-earth ions is hampered because of heterovalent substitution and the essential difference in the ionic radii of rare-earth ions and lattice cations. This report is concerned with investigation of impurity paramagnetic centers formed by  $Ce^{3+}$  ions in  $KZnF_3$  single crystal.

The crystals were grown using the Bridgman-Stockbarger method. The concentration of the impurity ions was 1.0 w%. EPR experiments was carried out using an X-band spectrometer ERS-231 (Germany) at  $T = 4.2$  K.

The parameters of the corresponding spin Hamiltonians, the ground states and their wave functions were determined. Structural models of the observed complexes were proposed. The analysis of the obtained results as compared to those obtained for the same paramagnetic ions in other hosts [1–3] was carried out.

This study was supported by the grant of the Presidium of the Russian Academy of Sciences no. 32 “Electron spin resonance, spin-dependent electron effects and spin technologies” and President of the Russian Federation “Leading Scientific Schools” (NSh-4653.2014.2).

1. Ibragimov I.R., Fazlizhanov I.I., Falin M.L. *et al.*: Sov. Phys. Solid State **34**, 1745 (1992)
2. Yamaga M., Honda M., Shimamura K. *et al.*: J. Phys.: Condens. Matter **12**, 5917 (2000)
3. Yamaga M., Honda M., Kawamata N. *et al.*: J. Phys.: Condens. Matter **13**, 3461 (2001)

## Membrane-Sucrose Interactions Probed by Spin-Label Pulsed EPR

**D. V. Leonov<sup>1,2</sup>, K. B. Konov<sup>3</sup>, K. Yu. Fedotov<sup>2</sup>, N. P. Isaev<sup>1</sup>,  
V. K. Voronkova<sup>3</sup>, and S. A. Dzuba<sup>1,2</sup>**

<sup>1</sup> Institute of Chemical Kinetics and Combustion, Russian Academy of Sciences,  
Novosibirsk 630090, Russian Federation

<sup>2</sup> Novosibirsk State University, Novosibirsk 630090, Russia Russian Federation

<sup>3</sup> Zavoisky Physical-Technical Institute, Russian Academy of Sciences, Kazan 420029,  
Russian Federation, ldmitryv.92@gmail.com

Sugars can stabilize biological systems under extreme desiccation and freezing conditions. Hypothetical molecular mechanisms suggest that stabilization effect may be determined either by specific interactions of sugars with biological molecules or by influence of sugars on the solvating shell of the biomolecule. To explore membrane-sugar interactions, electron spin echo envelope modulation (ESEEM) spectroscopy, a pulsed version of electron paramagnetic resonance (EPR), was applied to phospholipid bilayers with spin-labeled lipids added and solvated by aqueous deuterated sucrose solutions. The phospholipids were 1,2-dipalmitoyl-sn-glycero-3-phosphocholine (DPPC). The spin-labeled lipids were 1,2-dipalmitoyl-sn-glycero-3-phospho(TEMPO)choline (T-PCSL) with spin label TEMPO at the lipid polar head group. The deuterium ESEEM amplitude was calibrated using known concentrations of glassy deuterated sucrose solvents. The data obtained indicated the sucrose concentration near the membrane surface obeyed a simple Langmuir model of monolayer adsorption, which clearly implies direct sugar-molecule bonding to the bilayer surface.

The authors are thankful to N. E. Polyakov and M. Y. Volkov for NMR measurements.

This work was supported by the Russian Scientific Foundation (project # 15-15-00021).

## Magnetic Properties of Crystals of Partially Stabilized Zirconia

E. E. Lomonova<sup>1</sup>, F. O. Milovich<sup>2</sup>, N. Yu. Tabachkova<sup>2</sup>, R. M. Eremina<sup>3,4</sup>,  
and I. I. Fazlizhanov<sup>3,4</sup>

<sup>1</sup> Prokhorov General Physics Institute, RAS, Moscow 119991, Russian Federation

<sup>2</sup> National University of Science and Technology MISiS, Moscow 119991, Russian Federation,  
philippmilovich@gmail.com

<sup>3</sup> Zavoisky Physical-Technical Institute, Russian Academy of Sciences, Kazan 420029,  
Russian Federation

<sup>4</sup> Kazan Federal University, Kazan 420008, Russian Federation, REremina@yandex.ru

The crystals of partially stabilized zirconia (PSZ) possess unique mechanical characteristics such as high strength and fracture toughness, low friction coefficients, wear resistance, the chemical and biological inertness [1]. Such unique properties of the PSZ crystals are associated with the features of their phase composition and structure, namely, the degree of tetragonality of the phases and the presence of the domain–twin structure [2, 3]. Cations Y, Ce, Nd, Sc, Er can stabilize the PSZ crystal structure in the various degree due to the various dimensions of the ions, that eventually affects the physicochemical properties of PSZ.

In the frame of this work, we studied the crystals of partially stabilized zirconia by the oxides of yttrium and rare earth ions. It was established that all the samples possessed the developed domain twin structure. It was found that the impact of an additional amount of rare earth oxides on the phase composition, structure and properties of the crystals of the partially yttrium-stabilized zirconia depends on the type and concentration of the rare earth elements. For example, the additional introducing of 1.8 mol%  $\text{Er}_2\text{O}_3$  in PSZ ( $\text{ZrO}_2 - 1.0 \text{ mol}\% \text{ Y}_2\text{O}_3$ ) crystals (Fig. 1a) leads to a stabilization of the transformable phase *t*. The adding of 0.8 mol% erbium oxide to 2.0 mol% yttrium allows give a mixture of

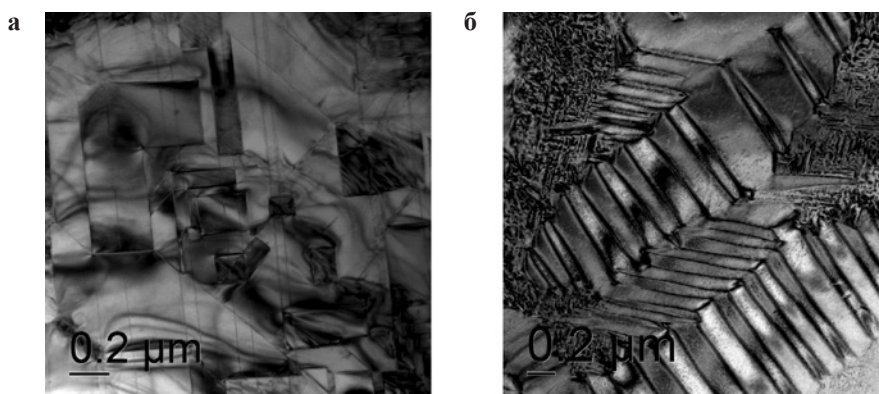


**Fig. 1.** TEM images of the PSZ structures with different concentrations of the stabilizing impurities: **a** 1.0 mol  $\text{Y}_2\text{O}_3$  +  $\text{Er}_2\text{O}_3$  1.8 mol%.  $\text{Er}_2\text{O}_3$ , **(b)** 2.0 mol  $\text{Y}_2\text{O}_3$  +  $\text{Er}_2\text{O}_3$  0.8 mol%.

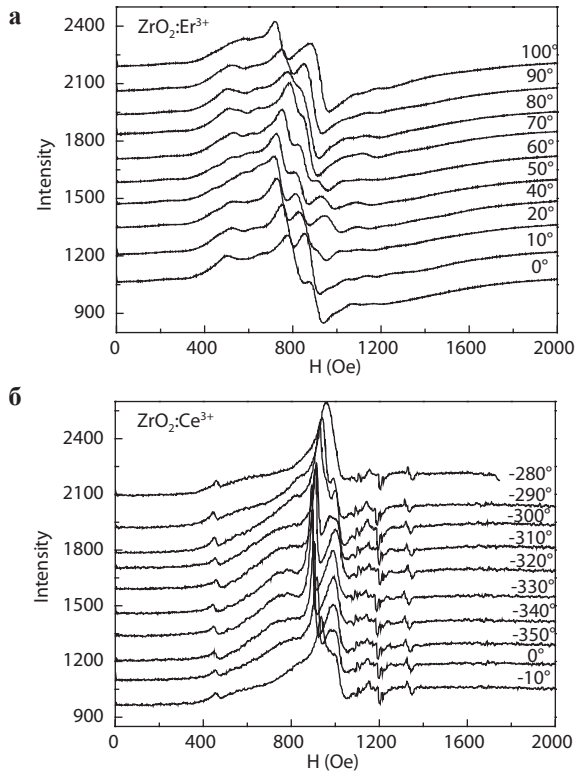


**Fig. 2.** Angular dependence of the ESR spectrum of  $\text{Er}^{3+}$  (a) and  $\text{Ce}^{3+}$  (b) magnetic ions in in  $\text{ZrO}_2$

transformable and non-transformable ( $t$  and  $t'$ ) phases, as in the case only of yttrium content of 2.8 mol% (Fig. 1b). Thus, it was shown that the replacing of the portion of yttrium by the rare earth element in PSZ ( $\text{ZrO}_2 - 2.8 \text{ mol\% Y}_2\text{O}_3$ ) do not always lead to the same phase composition and depends on the concentration of yttrium and rare earth ions with respect to each other.

To get the additional information about the microstructure of PSZ crystals, especially about the nearest neighbors of rare earth ions the crystals of partially stabilized zirconia ( $\text{ZrO}_2 + \text{Y}_2\text{O}_3 + \text{Er}_2\text{O}_3$  and  $\text{ZrO}_2 + \text{Y}_2\text{O}_3 + \text{Ce}_2\text{O}_3$ ) were investigated by the ESR method.

ESR spectrum of  $\text{ZrO}_2:\text{Er}^{3+}$  consists of the hyperfine structure of the cubic paramagnetic centrum  $\text{Er}^{3+}$  (isotope  $^{167}\text{Er}$   $J = 15/2$ ,  $I = 7/2$ ). ESR spectrum of  $\text{ZrO}_2:\text{Ce}^{3+}$  consists of the fine structure of two tetragonal paramagnetic centers of  $\text{Ce}^{3+}$  ( $J = 5/2$ ). The angular dependencies of ESR spectrum for both centers are presented in Fig. 2a,b, respectively.

The reported study was funded by RFBR according to the research project № 15-33-50153.

1. Gogotsi G.A., Lomonova E.E., Furmanova Y. *et al.*: Ceramurgia Int. **20**, 343 (1994)
2. Sakuma T.: Nippon Kinzoku Gakkaishi/Journal of the Japan Institute of Metals **29**, 879 (1988)
3. Alisin V.V., Borik M.A., Lomonova E.E. *et al.*: Mater. Sci. Eng., C **25**, 577 (2005)

## Calculations of Time-Resolved EPR Spectra in Photovoltaic Pair: Polymer Poly(3-Hexylthiophene) and [6-6]-Phenyl C61 – Butyric Acid Methyl Ester

**N. Lukzen<sup>1,2</sup> and J. Behrends<sup>3</sup>**

<sup>1</sup> International Tomography Center, Novosibirsk 630090, Russian Federation,  
luk@tomo.nsc.ru

<sup>2</sup> Novosibirsk State University, Novosibirsk 630090, Russian Federation

<sup>3</sup> Physics Department, Free University of Berlin, Berlin, Germany

Spin-dependent may be not only the chemical reactions but also many of the physical processes in nature. For instance, the transport of charge carriers in solar cells can be significantly affected by the presence of the spin degrees of freedom. A promising material in the study of the spin-dependent processes in organic cells is the mixture of the polymer poly(3-hexylthiophene) (P3HT) and fullerene derivatives for instance 6-6-phenyl C61 – butyric acid methyl ester (PCMB). Devices based on these materials are relatively cheap and provide high quantum yield of charge photo separation. One of the methods of observing paramagnetic carriers in solar cells is a direct recording of the EPR spectra. Recently there have been several experimental studies [1–3], which presents data on the EPR of organic solar cells when exposed to light: there were characteristic spectrum comprising absorption and emission lines. This indicates the formation of spin-correlated radical pairs in the singlet spin state under the sample irradiation. However, the theoretical description of the spectra obtained is still facing a number of difficulties. The paper [1] provides a qualitative interpretation of the spectra and modeling carried out without taking into account the anisotropy of the spin-spin interactions, which is valid for the EPR spectra in the liquid but not in solids. In the paper [2] simulations of the spectra with anisotropic  $g$ -tensor of paramagnetic particles and dipole-dipole interaction were performed, but there were unreasonable assumptions about the local order of the sample (axes of the tensors of all interactions in a certain way are oriented relative to each other) and a very short electron spin relaxation times (ca. 15 ns) was taken. In this work we carried out calculations of time-resolved X-band EPR spectra with taking into account  $g$ -tensor anisotropy of both radicals and averaging over all possible configurations was performed. The effect of paramagnetic relaxation also with account for Boltzmann populations of spin levels and effect of spin-spin interactions on appearance of the time-resolved spectra is considered in details. The financial support by the Russian Foundation for Basic Research (project No. 14-03-00453 and 14-03-00380) and the Alexander von Humboldt Foundation is gratefully acknowledged.

1. Behrends J., Sperlich A., Schnegg A., Biskup T., Teutloff C., Lips K., Dyakonov V., Bittl R.: *Phys. Rev. B* **85**, 125206 (2012)
2. Kobori Y., Noji R., Tsuganezawa S.: *J. Phys. Chem. C* **117**, 1589 (2013)
3. Uvarov M.N., Kulik L.V.: *Appl. Magn. Reson.* **44**, 97 (2013)

## Non Resonance Double Frequency NQR in $\text{NaNO}_2$

S. Mamadazizov<sup>1</sup>, G. Mozzhukhin<sup>2</sup>, B. Rameev<sup>2</sup>, and G. Kupriyanova<sup>3</sup>

<sup>1</sup> Immanuel Kant Baltic Federal University, Kaliningrad 236041, Russian Federation, sultonazar.mamadazizov@mail.ru

<sup>2</sup> Gebze Technical University, Gebze 41400, Turkey, mgeorge@gyte.edu.tr

<sup>3</sup> Immanuel Kant Baltic Federal University, Kaliningrad 236041, Russian Federation, galkupr@yandex.ru

In double frequency techniques usually the second channel is used to excite possible transition or suppress it by saturation. We estimated the influence of low frequency non-resonance pulse on echo.

Our system consists of two channel NQR spectrometer on the base of Apollo Tecmag and two frequencies probe. An object of our researches was  $\text{NaNO}_2$  with two different ranges of powder sizes: small (SF) and big (BF) fractions. We used double resonance pulse sequence, which is shown on figure 1 to estimate the influence of dressing pulse on NQR echo of  $\text{NaNO}_2$ .

Paper [2] describes size effects in NQR. According to this work decreasing of average powder sizes result in shortening of relaxation time  $T_2$  and also line broadening. It is true for our object. The average line width (see Table 1) of BF is smaller than the SF average line width. Moreover,  $T_2$  for SF equal to 795 ms and for BF it is equal to 880 ms [1]. But there is no obvious dependence of dressing pulse frequency on line width or relaxation time  $T_2$ .

During this work we detected the non-resonance attenuation of the echo signals (Fig. 2). On the second channel the pulse frequency changed in the range

**Table 1.** SF and BF line width comparison.

| Dressing pulse frequency (kHz) | Line width (Hz) |     |
|--------------------------------|-----------------|-----|
|                                | SF              | BF  |
| 900                            | 495             | 304 |
| 800                            | 343             | 256 |
| 700                            | 342             | 271 |
| 600                            | 388             | 281 |

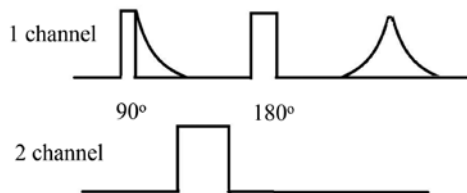


**Fig. 1.** Double frequency pulse sequence.



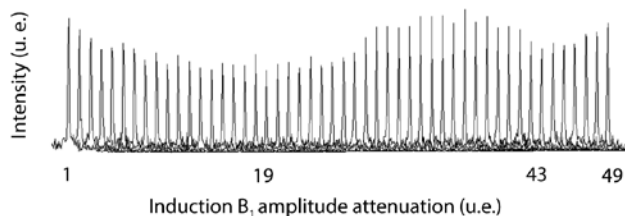


**Fig. 2.** Dependence of echo signal on changing amplitude of induction  $B_1$  for BF. Second pulse frequency is 400 kHz.

100 kHz–1000 kHz. We have noticed that the value of attenuation depends on pulse duration, amplitude of induction  $B_1$  and frequency. In addition, the vulnerable influence of pulse on second channel is observed at frequency range 400–1000 kHz. Moreover, for SF and BF the resulting echo attenuation on the same frequency is different due to size effect. We suggest that there also might be a piezoelectricity in small fraction.

It seems that the pulse on second channel destroys the spin coherency. As a result, we observe the attenuation of the signal in pulse sequence especially at frequency range 400–1000 kHz.

1. Sinyavsky N.Ya., Mershev I.G., Kupriyanova G.S.: *Zeitschrift für Naturforschung* **70**(6), 451–457 (2015)
2. Sinyavsky N.Ya., Mozzhukhin G.V., Dolinenkov Ph.: Size Effect in  $^{14}\text{N}$  Nuclear Quadrupole Resonance Spectroscopy. International Workshop “Magnetic Resonance Detection of Explosives and Illicit Materials”, Yalova, Turkey, 2011 p. 69–76.

## Compensation of the NQR Frequency Offset with Composite Pulses

**I. Mershiev** and **G. Kupriyanova**

Institute of Physics and Technology, Immanuel Kant Baltic Federal University, Kaliningrad 236041, Russian Federation, IMershiev@kantiana.ru

Composite pulses are widely used in NMR for compensation of the magnetic field inhomogeneity, frequency offset, and dipole-dipole interactions. In NQR in powders, excitation with composite pulses can increase signal-to-noise ratio through partial compensation of powder averaging and inhomogeneity of radiofrequency field [1]. Another possibility for increasing SNR is the use of composite pulses to compensate NQR frequency offset [2].

In this work, we design composite pulses for  $^{14}\text{N}$  NQR in powders with uniform excitation capability for a wide range of pulse angle and frequency offset. As the capability of phase modulation is usually limited with the spectrometer hardware, we use mixed-integer numerical optimization with genetic algorithm, to calculate length and phase of individual pulse in a sequence. In a numerical model, NQR spin system was implemented using fictitious operators approach [3]. Model suggests general case of  $I = 1$  NQR spin system ( $\eta \neq 0$ ). Results shows, that it is possible to keep excitation broadband with at least three parts in a composite pulse. Best results are obtained with

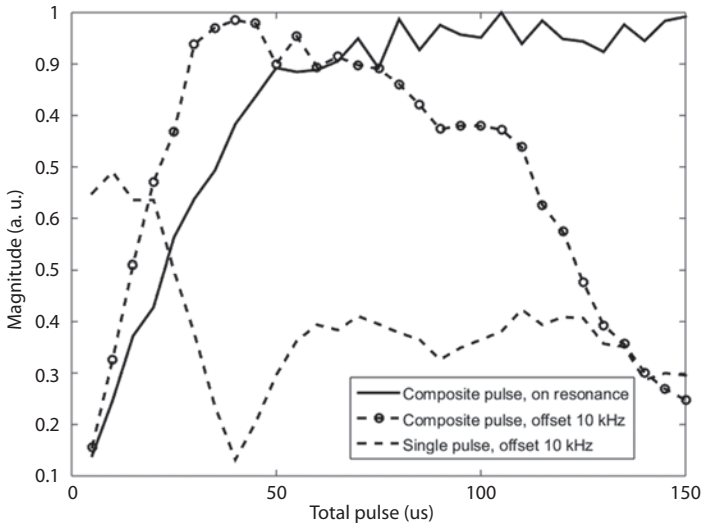


**Fig. 1.** Nutation experiments for single pulse and  $(0.430)_0-(0.30)_{180}-(0.270)_{90}$  composite pulse ( $\text{NaNO}_2$  powder sample, 3.608 MHz).

---

$(0.43\theta)_0-(0.3\theta)_{180}-(0.27\theta)_{90}$  composite pulse, where overall pulse length  $\theta$  can be varied in a wide range. Compensation of frequency offset can be useful in remote detection, where temperature and exact NQR frequency of the sample can be unknown.

1. Ramamoorthy A., Narasimhan P.T.: *Mol. Phys.* **73**, 207 (1991)
2. Mikhaltsevitch V.T., Rudakov T.N., Flexman J.H., Hayes P.A., Chisholm W.P.: *Solid State Nucl. Magn. Reson.* **25**, 61 (2004)
3. Vega S., Pines A.: *J. Chem. Phys.* **66**, 5624 (1977)

## Population Transfer in NQR of Compounds with Long $T_1$ Relaxation Parameter

**G. V. Mozzhukhin<sup>1</sup>, J. Barras<sup>2</sup>, B. Rameev<sup>1,3</sup>, and G. Kupriyanova<sup>4</sup>**

<sup>1</sup> Gebze Technical University, Gebze-Kocaeli 41400, Turkey, mgeorge@yandex.ru

<sup>2</sup> Department of Mechanical Engineering, King's College, London WC2R 2LS, UK

<sup>3</sup> Zavoisky Physical-Technical Institute, Russian Academy of Sciences, Kazan 420029, Russian Federation

<sup>4</sup> Baltic Federal State University, Kaliningrad 320014, Russian Federation

Two frequency method in NQR of N-14 nuclei may be used for lines reference in complex spectra [1], and although two and three frequency methods has application in explosives detection for increase of reliability and avoiding of transition processes in equipment. Usually, these applications take place in the substances with short  $T_1$  relaxation that has not allowed to estimate the influence of relaxation on the process of polarization transfer [2]. In this work we studied the polarization transfer in two frequency NQR with long  $T_1$  relaxation parameter.

Experimental setup: NQR experiments have been performed on Tecmag Apollo NQR/NMR console (0.1–100 MHz) (with two-channel transmitter and one-channel receiver modules for GIT group and single channel for King's college group). Tomco power amplifiers with output power of up to 500 W (or 250 W) have been used. For multifrequency NQR experiments the detector unit consists of the system of three orthogonal coils, each of which is connected to variable capacitor to form a serial/parallel resonance circuit tuned to its own resonance frequency. For single coil measurements the probe consisting of solenoid coil connected to a variable capacitor has been used. A low-noise single-channel preamplifier Miteq and auxiliary electronic circuits (Q-spoiler – see below, cross-diode boxes) have been connected between the probe and Tecmag NMR/NQR Console. The sample of our studies was carbamazepine ( $C_{15}H_{12}N_2O$ , 5H-Dibenz[b,f]azepine-5-carboxamide) produced by Sigma-Aldrich Company Ltd. was in the form of about 20 g of a plastic mixture placed inside a tube. The NQR spectrum of carbamazepine consists of two sets of three frequencies ( $\nu_+ = 3874$  kHz,  $\nu_- = 3827$  kHz and  $\nu_0 = 47$  kHz) [3]. One position of atom nitrogen N has asymmetry parameter  $\eta = 0.02$  and allows do the comparison the two frequency NQR for one and two coils.  $T_1$  is near 5s.

## Spin-Polarized Time-Resolved EPR Spectra of Pentadentate Fe(III) Complexes with Imidazole or Picoline as Co-Ligandes

**I. Ovchinnikov, T. Ivanova, A. Sukhanov, and O. Turanova**

Zavoisky Physical-Technical Institute, Russian Academy of Sciences, Kazan 420029,  
Russian Federation, igovchinnikov@gmail.com

Study of multifunctional mono [1] molecular and cluster [2] molecular systems with photoswitched physical properties is an actual problem. The spin-crossover complexes Fe(III) ( $d^5$  electron configuration,  ${}^6A_1$  (high spin HS) and  ${}^2T_2$  (low spin LS) terms with small differences in energy) are examples of similar systems. The spin-state photoswitching dynamics (spanning ten decades in time) was investigated recently on spin-crossover (LS  $\Rightarrow$  HS) compound [TPA Fe(III)TCC]PF<sub>6</sub> by femtosecond optical spectroscopy by the variation in the optical density [3, 4].

We presented results of the first investigation of photoswitching dynamics in accessible window  $5 \cdot 10^2$ – $5 \cdot 10^4$  ns to time-resolved EPR spectroscopy. The powder complexes [FeSaltL]BPh<sub>4</sub> with L = Him ( $S = 5/2$ ) and L = Pic ( $S = 1/2 \leftrightarrow 5/2$ ) were irradiated by pulse laser in the ligand-metal charge transfer band ( $\lambda = 532$  nm) at temperature interval 5–300 K. The emissive (spin polarized) spectra, coincides in form with the integral continuous-wave EPR spectra ( $g \approx 4$  for L = Him,  $g \approx 2$  for L = Pic) were observed. The kinetic parameters were characterized by two exponential functions describing the fast and slow kinetics. As well absorptive spectra at temperatures 40–60 K was appeared at time detection around 3000 ns in the range  $g \approx 22$  for samples with L = Him and Pic.

The possible interpretation of features observed under laser irradiation is discussed.

1. Venkataramani S., Jana U. *et al.*: Science **331**, 445 (2011)
2. Ohkoshi S., Imoto K. *et al.*: Nature Chem. **3**, 564 (2011)
3. Lorenc M., Balde Ch. *et al.*: Phys. Rev. B **85**, 05432 (2012)
4. Kaszub W., Buron-LeCointe M. *et al.*: Eur. J. Inorg. Chem. **2013**, 992 (2013)
5. Ovchinnikov I.V., Ivanova T.A. *et al.*: Russ. J. Coord. Chem. **39**, 598 (2013)

## Low-Temperature Dynamical Transition in Glassy *o*-Terphenyl

E. A. Pushkina<sup>1</sup>, D. V. Leonov<sup>1</sup>, and S. A. Dzuba<sup>1,2</sup>

<sup>1</sup> Physics Department, Novosibirsk State University, Novosibirsk 630090, Russian Federation, elenabiochem@gmail.com

<sup>2</sup> Voevodsky Institute of Chemical Kinetics and Combustion, Russian Academy of Sciences, Novosibirsk 630090, Russian Federation

The relationship between structural-dynamical properties and physiological activity of biological systems now is a subject of intensive investigations. In non-crystalline structures, intensive vibrations of atoms and molecules have been found recently by neutron scattering and Mossbauer absorption. These vibrations are harmonic below the temperature which is called a dynamic transition temperature,  $T_d$ , and are anharmonic or diffusive above this temperature. For biological systems,  $T_d$  ranges from 200 to 230 K.

In this work, this phenomenon is investigated by pulsed electron paramagnetic resonance (EPR) of spin probes and labels. The advantages of pulsed EPR, as compared with neutron scattering, are sensitivity to orientation motion of molecules and relative accessibility of the experiment. Moreover, it is possible to study the motion in the different parts of complex supramolecular structures, by using selective labeling.

The detailed temperature dependences of anisotropic spin relaxation rate ( $W_{anis}$ )( $W_{anis}$ ) for three types of radicals (**I**, **II** and **III**) (Figs. 2–4) in molecular

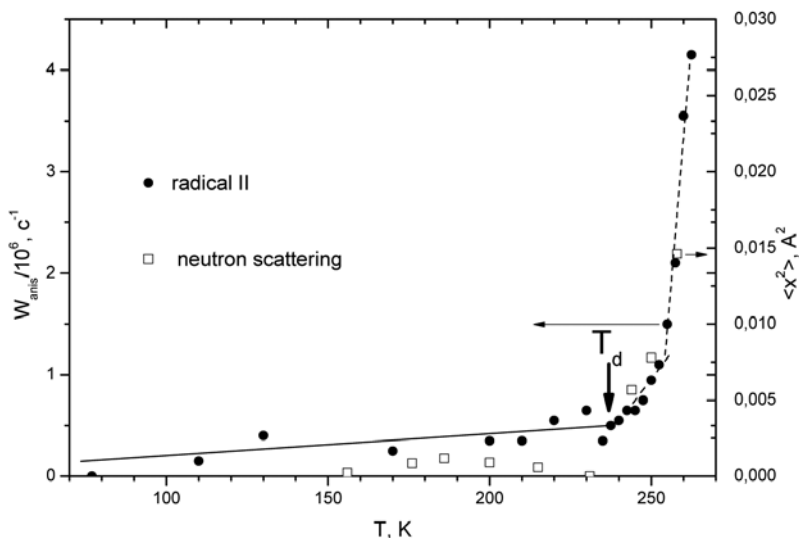


Fig. 1. The dependence between the temperature and the rate of anisotropic relaxation  $W_{anis}$  for radical **II** and mean square displacement  $\langle x^2 \rangle$  [1].

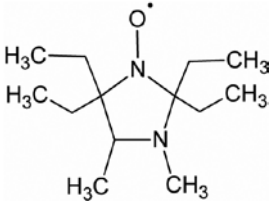


Fig. 2. Radical II.

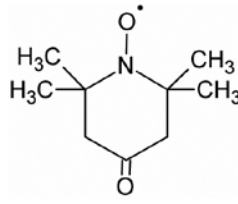


Fig. 3. Radical I.

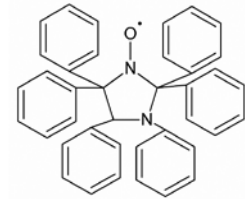


Fig. 4. Radical III.

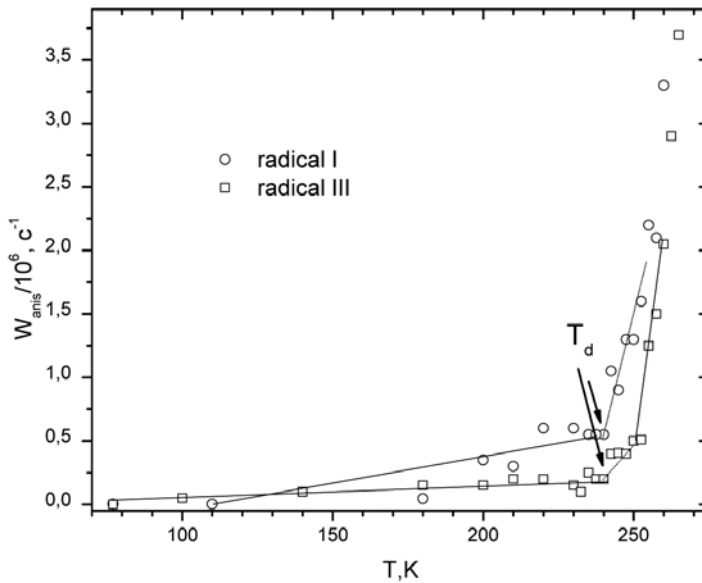


Fig. 5. The dependences between the temperature and the rate of anisotropic relaxation  $W_{anis}$  for radical I and radical III.

ortho-terphenyl glass were obtained. The drastic increase of the of  $W_{anis} W_{anis}$  for all three radicals was found above  $\sim 240$  K (Figs. 1 and 5). This increase is in good agreement with the published neutron scattering data [1] (see Fig. 1). The coincidence of both data sets can be explained as manifestation of the phenomenon of the dynamical transition in these both types of experiment.

Then, all three types of radicals are of remarkably different size, but their temperature dependences of  $W_{anis} W_{anis}$  look similarly. So, it is likely that cooperative molecular motions are responsible for the dynamical transition in glassy o-terphenyl.

## To the ESR Studies of the Topological Insulators

**V. O. Sakhin, E. F. Kukovitsky, Yu. I. Talanov, and G. B. Teitel'baum**

Zavoisky Physical-Technical Institute, Russian Academy of Sciences, Kazan 420029,  
Russian Federation, urfinjus67@gmail.com

Topological insulators (TI) represent a novel class of quantum materials having insulating bulk and dissipationless conducting surface. This surface state exhibits many exotic phenomena such as spin-momentum locking and topological protection against non-magnetic impurities and defects. This offers opportunities for future device applications. There has been a lot of research using various methods like APRES [1, 2], STM [2], and more, but still understanding of electronic properties of TI is troubled. Basic binary alloys, that reveal the TI nature, are  $\text{Bi}_2\text{Se}_3$ ,  $\text{Bi}_2\text{Te}_3$ , suffer from significant bulk contribution to transport properties, which masks the surface transport signals. Therefore, studies of topological phase behavior would require sensitive local method.

Electron spin resonance (ESR) could be effective for obtaining information about properties of TI due to its sensitivity to local magnetic fields. We propose here two possible approaches to implement it. The first one is to use the ultrathin paramagnetic layer deposited on a cleaved surface of TI. Such DPPH probe has narrow ESR signal, which should be very sensitive to the DC current flowing along the surface. Due to the spin-momentum locking of the surface charge carriers such a current will generate an additional magnetic field, which will shift the ESR signal of the probe. The nature of the shift can be verified by varying the direction and the value of current. The second possibility consists in doping of TI with the magnetic impurities. Their magnetic moments can be polarized due to the ESR pumping in the external magnetic field and to induce the spin current at the surface of TI. Due to the spin-momentum locking this will cause the flow of detectable electric current through sample.

To reduce the influence of the bulk transport contribution we performed the optimization of TI samples by doping with non-magnetic impurities, like Sn. The characterization of samples was carried out in the wide temperature range by the standard four-probe DC technique.

The financial support of the Foundation for Basic Research and the Government of the Tatarstan in frames of scientific project N 15-42-02477 is acknowledged.

1. Cao H. *et al.*: Phys. Status Solidi RRL **7**, 133 (2013)
2. Alpichshev Z. *et al.*: Phys. Rev. B **84**, 041104 (2011)



---

## Development of a Method for Separating Exchange and Dipole-Dipole Interactions to the Shape of EPR Spectra of Nitroxyl Radicals with Unresolved Proton Hyperfine Structure

**K. M. Salikhov<sup>1,2</sup>, R. T. Galeev<sup>1</sup>, B. Bales<sup>3</sup>, and M. M. Bakirov<sup>1</sup>**

<sup>1</sup> Zavoiisky Physical-Technical Institute, Russian Academy of Sciences, Kazan 420029, Russian Federation, [pinas1@yandex.ru](mailto:pinas1@yandex.ru)

<sup>2</sup> Kazan Federal University, Kazan 420008, Russian Federation

<sup>3</sup> Western Institute of Nanoelectronics, University of California, Los Angeles 18111, USA

The high sensitivity of the EPR spectra of stable nitroxide radicals to their chemical structure, the presence of paramagnetic additives, solvent polarity makes method of EPR oxymetry an effective tool. EPR of radicals is a perspective technique for direct measurement of tissue  $pO_2$ , which has several advantages over the other existing methods for applications in which the parameter of interest is the  $pO_2$  of tissues, and information is needed over a time course of minutes to hours, or for repetitive measurements over days or weeks.

EPR of radicals are widely known, but the description of the EPR of nitroxide radicals often use simplified algorithms that do not take into account all the processes due to exchange and dipole-dipole interactions. In papers [1, 2] different algorithms of separating dipole-dipole and Heisenberg Spin Exchange interactions are proposed. In this paper, we applied this routines for the case of simulated spectra. EPR spectra were simulated for the case nitroxide radicals with unresolved proton hyperfine structure.

1. Salikhov K.M.: *Appl. Magn. Reson.* **38**, 237–256 (2010)
2. Peric M., Bales B., Peric M.: *J. Phys. Chem. A* **116**, 2855–2866 (2012)
3. Molin Yu.N., Salikhov K.M., Zamaraev K.I.: *Spin exchange*. Springer Verlag, Berlin Heidelberg New York. 1980.

## Nuclear Magnetic Resonance in Low-Dimensional Compound $A_3Ni_2SbO_6$ ( $A = Na, Li$ )

**T. Salikhov<sup>1</sup>, M. Iakovleva<sup>1</sup>, K. Safiullin<sup>2</sup>, A. Klochkov<sup>2</sup>, M. Tagirov<sup>2</sup>,  
M. Stratan<sup>3</sup>, E. Zvereva<sup>3</sup>, V. Nalbandyan<sup>4</sup>, and E. Vavilova<sup>1</sup>**

<sup>1</sup> Zavoiisky Physical-Technical Institute, Russian Academy of Sciences, Kazan 420029, [tmsalikhov@gmail.com](mailto:tmsalikhov@gmail.com)

<sup>2</sup> Institute of Physics, Kazan Federal University, Kazan 420008, Russian Federation

<sup>3</sup> Faculty of Physics, Moscow State University, Moscow 119991, Russian Federation

<sup>4</sup> Chemistry Faculty, Southern Federal University, 344090, Russian Federation

In the last years the layered oxides of alkali and transition metals are intensively investigated due to their potential applications as solid electrolytes and electrode materials in modern ionics. Recently, a new generation of layered complex metal oxides with honeycomb-based crystal structure where ordered mixed-layers of magnetic cations alternate with non-magnetic alkali metal layers has been a subject of intense research worldwide. This work is devoted to the investigation of new quasi two-dimensional (2D) honeycomb-lattice compounds  $Li_3Ni_2SbO_6$ ,  $Na_3Ni_2SbO_6$ . Basic magnetic properties of  $Li_3Ni_2SbO_6$  and  $Na_3Ni_2SbO_6$  have been reported recently [1, 2]. We are here to present the results of studies a systematic study of their electronic and magnetic behavior by nuclear magnetic resonance.

We performed the  $^7Li$  ( $I = 3/2$ ) and  $^{23}Na$  ( $I = 3/2$ ) NMR experiments and found that the behavior of the NMR spectrum and relaxation at low temperature is caused by the interaction with the magnetic  $Ni^{2+}$  ions and reflects the dynamics of magnetic subsystem. Upon approaching the Neel temperatures the NMR lineshape of the sodium and lithium spectra change dramatically, that indicate the onset of long-range magnetic order. In addition, the calculations of different models of ordering have been performed. The best fit of the experimental data was obtained assuming a *zigzag* spin structure with spins oriented perpendicular to the plane. At 4.5 T the spin-flop phase is observed. At  $T > 300$  K the deviation of the  $1/\chi T_1 T$  from 1 shows the additional relaxation mechanism which becomes effective at these temperatures. We propose that the reason of this additional relaxation is the growth of in-plane lithium mobility.

The work was supported by Foundation for Basic Research (grant 14-02-01194 and 14-02-00245)

1. Zvereva E.A. *et al.*: Dalton Trans. **41**, 572 (2012).
2. Politaev V.V. *et al.*: J. Solid State Chem. **183**, 684 (2010)

## High-Frequency EPR Spectroscopy of ZnSe:Fe

**G. S. Shakurov<sup>1</sup>, D. S. Pytalev<sup>2</sup>, V. I. Kozlovsky<sup>3</sup>, and Yu. V. Korostelin<sup>3</sup>**

<sup>1</sup> Zavoisky Physical-Technical Institute, Russian Academy of Sciences, Kazan 420029,  
Russian Federation, shakurov@kfti.knc.ru

<sup>2</sup> Institute of Spectroscopy RAS, Moscow, Troitsk 142190, Russian Federation

<sup>3</sup> P.N. Lebedev Physical Institute, Moscow 119991, Russian Federation

ZnSe:Fe<sup>2+</sup> crystal is the promising laser material for a mid IR range. The EPR spectroscopy study of this crystal performed with X-band spectrometer reveals only Fe<sup>3+</sup> ions in the cubic environment [1]. The EPR spectra of Fe<sup>2+</sup> ions are unknown. We carried out the wide-band high-frequency (37–850 GHz) EPR measurements of ZnSe:Fe. Two types of the spectra were found. The first belongs to Fe<sup>2+</sup> ion. The resonance transitions between ground singlet and excited triplet were observed. The zero-field-splitting was about 15 cm<sup>-1</sup> which is consistent with previously far infrared measurements of ZnS:Fe<sup>2+</sup> [2]. The second type is the spectra from monoclinic Fe<sup>3+</sup> ions. The energy distances between the ground and excited doublets are similar to the associate ZnSe:Fe-Cu ones [3].

1. Dieleman J.: Philips Res. Rep. **20**, 206 (1965)
2. Slack G.A., Roberts S., Ham F.: Phys. Rev. **155**, 170 (1967)
3. Holton W.C. *et al.*: Phys. Rev. **169**, 359 (1968)

## EPR Study of the Inclusion Complex of Nitronyl Nitroxide Covalently Linked with Permethyl-B-Cyclodextrin

**R. K. Strizhakov<sup>1</sup>, O. A. Krumkacheva<sup>2</sup>, E. V. Tretyakov<sup>2</sup>,  
A. S. Medvedeva<sup>3</sup>, V. V. Novokshonov<sup>3</sup>, V. G. Vasiliev<sup>3</sup>,  
V. I. Ovcharenko<sup>2</sup>, and E. G. Bagryanskaya<sup>1</sup>**

<sup>1</sup> N. N. Vorozhtsov Novosibirsk Institute of Organic Chemistry, Novosibirsk 630090, Russian Federation

<sup>2</sup> International Tomography Center, Novosibirsk 630090, Russian Federation

<sup>3</sup> A. E. Favorsky Irkutsk Institute of Chemistry, Irkutsk 664033, Russian Federation  
Rodion.Strizhakov@tomo.nsc.ru

Cyclodextrins (CD) are widely used in science, technology and industry since they have hydrophobic cavity. That's why CDs may produce various inclusion complexes with other molecules including nitroxides [1]. Depending on the specific nitroxide the modified CDs may be used as selective luminescence quenchers [2], high-sensitive radical detecting systems [3], and so on.

In this study we investigated adduct of permethyl- $\beta$ -CD (Trimeb) and covalently linked nitronyl nitroxide (NN). Similar spin adducts have longer lifetime than free nitroxides in case of radical fragment being deeply-included in the CD cavity [4]. We investigated the behavior of this complex (NN-Trimeb) using Electron Spin Echo Envelope Modulation (ESEEM) and Continuous Wave EPR (CW-EPR) methods.

ESEEM indicated the formation of the inclusion complex between NN and Trimeb cavity. However there is the equilibrium between the complex with NN being outside and capping the cavity. CW-EPR method was employed to measure

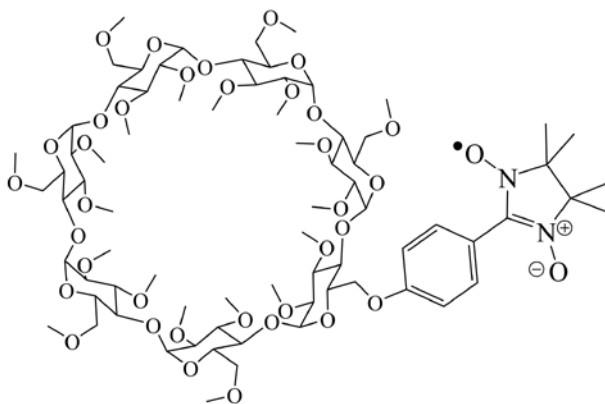


**Fig. 1.** Structure of the complex.

---

the NN-Trimethyl constant of reduction by ascorbic acid, which was close to the free nitroxide one. It agreed with ESEEM results well.

The financial support of the Russian Foundation for Basic Research (No. 14-03-32024).

1. Krumkacheva O., Fedin M. *et al.*: Phys. Chem. B, **117** (27), 8223 (2013)
2. Krumkacheva O., Tanabe M., Yamauchi S. *et al.*: Appl. Magn. Reson. **42** (1), 29 (2012)
3. Han Y., Liu Y., Zweier J.L. *et al.*: J. Org. Chem., **74**, 5369 (2009)
4. Karoui H., Tordo P.: Tetr. Lett. **45**(5), 1043 (2004)

## Influence of Fe-Fe and Fe-Ln Spin-Spin Interactions on the Magnetisation Dynamics of Mixed Clusters

**A. Sukhanov<sup>1</sup>, R. Galeev<sup>1</sup>, L. Mingalieva<sup>1</sup>, V. Voronkova<sup>1</sup>,  
A. Baniodeh<sup>2</sup>, and A. Powell<sup>2</sup>**

<sup>1</sup> Zavoiisky Physical-Technical Institute, Russian Academy of Sciences, Kazan 420029, Russian Federation, vio@kfti.knc.ru

<sup>2</sup> Karlsruhe Institute of Technology, University of Karlsruhe, Karlsruhe, Germany

The design, synthesis, and magnetic investigation of so-called single molecule-magnets (SMMs) have attracted widespread attention after the discovery that a molecular transition metal coordination compound could, at liquid-helium temperatures, retain magnetization for long periods of time at a certain blocking temperature in the absence of an external magnetic field [1]. In 3d-SMMs, the reversal of the magnetization is blocked by a combination of two properties, the Ising-type magnetic anisotropy, which can be expressed as the axial zero-field splitting parameter,  $D$ , and the total spin on the molecule,  $S$ . In recent years intensively synthesized and investigated clusters built up of transition metal and rare-earth ions as perspective candidates for the design of new SMMs [2], special clusters containing dysprosium ions. The SMM behavior of these clusters is due to the strong magnetic anisotropy which is characteristic for dysprosium ions in the low-symmetry environment. The design of new SMMs on the basis of clusters with dysprosium ions requires the understanding of the correlation between the relaxation rate of the magnetization, anisotropy of the local magnetic properties of the  $Dy^{3+}$  ion and spin-spin interactions in cluster. The influence of the spin-spin interactions on SMMs properties of dysprosium containing clusters today is poorly studied. EPR is a useful method for investigations of the local magnetic properties of the paramagnetic ions and spin-spin interaction between ions in clusters.

This investigation focuses on the study of Fe-Fe and Fe-Dy spin-spin interactions in the mixed  $FeLn_2$ ,  $Fe_2Ln_2$  and  $Fe_3Ln$  ( $Ln = Y^{3+}$ ,  $Dy^{3+}$ ) clusters. It has been previously shown that the low-temperature spectra of  $Fe_2Ln_2$  compounds are determined by magnetic properties of rare-earth ions and the dipole-dipole interactions between the Ln ions [3]. The study of a family of  $Fe_2Dy_2$  clusters in the compounds with different substituted benzoate ligands [ $Fe_2Dy_2(OH)_2(teaH)_2(R-C_6H_4COO)_6$ ] showed that the nature and position of the substituents affect the SMMs properties [4]. Here we report the results of the EPR investigation of some tetranuclear  $Fe_2Dy_2$  clusters and other clusters to understand the reason for the change of SMMs properties and character of influence of the spin-spin interactions on these properties. The EPR spectra of

---

polycrystalline samples were measured at X- and Q-bands in the temperature range of 50–4 K.

This research is supported in part by the Russian Foundation for Basic Research (project no. 13-02-01157) and Program of Presidium RAS.

1. Sessoli R., Gatteschi D., Caneschi A., Novak M.A.: *Nature* **365**, 141 (1993)
2. Woodruff D.N., Winpenny R.E.P., Layfield R.A.: *Chemical Reviews* **113**(7) (2013)
3. Baniodeh A., Lan Y., Novitchi G., Mereacre V., Sukhanov A., Ferbinteanu M., Voronkova V., Anson C.E., Powell A.K.: *Dalton Trans.* **42**, 8926–8938 (2013)
4. Baniodeh A., Mereacre V., Lan Y., Wolny J.A., Anson Ch.E., Schünemann V., Powell A.K.: *Chem. Comm.* **49**, 9666 (2013)

## ESR Study of the $\text{Bi}_2\text{Te}_3$ Doped with Manganese

**Yu. Talanov, E. Kukovitsky, V. Sakhin, and G. Teitel'baum**

Zavoisky Physical-Technical Institute, Russian Academy of Sciences, Kazan 420029,  
Russian Federation, talanov@kfti.knc.ru

A novel approach to processing spin and charge currents in topological insulators (TI) consists in pumping of polarized spins using thin ferromagnetic layer deposited on TI [1]. Unfortunately, the application of this very interesting approach is complicated by the limitations on the magnetization transfer between these two different media. These restrictions stimulate the search for possibilities to create the spin polarization in the TI directly. As one of possible steps in this direction, we suggest to use magnetic impurities doped in the bulk of TI. Here we report here our results of the ESR and magnetometric studies of the TI compound  $\text{Bi}_2\text{Te}_3$  doped with magnetic manganese ions. We presume that these findings will shed some light on the new possibility of the spin-pumping in TI.

Single-crystal samples of  $\text{Bi}_{2-x}\text{Mn}_x\text{Te}_3$  were grown in quartz crucibles under the enhanced pressure (2 bars) of the inert gas by means of slow cooling melt in the temperature gradient field with the axial symmetry. The manganese concentration in the initial material corresponded to two nominal values of  $x = 0.005$  and  $0.05$ . Crystals are easily flaked along the  $ab$ -plane. The characteristic sizes of samples studied are  $4 \times 2 \times 0.1 \text{ mm}^3$ .

The magnetic susceptibility measurements using a homebuilt SQUID magnetometer indicate that the sample susceptibility varies with temperature according to the Curie-Weiss law:  $\chi = C/(T - \Theta)$  with  $\Theta$  being the Curie-Weiss temperature. In crystals with  $x = 0.005$   $\Theta = 0$ , i.e. the magnetic ordering is absent. The samples with  $x = 0.05$  have  $\Theta = 11 \text{ K}$ . Below this temperature they are completely ferromagnetically ordered.

The ESR study on an X-band spectrometer confirms this statement. The ESR signal of Mn ions has properties inherent to ferromagnetic resonance (FMR): the resonance field value is minimal ( $\sim 900 \text{ Oe}$ ), when the applied field is parallel to the  $ab$ -plane of crystal; and it is maximal ( $> 7000 \text{ Oe}$ ) in the field perpendicular to the plane.

We found that the similar behavior of the ESR signal holds also above  $T = \Theta$  (the  $\Theta$  value is obtained from the susceptibility measurements in low fields). Moreover, the analysis of the temperature and angular dependence of the ESR spectra provides reasons to suggest the presence of the fluctuating ferromagnetic inclusions at  $T > \Theta$ . The application of the magnetic field of several kilooersteds leads to their ordering, large magnetization and large ESR signal shift accordingly. Note that the similar magnetization behavior was observed in the magnetic



measurements of Mn-doped  $\text{Bi}_2\text{Te}_3$  [2]. Our results favor the possibility to control spin currents in TI via tuning the ferromagnetically correlated clusters formed by doped magnetic ions.

The work is supported by the Russian Foundation for Basic Research (project no 15-42-02477).

1. Shiomi Y., Nomura K., Kajiwara Y.: Phys. Rev. Lett. **113**, 196601 (2014)
2. Watson M.D., Collins-McIntyre L.J. *et al.*: New Journal of Physics **15**, 103016 (2013)

## Dimer Self-Organization of Er<sup>3+</sup> Impurity Ions in Synthetic Forsterite

**V. F. Tarasov<sup>1</sup>, L. V. Mingalieva<sup>1</sup>, K. A. Subbotin<sup>2</sup>, R. B. Zaripov<sup>1</sup>,  
and E. V. Zharikov<sup>2,3</sup>**

<sup>1</sup> Zavoiisky Physical-Technical Institute, Russian Academy of Sciences, Kazan 420029,  
Russian Federation, tarasov@kfti.knc.ru

<sup>2</sup> Prokhorov General Physics Institute of the Russian Academy of Sciences, Moscow 119991,  
Russian Federation, evzh@mail.ru

<sup>3</sup> Mendeleev University of Chemical Technology of Russia, Moscow, 125047, Russian Federation,  
evzh@mail.ru

It was found earlier that some trivalent impurity ions in synthetic forsterite have a tendency to the formation of dimer associates consisting of two closely situated impurity ions with a magnesium vacancy between them. The mechanism leading to the association of the impurity ions into the dimers is related with the necessity to conserve the total cation charge during the heterogeneous substitution. In this case three Mg<sup>2+</sup> cations are replaced by a dimer associate of the two trivalent impurity ions with magnesium vacancy between them. This effect of the dimer self-organization of trivalent ions in forsterite was observed for the Cr<sup>3+</sup> [1], Ho<sup>3+</sup> [2] and Tb<sup>3+</sup> [3] ions and was not observed for Tm<sup>3+</sup> [4] ions. Here we present the results of the application of X- and Q-band electron paramagnetic resonance (EPR) to studying structure of paramagnetic centers formed by the Er<sup>3+</sup> ions in forsterite.

The measurements were performed at helium temperatures by the EMX plus and ELEXSYS E580 EPR spectrometers in the X- and Q-bands respectively. It is found that erbium ions substitute Mg<sup>2+</sup> ions in M1 positions of the forsterite crystal lattice as single ions and dimer associates. The concentration of the dimer associates was much higher than that to be expected for the statistical distribution of the impurity ions in the forsterite host. The magnetic properties are determined for both Er<sup>3+</sup> centers.

This work was supported in part by RFBR and the Government of the Republic of Tatarstan according to the research project № 15-42-02324 a.

1. Shakurov G.S., Tarasov V.F.: *Appl. Magn. Reson.* **21**, 597 (2001)
2. Konovalov A.A., Lis D.A., Malkin B.Z. *et al.*: *Appl. Magn. Reson.* **28**, 267(2005)
3. Konovalov A.A., Lis D.A., Subbotin K.A. *et al.*: *Appl. Magn. Reson.* **45**, 193 (2014)
4. Konovalov A.A., Lis D.A., Subbotin K.A. *et al.*: *Appl. Magn. Reson.* **30**, 673 (2006)

## Formation of $(\text{Ni}^{3+}-\text{F}_{\text{int}}^-)$ Associates in the $\text{BaF}_2$ Crystals Activated by Nickel: Results of EPR Study

V. A. Ulanov<sup>1,2</sup>, R. R. Zainullin<sup>2</sup>, I. V. Yatsyk<sup>1</sup>, and E. R. Zhiteitsev<sup>1</sup>

<sup>1</sup> Zavoisky Physical-Technical Institute, Russian Academy of Sciences, Kazan 420029, Russian Federation

<sup>2</sup> Kazan State Power Engineering University, Kazan 420066, Russian Federation

Nickel impurity centers in the fluorite group crystals ( $\text{CdF}_2$ ,  $\text{CaF}_2$ ,  $\text{SrF}_2$  and  $\text{BaF}_2$ ) were the objects of number EPR investigations. As it was found in these works, in the fluorite group crystals the nickel impurities substituted for host cations and stabilized in the  $\text{Ni}^+$ ,  $\text{Ni}^{2+}$  and  $\text{Ni}^{3+}$  valence states. In a cubic crystal field induced in positions of nickel impurities by nearest eight  $\text{F}^-$  ions, the ground term of  $\text{Ni}^+(3d^9, {}^2D)$  is splitted into excited orbital doublet  ${}^2E_{2g}$  and ground orbital triplet  ${}^2T_{2g}$ . In the same situation the ground term of  $\text{Ni}^{2+}(3d^8, {}^3F)$  gives the ground  ${}^3T_{1g}$  orbital triplet and the one of  $\text{Ni}^{3+}(3d^7, {}^4F)$  gives the  ${}^4A$  orbital singlet. Consequently, in the fluorite group crystals the  $\text{Ni}^+$  and  $\text{Ni}^{2+}$  can demonstrate the Jahn-Teller properties. As to  $\text{Ni}^{3+}$  centers, their dynamical properties depend on a size of the coordination cube formed by eight nearest fluorine neighbours and on the nature of the chemical bonds with these neighbours.

Earlier EPR investigations [1-3] gave the following results. Impurity centers of the  $\text{Ni}^+$  ions were got by X-ray irradiation of the  $\text{CaF}_2:\text{Ni}$ ,  $\text{SrF}_2:\text{Ni}$  and  $\text{BaF}_2:\text{Ni}$  crystals [2, 3]. Magnetic properties of the  $\text{Ni}^+$  centers revealed by [2, 3] had a tetragonal symmetry, and the impurity  $\text{Ni}^+$  ions were found in off-center positions of a tetragonal type. The off-center shift of  $\text{Ni}^+$  was found about 1 Å. It was proposed by authors of [2, 3] that this off-center shift was realized due to a Jahn-Teller effect combined with a pseudo-Jahn-Teller effect. The  $\text{Ni}^{3+}$  centers

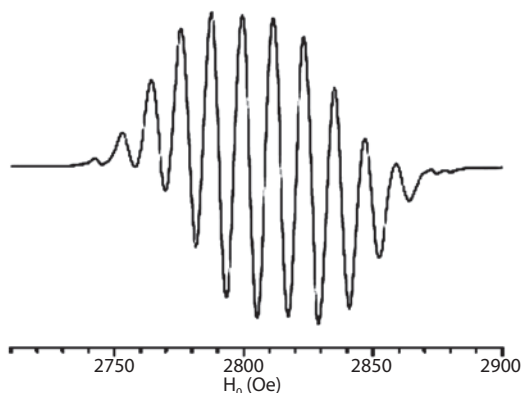


**Fig. 1.** The fragment of EPR spectrum of  $\text{BaF}_2:\text{Ni}$  sample relating to the four type parallel centers ( $H_0 \parallel \langle 001 \rangle$ ,  $T = 20$  K).

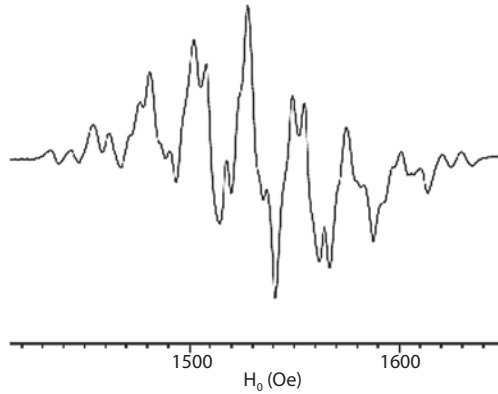


**Fig. 2.** The fragment of the EPR spectrum of  $\text{BaF}_2:\text{Ni}$  sample relating to the four type perpendicular centers ( $H_0 \parallel \langle 001 \rangle$ ,  $T = 20 \text{ K}$ ).

observed in the irradiated  $\text{CaF}_2:\text{Ni}$  crystals [2] had a cubic symmetry and this result corresponds to a prediction which based on the fact that the ground state of the  $\text{Ni}^{3+}$  ions formed these centers is orbital singlet. The  $\text{Ni}^{2+}$  centers of trigonal symmetry were revealed in the  $\text{CdF}_2:\text{Ni}$  and  $\text{CaF}_2:\text{Ni}$  crystals [3]. The authors of [3] proposed that the trigonal symmetry of the  $\text{Ni}^{2+}$  centers was realized due to a strong Jahn-Teller effect in the ground triplet orbital state.

Our interest to the  $\text{BaF}_2$  crystals activated by paramagnetic ions is associated with the fact that these crystals are often used as substrates in various semiconducting devices. It seems to us the paramagnetic centers in such substrate can allow an operation the charge transport processes in semiconducting layers by optical irradiation of the substrate.

In the present work the  $\text{BaF}_2$  crystals activated by nickel impurities were investigated by EPR method. The  $\text{BaF}_2:\text{Ni}$  crystals were grown by the vertical Bridgman method in a graphite crucible. A helium and fluorine gas mixture was used as an atmosphere for a crystal growth process. Nickel was introduced into the melt as a metallic powder. The crystalline samples grown by such a way had a green color. They were investigated by EPR method using the X-band Bruker spectrometer EMSplus ( $f = 9386 \text{ MHz}$ ). The crystals under investigation were not exposed to X-ray irradiation. To obtain temperatures ranging from 4.2 to 100 K, the Oxford Instruments continuous-flow helium cryostat was used. The *dc* magnetic field was modulated at 100 kHz.

Analysis of the angular positions of the EPR spectra lines allowed us to observe at  $T = 5 \text{ K}$  four types of paramagnetic centers were revealed in the EPR spectra of the samples under investigation. First of them were subscribed to  $\text{Mn}^{2+}$  centers of cubic symmetry which proved to be an uncontrolled impurities in the  $\text{BaF}_2:\text{Ni}$  samples. The EPR lines corresponding to these manganese centers were rather weak. Later these lines were used by us to analyze the temperature dependencies of EPR line amplitudes of the nickel impurity centers studied. The second type centers had a monoclinic symmetry and were attributed to  $\text{Ni}^{2+}$  ions associated with interstitial fluorine ions being at tetragonal positions

relative to  $\text{Ni}^{2+}$ . Monoclinic symmetry of their magnetic properties was due to the Jahn-Teller effect. The third type centers had a tetragonal symmetry and were subscribed to  $(\text{Ni}^+-\text{Ni}^{3+})$  bound each with other by exchange of ferromagnetic nature. Above mentioned centers were observed as well in the  $\text{BaF}_2:\text{Ni}$  crystals grown by us earlier in the helium atmosphere with a low concentration of fluorine gas. In this work we investigated the  $\text{BaF}_2:\text{Ni}$  samples grown in the helium atmosphere with a rather high concentration of fluorine gas. Obviously, due to this fact we observed new paramagnetic centers with tetragonal symmetry of magnetic properties. The fragments of EPR spectra of the  $\text{BaF}_2:\text{Ni}$  samples corresponding to new centers (four type centers) are represented in Figs. 1 and 2. In Fig.1 one can see the spectrum arising due to the four type centers with axes of tetragonality oriented parallel to the direction of the  $dc$  magnetic field  $\vec{H}_0$  (parallel centers).

The spectrum of the four type centers oriented perpendicular to the  $\vec{H}_0$  (perpendicular centers) is represented in Fig. 2. Angular dependencies in the spectra of these centers are described well with  $g_{\parallel} = 2.387 \pm 0.001$  and  $g_{\perp} = 4.370 \pm 0.001$ . These spectra are characterized by the well resolved superhyperfine structures arising due to superhyperfine interaction (SHFI) of electron magnetic momentum with three groups of nuclear magnetic moments of  $\text{F}^-$  ions (4+4+1). The models of the centers and its characteristics are discussed.

1. Alonso P.J., Casas Gonzalez J., den Hartog H.W.: Phys. Stat. Sol. (b) **102**, 721 (1980)
2. Alonso P.J., Casas Gonzalez J., den Hartog H.W., Alcalá R.A.: J. Phys. C: Solid State Phys. **16**, 3593 (1983)
3. Gehlhoff W., Ulrici W.: Phys. Stat. Sol. (b) **102**, 11 (1980)

## EPR Investigation of Trinuclear Copper Cluster in Hyperbranched Polyesterpolyacrylic Acid

**S. V. Yurtaeva<sup>1</sup>, I. V. Ovchinnikov<sup>1</sup>, M. P. Kutyreva<sup>2</sup>, A. R. Gataulina<sup>2</sup>,  
N. A. Ulakhovich<sup>2</sup>, and A. A. Rodionov<sup>3</sup>**

<sup>1</sup> Zavoisky Physical-Technical Institute, Russian Academy of Sciences, Kazan 420029, Russian Federation, yurtaeva@mail.knc.ru

<sup>2</sup> Institute of Chemistry, Kazan Federal University, Kazan 420008, Russian Federation, Marianna.Kutyreva@kpfu.ru

<sup>3</sup> Institute of Physics, Kazan Federal University, Kazan 420008, Russian Federation, rodionovshurik@yandex.ru

The chemistry and physics of trinuclear Cu(II) complexes has drawn considerable interest due to their identification as the active sites of oxidases and oxygenases. Over the years, however, there has also been much interest in these complexes for the development of new inorganic materials showing molecular ferromagnetism.

In this research we investigated Cu(II) complexes with hyperbranched polyesterpolyacrylic acid of third generation, containing six fragments of acrylic acid in terminal positions. Concentrated sample (blue powder) and a frozen solution of complex were investigated by EPR. In powder samples trinuclear Cu(II) complexes were detected and in solutions mononuclear paramagnetic Cu(II) centers were observed. The EPR spectrum of powder sample at room temperature demonstrated 4 lines corresponding to trinuclear Cu(II) cluster. To understand its nature the temperature behavior of EPR spectrum was investigated. The temperature dependence of integral intensity was determined. At the temperatures of 8–9 K ferromagnetic ordering occurs. Ferromagnetic nature of the coupling between Cu(II) ions is suggested. The model of structure of trinuclear Cu(II) cluster is suggested, carbonate anion serves as a tridentate bridge. According to IR data the coordination environment of each copper ion is tetrahedral. The interaction

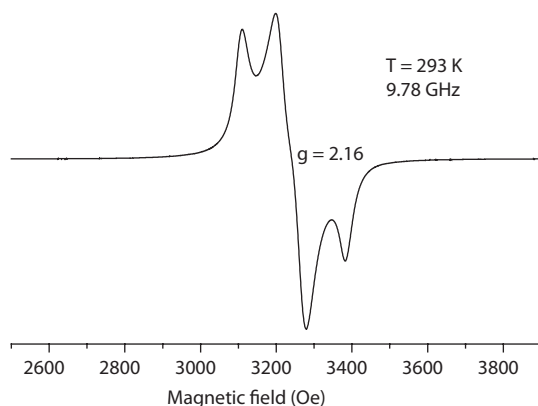


Fig. 1.

---

among the Cu(II) ions is weakly ferromagnetic and complex exhibits a  $S = 3/2$  quartet ground state. At low temperatures only three ground state transitions are observed ( $-3/2 \rightarrow -1/2$ ); ( $-1/2 \rightarrow 1/2$ ); ( $1/2 \rightarrow 3/2$ ). At room temperature upper doublet state with  $S = 1/2$  is populated and ( $-1/2 \rightarrow 1/2$ ) transition from excited doublet state ( $S = 1/2$ ) is also observed.

The nature of ferromagnetic interaction of Cu(II) ions in trinuclear Cu cluster is discussed.

## The Influence of the Frequency of the Microwave Field on the Dispersion Curves of the Spin-Wave Resonance Spectra

A. M. Zuyzin, M. A. Bakulin, S. V. Bezborodov, V. V. Radaikin,  
and S. N. Sabaev

Mordovian State University, Saransk, sergei2089@mail.ru

The purpose of this study was to investigate the influence of the frequency of the microwave field on the dispersion dependence of the spectra of the spin-wave resonance (SWR) bilayer films with perpendicular and parallel orientations of the static magnetic field  $H$  relative to the film plane.

Registration of the spectra spin-wave resonance (SWR) had been producing by EPR spectrometer X- and Q-band EMX Plus (Bruker) at frequencies of the microwave field  $f_1 = 9.4$  GHz and  $f_2 = 34$  GHz. Investigations were made on the two-layer single-crystal garnet-ferrite films, which were grown by method of liquid phase epitaxy. The parameters of the films are shown in Table 1.

Table 1.

| Sample no. | Layer no. | Composition   | h (μm) | 4πM (G) | α     | γ, 10 <sup>7</sup> (Oe <sup>-1</sup> s <sup>-1</sup> ) | H <sub>k</sub> <sup>eff</sup> (Oe) |
|------------|-----------|---|--------|---------|-------|--|------------------------------------|
| 1          | 1*        | Y <sub>2.98</sub> Sm <sub>0.02</sub> Fe <sub>5</sub> O <sub>12</sub>                        | 0.42   | 1740    | 0.003 | 1.76   | -1715                              |
|            | 2*        | Sm <sub>0.43</sub> Er <sub>2.55</sub> Fe <sub>5</sub> O <sub>12</sub>                       | 2.5    | 1330    | 0.2   | 1.38   | 96                                 |
| 2          | 1*        | Y <sub>2.98</sub> Sm <sub>0.02</sub> Fe <sub>5</sub> O <sub>12</sub>                        | 0.98   | 1740    | 0.003 | 1.76   | -1715                              |
|            | 2*        | Er <sub>2.58</sub> La <sub>0.42</sub> Fe <sub>3.95</sub> Ga <sub>1.05</sub> O <sub>12</sub> | 1.2    | 450     | 0.84  | 1.66   | -78                                |

1\* denotes the layer of the excitation, 2\* is the spin-pinned layer.

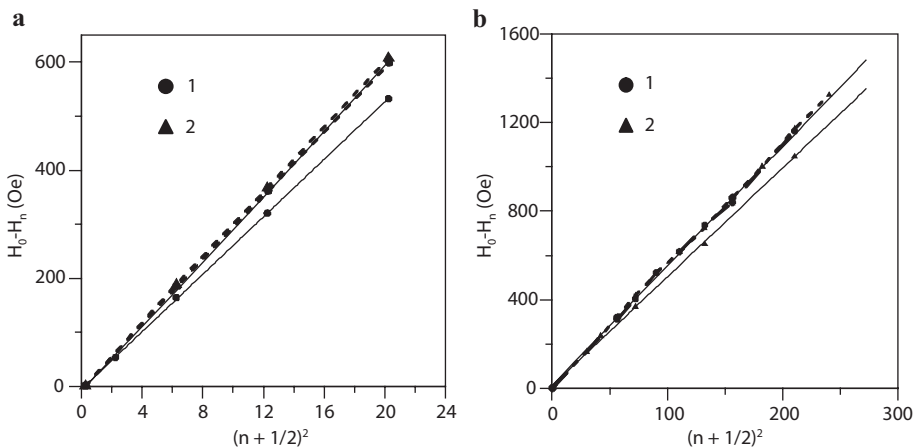


Fig. 1. Dispersion curves  $H_0 - H_n = f(n + 1/2)^2$ : **a** sample number 1, **b** sample number 2. Solid lines – band, dashed lines – band. 1 – normal orientation. 2 – parallel orientation.



The experiments revealed that with the increasing of frequency of the microwave field there are significant changes in the spectrum of the SWR. It was found that the misalignment between the dispersion curves for the parallel and perpendicular orientations of the magnetic field with respect to the plane of the film is markedly reduced (Fig. 1) [1, 2].

The increase in the angle of the dispersion slope with increasing frequency of the microwave field in the sample №1 for the perpendicular orientations of the magnetic field layer associated with the transition the spin-pinned layer from the state of reactive medium in dispersive when the perpendicular orientation  $\mathbf{H}$  with respect to the film. This transition is due to different values  $\gamma$  in the layers. Change in the slope of the dispersion curve of the sample №2 with increasing frequency due to the increasing influence of the dissipative mechanism of spin pinning. This leads to a change in the spatial phase of the standing spin waves at the interface between the layers and the corresponding change in the wave number.

1. Zuzin A. M., Bazhanov A. G., Radaïkin V.V.: Technical Physics. The Russian Journal of Applied Physics. **44**, 11, 1351–1355 (1999)
2. Zyuzin A.M., Sabaev S.N., Kulyapin A.V.: Physics of the Solid State **45**, 12, 2313–2319 (2003)

## Spin-Wave Resonance in Films with a Uniform Gradient of Field Uniaxial Anisotropy

A. M. Zyuzin and N. V. Yantsen

Mordovia State University, Saransk 430000, Russian Federation, nikitos13rus@mail.ru

Have been investigated features of the spectra spin-wave resonance (SWR) in films with linearly varying uniaxial anisotropy field by their thickness  $H_k = B_z + C$ . Calculation of the spectra SWR produced by solving the wave equations

$$\frac{2A}{M} \frac{\partial^2 m}{\partial z^2} - \left( H + Bz + C - \frac{\omega}{\gamma} \right) m = 0,$$

where  $m$  is variable magnetization. The solution of this equation is a linear combination of Airy functions [1].

The calculation results revealed that SWR spectrum consists of two sections. In the first section are excited volume spin-wave (SW) mods, the intensity of which is very high. In contrast to homogeneous films with surface anisotropy or bilayer film, in which the intensity varies as a  $I_n/I_0 \sim 1/n^2 \div 1/n^4$  [2] (where  $n$  is the number of SW-mod), in the investigated films, as follows from Fig. 1, the intensity of the 26-th SW-mod is not reduced by more than twice compared with intensity of the first SW-mod.

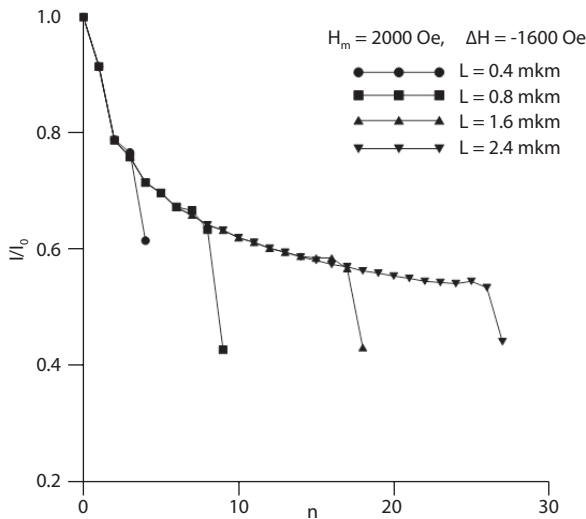


Fig. 1. The relative intensity of SW-mod.

One interesting results is that at invariable gradient field anisotropy the number of high-intensity mods and the frequency interval at invariable value of the external magnetic field is directly dependent on the film thickness. It is shown that with decreasing the thickness decreases the number of mods with a high intensity. But the distribution of resonance fields and intensities in the initial section remains essentially unchanged. In such a way variation in the thickness can be adjusted frequency interval excited SWR-mods. It is also shown that the distribution of the absorption peaks spin-wave modes in frequency of the microwave field close to linear.

1. Hoekstra B., Stapele R.P., Robertson J.M.: *J. Appl. Phys.* **48**, 382 (1977)
2. Zyuzin A.M., Sabaev S.N., Radaykin V.V. *et al.*: *Tech. Phys. Lett.* **34**, 16, 53–57 (2008)

---

## AUTHOR INDEX

|                            |                  |
|----------------------------|------------------|
| Abdulmalic, M. A.          | 19               |
| Abramova, T.               | 93               |
| Abrosimov, N. V.           | 110              |
| Akhmetov, M. M.            | 78, 99           |
| Alakshin, E. M.            | 50               |
| Albertini, M.              | 66               |
| Alfonsov, A.               | 34, 103          |
| Aliabadi, A.               | 19               |
| Alloul, H.                 | 41               |
| Andreev, N. V.             | 39               |
| Andrianov, V. V.           | 96               |
| Astakhov, G.               | 75               |
| Atsarkin, V. A.            | 2, 6             |
| Audran, G.                 | 48               |
| <b>Bagryanskaya, E. G.</b> | 12, 28, 114, 132 |
| Bakirov, M. M.             | 129              |
| Bakulin, M. A.             | 144              |
| Bales, B.                  | 129              |
| Baniodeh, A.               | 134              |
| Baranov, P. G.             | 75               |
| Barras, J.                 | 124              |
| Behrends, J.               | 119              |
| Belyaev, B. A.             | 106              |
| Berezin, A. S.             | 80               |
| Bezborodov, S. V.          | 144              |
| Biziyaev, D. A.            | 54               |
| Bogaychuk, A.              | 82               |
| Borisenko, I. V.           | 6                |
| Bowman, M. K.              | 16               |
| Brémond, P.                | 48               |
| Broderick, T.              | 68               |
| Büchner, B.                | 19, 34, 37, 103  |
| Budarin, L. I.             | 56, 86           |
| Bukharaev, A. A.           | 54               |
| Carbonera, D.              | 66               |
| Chen, H.                   | 16               |
| Cherepnev, G. V.           | 104              |
| Chervonova, U.             | 84               |
| Chichkov, V. I.            | 39               |
| Chupakhina, T. I.          | 90               |
| Chushnikov, A. I.          | 104              |
| Curro, N. J.               | 37               |

---

|                       |                   |
|-----------------------|-------------------|
| Degtyarev, E. N.      | 27                |
| Demidov, E.           | 56, 58, 86        |
| Demidov, V. V.        | 6                 |
| Deminov, R. G.        | 95                |
| Demishev, S. V.       | 9                 |
| Denisov, A. A.        | 96                |
| Detochenko, A. A.     | 110               |
| Dioguardi, A. P.      | 37                |
| Di Valentin, M.       | 66                |
| Dmitriev, A.          | 35                |
| Domracheva, N.        | 84                |
| Dooglav, A. V.        | 41                |
| Drechsler, S.-L.      | 34                |
| Dyakonov, V.          | 75                |
| Dzheparov, F. S.      | 70                |
| Dzuba, S. A.          | 14, 107, 116, 126 |
| Eremina, R. M.        | 39, 89, 90, 117   |
| Earle, K. A.          | 68                |
| Ezhevskii, A. A.      | 110               |
| Falin, M. L.          | 92, 115           |
| Fazlizhanov, I. I.    | 117               |
| Fedin, M. V.          | 12, 28, 114       |
| Fedorova, O. S.       | 22                |
| Fedotov, K. Yu.       | 116               |
| Fel'dman, E. B.       | 69                |
| Filimonov, Yu.        | 58                |
| Fishman, N.           | 31, 93            |
| Fittipaldi, M.        | 7                 |
| Fominov, Ya. V.       | 95                |
| Fraerman, A. A.       | 56                |
| Fuchs, F.             | 75                |
| Gaifullin, R. R.      | 95                |
| Gainutdinov, Kh. L.   | 96                |
| Galeev, R.            | 98, 129, 134      |
| Gataulina, A. R.      | 142               |
| Gatteschi, D.         | 3, 7              |
| Gavrilova, T. P.      | 39, 90            |
| Gavrilyachenko, V. G. | 90                |
| Gazizulin, R. R.      | 50                |
| Gilmanov, M. I.       | 9                 |
| Gilmutdinov, I. F.    | 41, 90            |
| Glushkov, V. V.       | 9                 |
| Gobbo, M.             | 66                |
| Goenko, I. A.         | 99                |
| Golubov, A. A.        | 95                |
| Gorev, R. V.          | 54, 58            |
| Gorkin, A.            | 82                |

|                      |              |
|----------------------|--------------|
| Goryunov, Yu.        | 101          |
| Grafe, H.-J.         | 34, 37, 103  |
| Gräfe, U.            | 37           |
| Grampp, G.           | 31           |
| Gritsan, N.          | 35           |
| Gruzdev, M.          | 84           |
| Gumarov, G. G.       | 78, 99       |
| Guseinov, D. V.      | 110          |
| Gusev, N. S.         | 56           |
| Hammerath, F.        | 37           |
| Hofer, P.            | 45           |
| Iakovleva, M.        | 34, 103, 130 |
| Ibragimova, M. I.    | 104          |
| Isaev, N. P.         | 16, 116      |
| Ivanov, K.           | 71, 74       |
| Ivanova, T.          | 125          |
| Iyudin, V. S.        | 96           |
| Izotov, A. V.        | 106          |
| Jeschke, G.          | 71           |
| Kabirov, Yu. V.      | 90           |
| Kandrashkin, Yu. E.  | 54           |
| Kardash, M. E.       | 107          |
| Karminskaya, T. Yu.  | 95           |
| Karzanov, V. V.      | 86           |
| Kataev, V.           | 19, 34, 103  |
| Khaibullin, R.       | 60           |
| Khairuzhdinov, I. T. | 109          |
| Khaliullin, G.       | 36           |
| Khanipov, T. F.      | 54           |
| Khivintzev, Yu.      | 58           |
| Khotyanovich, M. O.  | 96           |
| Khramtsova, E. A.    | 25           |
| Kirilyuk, I. A.      | 28           |
| Kiryutin, A.         | 22, 93       |
| Kiyamov, A. G.       | 90           |
| Klauss, H.-H.        | 103          |
| Klingeler, R.        | 61           |
| Klochkov, A.         | 50, 130      |
| Kokorin, A. I.       | 27           |
| Kolbanev, I. V.      | 27           |
| Kolker, A.           | 84           |
| Konakov, A. A.       | 110          |
| Konov, A. B.         | 78, 111      |
| Konov, K. B.         | 29, 116      |
| Konygin, G. N.       | 78, 99       |
| Koo, C.              | 61           |
| Korableva, S. L.     | 115          |

---

|                      |                            |
|----------------------|----------------------------|
| Koroleva, A. V.      | 110                        |
| Korostelin, Yu. V.   | 131                        |
| Kozlovsky, V. I.     | 131                        |
| Kraus, H.            | 75                         |
| Krivenko, S. A.      | 41                         |
| Krumkacheva, O. A.   | 12, 28, 114, 132           |
| Kruppa, A. I.        | 20                         |
| Kudrin, A. V.        | 110                        |
| Kukovitsky, E.       | 128, 136                   |
| Kulchitchkii, V. A.  | 96                         |
| Kupriyanov, M. Yu.   | 95                         |
| Kupriyanova, G. S.   | 72, 82, 112, 120, 122, 124 |
| Kutyreva, M. P.      | 142                        |
| Kuzhelev, A. A.      | 12, 28, 114                |
| Kuzmin, V. V.        | 50                         |
| Kuznetsov, D.        | 45                         |
| Kuznetsov, N. A.     | 22                         |
| Lang, G.             | 37                         |
| Latypov, V. A.       | 92, 115                    |
| Lavrenova, L. G.     | 80                         |
| Leonov, D. V.        | 116, 126                   |
| Leshina, T. V.       | 20, 25                     |
| Lesnikov, V. P.      | 86                         |
| Lightfoot, P.        | 61                         |
| Likhtenshtein, G. I. | 23                         |
| Lomonova, E. E.      | 117                        |
| Lomzov, A. A.        | 12                         |
| Luetkens, H.         | 103                        |
| Lukzen, N.           | 119                        |
| Lyadov, N. M.        | 90                         |
| Lyubenova, S.        | 45                         |
| Magin, I. M.         | 20                         |
| Maiti, T.            | 89                         |
| Malferrari, M.       | 17                         |
| Maljuk, A.           | 103                        |
| Mamadazizov, S.      | 120                        |
| Mamedov, M.          | 17                         |
| Marque, S.           | 48                         |
| Maryasov, A. G.      | 16                         |
| Matysik, J.          | 71                         |
| Medvedeva, A. S.     | 132                        |
| Mershiev, I.         | 122                        |
| Milovich, F. O.      | 117                        |
| Mingalieva, L. V.    | 54, 134, 138               |
| Mironov, V. L.       | 54, 56, 58                 |
| Möbius, K.           | 17                         |
| Molchanov, V. V.     | 112                        |

|                      |               |
|----------------------|---------------|
| Morozova, O. B.      | 18, 31, 93    |
| Mozzhukhin, G. V.    | 112, 120, 124 |
| Mukhamedshin, I. R.  | 41            |
| Munao, I.            | 61            |
| Nadolinny, V. A.     | 80            |
| Nalbandyan, V.       | 130           |
| Nateprov, A.         | 101           |
| Nojiri, H.           | 34            |
| Novokshonov, V. V.   | 132           |
| Nurgazizov, N. I.    | 54            |
| Orlinskii, S. B.     | 75            |
| Orlova, A. N.        | 72            |
| Ovcharenko, V. I.    | 132           |
| Ovchenkov, Y. A.     | 61            |
| Ovchinnikov, S. G.   | 51            |
| Ovchinnikov, I. V.   | 125, 142      |
| Ovsyannikov, G. A.   | 6             |
| Panov, M. S.         | 22, 31, 93    |
| Parfenov, V. V.      | 39            |
| Pashkevich, S. G.    | 96            |
| Petr, A.             | 19            |
| Petrov, S. V.        | 92            |
| Petukhov, V. Yu.     | 78, 99, 104   |
| Podol'skii, V. V.    | 86            |
| Polyakov, N. E.      | 20            |
| Popkov, S. A.        | 110           |
| Povarov, K. Yu.      | 49            |
| Powell, A.           | 134           |
| Pravdivtsev, A. N.   | 74            |
| Purtov, P. A.        | 20, 25        |
| Pushkina, E. A.      | 126           |
| Pyataev, A.          | 84            |
| Pyshnyi, D.          | 12            |
| Pytalev, D. S.       | 131           |
| Radaikin, V. V.      | 144           |
| Rameev, B.           | 60, 120, 124  |
| Rautskii, M. V.      | 51            |
| Riemann, H.          | 110           |
| Rodionov, A. A.      | 142           |
| Rogozhnikova, O. Yu. | 12, 16, 114   |
| Rüffer, T.           | 19            |
| Rybin, D. S.         | 78            |
| Sabaev, S. N.        | 144           |
| Sadykov, M. F.       | 111           |
| Safullin, K.         | 50, 130       |
| Sakhin, V.           | 128, 136      |



---

|                    |              |
|--------------------|--------------|
| Salikhov, K. M.    | 19, 109, 129 |
| Salikhov, T.       | 130          |
| Samarin, A. N.     | 9            |
| Samoilova, R. I.   | 16           |
| Savitsky, A.       | 17           |
| Semeno, A. V.      | 9            |
| Semenov, A.        | 17           |
| Severin, E. A.     | 112          |
| Shakurov, G. S.    | 131          |
| Sharipov, K. R.    | 90           |
| Shevelev, G. Y.    | 12, 28       |
| Shukla, A. K.      | 89           |
| Shustov, V. A.     | 43           |
| Sinyavsky, N.      | 82           |
| Sivak, M. V.       | 27           |
| Skorohodov, E.     | 58           |
| Sluchanko, N. E.   | 9            |
| Smirnov, A. I.     | 49           |
| Soldatov, T. A.    | 49           |
| Soltamov, V.       | 75           |
| Sorokin, B. V.     | 6            |
| Sosnovsky, D. V.   | 25, 71       |
| Soukhorukov, A. V. | 110          |
| Stratan, M.        | 130          |
| Streletsky, A. N.  | 27           |
| Strizhakov, R. K.  | 28, 132      |
| Sturza, M.-I.      | 34           |
| Subbotin, K. A.    | 138          |
| Sukhanov, A.       | 125, 134     |
| Suturina, E.       | 35           |
| Tabachkova, N. Yu. | 117          |
| Tagirov, L. R.     | 95           |
| Tagirov, M. S.     | 50, 130      |
| Talanov, Yu. I.    | 128, 136     |
| Tarasov, A. S.     | 51           |
| Tarasov, V. F.     | 138          |
| Teitel'baum, G. B. | 128, 136     |
| Tirkiya, A.        | 111          |
| Tormyshev, V. M.   | 12, 16, 114  |
| Tretyakov, E. V.   | 132          |
| Troitskaya, T. I.  | 114          |
| Tronov, A. A.      | 86           |
| Trukhin, D. V.     | 12, 114      |
| Tsirlin, A. A.     | 61           |
| Turanova, O.       | 125          |
| Ulakhovich, N. A.  | 142          |
| Ulanov, V. A.      | 43, 139      |

|                    |                      |
|--------------------|----------------------|
| Varnakov, S. N.    | 51                   |
| Vasiliev, A. N.    | 61                   |
| Vasiliev, V. G.    | 132                  |
| Vavilova, E. L.    | 19, 34, 103 130      |
| Venturoli, G.      | 17                   |
| Vieth, H.-M.       | 74                   |
| Volkov, N. V.      | 51                   |
| Volkova, O. S.     | 61                   |
| Vorobeva, V.       | 84                   |
| Voronkova, V. K.   | 19, 116, 134         |
| Wurmehl, S.        | 34, 103              |
| Yafarova, G. G.    | 96                   |
| Yakubov, R.        | 58                   |
| Yantsen, N. V.     | 146                  |
| Yatzyk, I. V.      | 39, 90, 99, 104, 139 |
| Yavkin, B.         | 75                   |
| Yurkovskaya, A. V. | 18, 22, 31, 74, 93   |
| Yurtaeva, S. V.    | 142                  |
| Zainullin, R. R.   | 43, 139              |
| Zaripov, R. B.     | 19, 138              |
| Zharikov, E. V.    | 138                  |
| Zhiteitsev, E. R.  | 43, 139              |
| Ziatdinov, A. M.   | 52                   |
| Zimmermann, S.     | 103                  |
| Zubin, A. Y.       | 72                   |
| Zurlo, E.          | 66                   |
| Zuyzin, A. M.      | 144, 146             |
| Zvereva, E. A.     | 61, 130              |



